Supporting Information

Mechanistic and Kinetic Understanding of the UV_{254} Photolysis of Chlorine and Bromine Species in Water and Formation of Oxyhalides

Woorim Lee[1], Yuri Lee[1], Sebastien Allard[2], Jiwoon Ra[1], Seunghee Han[1], Yunho Lee[1]*

[1]*School of Earth Sciences and Environmental Engineering, Gwangju Institute of Science and Technology (GIST), Gwangju 61005, Republic of Korea*

[2]*Department of Chemistry, Curtin University, GPO Box U1987, Perth Western Australia 6845, Australia*

*Corresponding author. Mailing address: School of Earth Sciences and Environmental Engineering, Gwangju Institute of Science and Technology (GIST), Gwangju 61005, Republic of Korea.

Phone: 82-62-715-2468, fax: 82-62-715-2434, email: yhlee42@gist.ac.kr

This SI includes 13 texts, 9 tables, 23 figures, and 1 scheme as supplementary materials, data, discussions and kinetic modeling.

Supporting Texts

SI-Text-1. Standards and Reagents

Atrazine (analytical standard), 2,2′-Azino-bis(3-ethylbenzothiazoline-6-sulfonic acid) diammonium salt (i.e. ABTS, ≥98%), benzoic acid (≥99.5%), bromate standard solution (1000 mg L^{-1}), 2,4-dinitrophenylhydrazine (i.e. DNPH, 97%), formaldehyde solution (37% in H_2O), methanol (≥99.9%), nitrobenzene (≥99.0%), phosphoric acid (H_3PO_4, 85% in H_2O), potassium chlorate (≥99.0%), sodium bromide (≥99.0%), sodium chloride (≥99.0), sodium formate (≥99.0%), sodium hydroxide solution (NaOH, 50% in H_2O), sodium hypochlorite (NaOCl, 4-5%), sodium phosphate dibasic dihydrate (≥99.5%), sodium phosphate monobasic dihydrate (≥99.0%), sodium tetraborate decahydrate (≥99.5%), sodium thiosulfate pentahydrate (99.5%) and *tert*-butanol (≥99.0%) were purchased from Sigma-Aldrich (St. Louis, MO). Acetonitrile (99.9%) was purchased from Thermo Fisher scientific (Waltham, MA). Phosphate buffer solutions (pH 5 and 6) were prepared by using Na_2HPO_4 and NaH_2PO_4. Borate buffer solutions (pH 10) were prepared by using $Na_2B_4O_7$ and NaOH.

Chemical solutions were prepared with ultrapure water (≥18.2 MΩ-cm) obtained using a Barnstead purification system (Thermo Fisher Scientific). Chlorine stock solutions (20–100 mM) were prepared by diluting sodium hypochlorite solution (NaOCl, 4–5% active chlorine) and standardized by measuring the ultraviolet absorbance at 292 nm and the molar absorption coefficient of 362 $M^{-1}cm^{-1}$ for OCl^-.[1] Bromine stock solutions (20 mM) were prepared by reacting equal volumes of 20 mM of NaOCl solution with 21 mM of sodium bromide (NaBr) solution at pH 11 for three days.[2] After completion of the reaction (i.e., $OCl^- + Br^- \rightarrow OBr^- + Cl^-$, $k = 0.9\times10^{-3}$ $M^{-1}s^{-1}$),[3] the bromine stock solution was standardized spectrophotometrically using the molar absorption coefficient of 332 $M^{-1}cm^{-1}$ at 329 nm for OBr^-.[4] The concentration of the formaldehyde stock solution was determined by the Nash method[5] using the UV absorbance at 412 nm and the corresponding molar absorption coefficient of 7530 $M^{-1}cm^{-1}$. All stock solutions were stored at 4°C in darkness before use.

SI-Text-2. UV experiments

UV photolysis was performed in a quasi-collimated beam system equipped with a low-pressure mercury lamp emitting UV light primarily at 254 nm (TUV 130W XPT, Philips, Amsterdam). The prepared samples (100 mL) were placed in glass Petri dishes (ø 8 cm and sample depth of 2 cm) and irradiated with UV at the fluence rate of 0–2000 mJ cm^{-2}. The applied UV fluence rate was ~4 mW cm^{-2}, which was determined by atrazine chemical actinometry[6,7] or using a UVX digital radiometer (Ultra-Violet Products Ltd., Upland, CA). The reaction solution was sampled at different UV fluence levels and analyzed directly without any sample treatment (for determining the residual oxidant concentration) or with added sodium thiosulfate (at 10-fold the initial chlorine concentration) to quench the residual chlorine. Samples were stored at 4°C until sample analysis. Decreases of the sample volume due to sampling did not exceed 10% of the initial volume. Experiments were conducted in triplicate, from which average values with standard deviation were reported.

SI-Text-3. Analytical methods

HPLC/UV. A high-performance liquid chromatography (HPLC) system (Ultimate 3000, Dionex, Sunnyvale, CA), equipped with a UV diode array detector was used to quantify nitrobenzene (NB), benzoic acid (BA), and formaldehyde. Separation of NB and BA was achieved with a Nucleosil C18 column (5 μm, 4×125 mm) using acetonitrile and water containing phosphoric acid (25 mM) as the mobile phase. A gradient eluent was programmed as follows: 0–4 min with 40% acetonitrile; 4–5 min with 40%–20% acetonitrile; 5–7 min with 20% acetonitrile; 7–8 min with 20%–40% acetonitrile; 8–10 min with 40% acetonitrile. Formaldehyde was determined based on pre-column derivatization with 2,4-dinitrophenylhydrazine (DNPH) and HPLC/UV analysis of the derivatization product.[8] Separation of derivatization product was achieved using 40% acetonitrile and 60% water isocratically. The

injection volume was 100 μL, and the flow rate was 1 mL min^{-1}.

IC/conductivity. An ion-chromatography (IC) with a conductivity detector (Professional IC Vario, Metrohm, Herisau) was used to quantify chlorite (ClO_2^-) and chlorate (ClO_3^-). Separation was achieved using an anion exchange column (Metrosep A Supp 5-150/4.0) with 3.2 mM Na_2CO_3/1 mM $NaHCO_3$ solution (flow rate of 0.5 mL min^{-1}) as the eluent. The limits of detection (LOD) were 10 nM (= 0.7 μg L^{-1}) for ClO_2^- and 13 nM (= 1.4 μg L^{-1}) for ClO_3^-.

HPLC/ICP/MS. A HPLC (Agilent 1100, Agilent, Santa Clara, CA) coupled with an inductively coupled plasma mass spectrometry (Agilent 7500) was used to quantify bromate (BrO_3^-). Separation was achieved with an IonPac™ AS 19 column (2×250 mm, Dionex) using a solution containing ammonium nitrate/nitric acid (25 mM/5 mM) as the eluent at a flow rate of 0.25 mL min^{-1}. The LOD of BrO_3^- was 3 nM (= 0.5 μg L^{-1}).

UV/vis. UV/vis absorption spectra were obtained using an Evolution 201 UV/vis spectrophotometer (Thermo Fisher Scientific).

SI-Text-4. Apparent quantum yields for the halogen oxidant decomposition

The decomposition of chlorine and bromine (initial concentration = 140 μM) under UV irradiation followed first-order kinetics with respect to the UV fluence under all tested conditions (Figure S1). In organic-free solutions (Figure S1a), the oxidant decomposition rate was the highest for chlorine at pH 6 (HOCl, 4.9×10^{-4} cm^2 mJ^{-1}), followed by chlorine at pH 10 (OCl^-, 4.0×10^{-4} cm^2 mJ^{-1}), bromine at pH 6 (HOBr, 2.3×10^{-4} cm^2 mJ^{-1}), and bromine at pH 10 (OBr^-, 7.2×10^{-5} cm^2 mJ^{-1}), in which the parentheses show the major halogen oxidant species and the fluence-based first-order rate constants of oxidant decomposition (k_{Ox}) at each condition (Table S1). The apparent quantum yields for the oxidant decomposition (Φ_{Ox}^{app}) could be calculated based on Equation S1, and were 1.58 for HOCl, 1.45 for

OCl^-, 0.55 for HOBr, and 0.74 for OBr^-.

$$\Phi_{Ox}^{app} = \frac{k_{Ox} \times U_{254}}{2.303 \times \varepsilon_{254}} \quad \text{(S1)}$$

U_{254} is the molar photon energy at 254 nm (= 4.72×10^5 J einstein^{-1})[9] and ε_{254} ($M^{-1}cm^{-1}$) is the molar absorption coefficient of the halogen oxidant specie at 254 nm (see Table S2 and Figure S2). The obtained Φ_{Ox}^{app} values for HOCl and OCl^- were consistent with those reported in literature (Table S2). Quantum yields of more than 1 can be rationalized as the decomposition of chlorine species by $^{\bullet}OH$ and RCS in addition to their direct UV photolysis. The contribution of the different radicals to the chlorine decomposition can vary depending on the solution composition, including the initial chlorine concentration and pH. This explains the wide variations of the Φ_{Ox}^{app} for chlorine species reported in literature. For the bromine species, Guo et al. reported Φ_{Ox}^{app} values of 0.69(±0.03) for HOBr and 0.37–0.55 for OBr^-,[10] which were somewhat different from those of this study. It was found that the molar absorption coefficients at 254 nm (ε_{254}) of bromine species used in this study (84 $M^{-1}cm^{-1}$ for HOBr and 20 $M^{-1}cm^{-1}$ for OBr^-) were different from those in Guo et al. (77 $M^{-1}cm^{-1}$ for HOBr and 28 $M^{-1}cm^{-1}$ for OBr^-). When the ε_{254} values of this study were applied to the data of Guo et al., the Φ_{Ox}^{int} values of Guo et al. were changed to 0.63 for HOBr and 0.52–0.77 for OBr^-. These new Φ_{Ox}^{int} values are reasonably close to those from this study. Another study reported Φ_{Ox}^{app} values which were determined in synthetic phosphate-buffered solutions at pH 6.5 and 8.5 in which HOBr and OBr^- coexisted.[11] In that study, Φ_{Ox}^{app} value of 4.4 at pH 6.5 was reported, which was much larger than the value in this study (0.55 at pH 6). The reason for this discrepancy is unclear.

In the presence of *tert*-butanol (50 mM), the decomposition rates of HOCl and OCl^- were similar to those in the organic compound-free experiments, while the decomposition rates of HOBr and OBr^- increased by a factor of about two (Figure S1b and Table S1). *Tert*-butanol can effectively terminate the radical chain reaction by converting the primary radicals ($^{\bullet}OH$ and $X^{\bullet}$) to non-radical products (SI-

Text-5), which is consistent with the small difference in the oxidant decomposition rate in the presence of *tert*-butanol. In the presence of methanol (50 mM), the decomposition rates of all halogen oxidant species except OCl^- increased substantially, by a factor of 90 for OBr^-, 67 for HOCl, and 10 for HOBr. The decomposition rate of OCl^- increased marginally by a factor of 1.6 (Figure S1c, Table S1). The reactions of $^{\bullet}OH$ and $X^{\bullet}$ with methanol efficiently produce $O_2^{\bullet-}$ via peroxyl radical chemistry.[12] As $O_2^{\bullet-}$ rapidly reacts with HOCl, HOBr, and OBr^- generating $^{\bullet}OH$ or $X^{\bullet}$, a radical-chain reaction can be initiated with $^{\bullet}OH/X^{\bullet}$ and $O_2^{\bullet-}$ as the chain carrier. By contrast, the reaction of $O_2^{\bullet-}$ with OCl^- is known to be slow. The chemistry in the UV/halogen oxidant/methanol system is also discussed below (SI-Text-5). Overall, our results indicate that the generation of $O_2^{\bullet-}$ by dissolved organic matter (DOM) from its reaction with $^{\bullet}OH/X^{\bullet}$ (e.g., no $O_2^{\bullet-}$ from *tert*-butanol-type DOM versus facile $O_2^{\bullet-}$ formation from methanol-type DOM) is important for the oxidant decomposition rates and consequent radical generation during water treatment applications of UV/halogen oxidant systems. Similar DOM-involved radical chain reaction has also been shown to be important for the decomposition of ozone and consequent $^{\bullet}OH$ formation.[13] Further investigation is needed to better understand the impact of organic compounds with more diverse functional groups and real DOM on the chemistry of UV/halogen oxidant systems.

SI-Text-5. Chemistry of the UV/chlorine and UV/bromine systems in the presence of excess *tert*-butanol or methanol

Tert-Butanol. To determine the total yield of primary radicals in the UV/chlorine and UV/bromine system, a radical scavenging assay was performed using *tert*-butanol. In the presence of excess *tert*-butanol, the primary radicals generated from UV photolysis of chlorine ($^{\bullet}OH$ and $Cl^{\bullet}$) and bromine ($^{\bullet}OH$) can be fully scavenged by *tert*-butanol. The $Br^{\bullet}$ in UV/bromine system is found to be partially

scavenged by *tert*-butanol (see SI-Text-6 for the details). The reaction of the primary radicals with *tert*-butanol generates secondary radicals/products, including formaldehyde. Thus, the yields of the primary radicals in the UV/chlorine and UV/bromine systems can be determined by measuring formaldehyde formation. Here, the chemistry of the UV/chlorine and UV/bromine systems with excess *tert*-butanol is described.

The reaction of $^{\bullet}OH$ with *tert*-butanol in an oxygenated aqueous solution produces 2-methyl-2-hydroxypropyl radicals and $^{\bullet}CH_2(CH_3)_2COH$ (Equation S2).[14,15] $Cl^{\bullet}$ also reacts rapidly with *tert*-butanol, forming $^{\bullet}CH_2(CH_3)_2COH$ (Equation S3).[16] $Br^{\bullet}$ can also react with *tert*-butanol to produce $^{\bullet}CH_2(CH_3)_2COH$ (Equation S4).[17] The formed $^{\bullet}CH_2(CH_3)_2COH$ reacts rapidly with O_2, forming the peroxyl radical $^{\bullet}OOCH_2(CH_3)_2COH$ (Equation S5).[14,15] The $^{\bullet}OOCH_2(CH_3)_2COH$ mainly decays bi-molecularly and decomposes into H_2O_2, CH_2O, and other oxygenated organic compounds (Equation S6).[14,15,18] In a radiolytic system saturated with a N_2O/O_2 (80/20 v/v) mixture, the molar yields of H_2O_2 and CH_2O were 0.38 and 0.25 per $^{\bullet}OH$, respectively.[15,18] $O_2^{\bullet-}$ ($HO_2^{\bullet}$) is also formed at a low yield (a molar yield of less than 0.05 per $^{\bullet}OH$).[19] Overall, the reaction of $^{\bullet}OH$ with *tert*-butanol produces mostly non-radical products, leading to effective termination of the radical reactions. Nevertheless, the formation of $O_2^{\bullet-}$, despite its low yield, can lead to some additional decomposition of the halogen oxidant species, as $O_2^{\bullet-}$ reacts rapidly with HOCl, HOBr, and OBr^- (see below the methanol section). The reaction of H_2O_2 with chlorine/bromine is rapid and produces O_2 and Cl^-/Br^- (Equations S7 and S8).[20,21] Thus, the apparent quantum yields in the *tert*-butanol system should also account for the reaction of the halogen oxidants with H_2O_2.

$$^{\bullet}OH + (CH_3)_3COH \rightarrow H_2O + {}^{\bullet}CH_2(CH_3)_2COH \qquad k = 6\times10^8\ M^{-1}s^{-1}\ [14,15] \qquad (S2)$$

$$Cl^{\bullet} + (CH_3)_3COH \rightarrow Cl^- + {}^{\bullet}CH_2(CH_3)_2COH \qquad k = 1.5\times10^9\ M^{-1}s^{-1}\ [16] \qquad (S3)$$

$$Br^{\bullet} + (CH_3)_3COH \rightarrow Br^- + {}^{\bullet}CH_2(CH_3)_2COH \qquad k = 1.4\times10^4\ M^{-1}s^{-1}\ [17] \qquad (S4)$$

$^{\bullet}CH_2(CH_3)_2COH + O_2 \rightarrow {}^{\bullet}OOCH_2(CH_3)_2COH \quad k = 1.4\times10^9\ M^{-1}s^{-1}$ [14,15] (S5)

$2\,{}^{\bullet}OOCH_2(CH_3)_2COH \rightarrow \rightarrow H_2O_2 + CH_2O +$ oxygenated organic products (S6)

$HO_2^- + HOCl \rightarrow O_2 + H_2O + Cl^- \quad k = 4.4\times10^7\ M^{-1}s^{-1}$ [20] (S7)

$HO_2^- + HOBr \rightarrow O_2 + H_2O + Br^- \quad k = 7.6\times10^8\ M^{-1}s^{-1}$ [21] (S8)

Methanol. The results in the presence of methanol could be explained by scavenging of $^{\bullet}OH$ and $X^{\bullet}$ by methanol, subsequent formation of secondary radicals or products, and the reaction of secondary radicals/products with the halogen oxidant species to different extents depending on the oxidant species. The reactions of $^{\bullet}OH$ and $Cl^{\bullet}$ with methanol are rapid and produce $^{\bullet}CH_2OH$ (Equations S9 and S10),[17] while the reaction of $Br^{\bullet}$ with methanol is relatively slow (Equation S11).[17] The formed $^{\bullet}CH_2OH$ reacts rapidly with O_2 to generate the peroxyl radical $^{\bullet}OOCH_2OH$. The reaction of $^{\bullet}CH_2OH$ with the halogen oxidant is negligible, considering the high rate of Equation S12 and high relative concentration of O_2 (~0.25 mM) compared with the halogen oxidant (0.14 mM).[12] $^{\bullet}OOCH_2OH$ is known to quickly decompose to $O_2^{\bullet-}$ and CH_2O ($k > 10^3\ s^{-1}$ at pH ≥ 6, Equation S13).[12] The $^{\bullet}OOCH_2OH$ can also decay via a bimolecular reaction, which produces formic acid and H_2O_2 (Equation S14).[22] However, the yield of formic acid was less than ~3% that of CH_2O (data not shown), indicating that bimolecular decay of $^{\bullet}OOCH_2OH$ was insignificant in our reaction system.

$^{\bullet}OH + CH_3OH \rightarrow H_2O + {}^{\bullet}CH_2OH \quad k = 9\times10^8\ M^{-1}s^{-1}$ [17] (S9)

$Cl^{\bullet} + CH_3OH \rightarrow Cl^- + {}^{\bullet}CH_2OH + H^+ \quad k = 1.0\times10^9\ M^{-1}s^{-1}$ [17] (S10)

$Br^{\bullet} + CH_3OH \rightarrow Br^- + {}^{\bullet}CH_2OH + H^+ \quad k = 3.5\times10^5\ M^{-1}s^{-1}$ [17] (S11)

$^{\bullet}CH_2OH + O_2 \rightarrow {}^{\bullet}OOCH_2OH \quad k = 4.2\times10^9\ M^{-1}s^{-1}$ [12] (S12)

$^{\bullet}OOCH_2OH \rightarrow O_2^{\bullet-} + CH_2O + H^+ \quad k > 10^3\ s^{-1}$ at pH ≥ 6 [12] (S13)

$2\,{}^{\bullet}OOCH_2OH \rightarrow 2HCO_2H + H_2O_2 \quad k = 2.1\times10^9\ M^{-1}s^{-1}$ [22] (S14)

The reaction of $O_2^{\bullet-}$ with HOCl is rapid ($k = 7.5\times10^6\ M^{-1}s^{-1}$) and known to produce O_2, Cl^-, and

•OH (Equation S15) while the reaction of $O_2^{\bullet-}$ with OCl^- is slow and insignificant.[23,24] The reaction of $O_2^{\bullet-}$ with HOBr is rapid ($k = 3.5\times10^9$ $M^{-1}s^{-1}$) and produces O_2, OH^-, and Br• (Equation S16).[25] For the reaction of $O_2^{\bullet-}$ with OBr^- (Equation S17), a k value of 2×10^8 $M^{-1}s^{-1}$ has been reported as an upper limit.[25] Thermodynamic calculations have shown that the formation of •OH is favored over the formation of Cl• (Equation S15), while the formation of Br• is favored over the formation of •OH (Equation S16) at near-neutral pH.[26] A radical chain reaction is initiated when •OH, Cl•, and Br• react further with methanol. This explains the high quantum yields observed for the decomposition of HOCl, HOBr, and OBr^- in the presence of methanol. The poor reactivity of $O_2^{\bullet-}$ with OCl^- is also consistent with the much lower quantum yield obtained for OCl^-. For the OCl^- system, the reaction of $O_2^{\bullet-}$ with $^{\bullet}OOCH_2OH$ (Equation S18)[12] or the bimolecular reactions of $^{\bullet}OOCH_2OH$ (Equation S14) may quickly terminate the radical chain reactions. These radical chain reactions led to high quantum yields.

$$O_2^{\bullet-} + HOCl \rightarrow O_2 + {}^{\bullet}OH + Cl^- \qquad k = 7.5\times10^6\ M^{-1}s^{-1}\ [23,24] \qquad \text{(S15)}$$

$$O_2^{\bullet-} + HOBr \rightarrow O_2 + OH^- + Br^{\bullet} \qquad k = 3.5\times10^9\ M^{-1}s^{-1}\ [25] \qquad \text{(S16)}$$

$$O_2^{\bullet-} + OBr^- + H^+ \rightarrow O_2 + OH^- + Br^{\bullet} \qquad k < 2\times10^8\ M^{-1}s^{-1}\ [25] \qquad \text{(S17)}$$

$$O_2^{\bullet-} + {}^{\bullet}OOCH_2OH \rightarrow O_2 + HOOCH_2OH \qquad k \approx 10^7\ M^{-1}s^{-1}\ [12] \qquad \text{(S18)}$$

SI-Text-6. Kinetics modeling of the UV/halogen oxidant systems in the absence and presence of *tert*-butanol

The UV/chlorine and UV/bromine systems were kinetically modeled using the chemical kinetics simulation software Kintecus® 6.51.[27] The model was based on the key kinetic information from this study, such as the intrinsic quantum yield of radical formation (Table S2) and the rate constants of •OH reactions with chlorine species and information available in the literature. A preliminary kinetic model was developed containing all of the relevant reactions found in the literature for UV/chlorine and

UV/bromine. The preliminary kinetic model was analyzed by Atropos© 1.20,[28] to identify significant reactions based on sensitivity analysis. Table S3 and Table S4 summarize the reactions used in the final versions of the UV/chlorine and UV/bromine systems, respectively. Table S5 shows a list of reactions excluded from the final version of the kinetic model due to their relatively less contribution. The reactions of phosphate species (used as a buffer) with radicals (e.g., HPO_4^{2-} + $^{\bullet}OH$ → products, k = 1.5×10^5 $M^{-1}s^{-1}$)[29] were also excluded from the final kinetic model due to their negligible contribution. The kinetic model comprised of sub-set reactions such as 'photolysis of chlorine/bromine species', 'reactions of oxygen atoms ($O(^1D)$ and $O(^3P)$)', 'formation of hydrogen peroxide (H_2O_2) and ozone (O_3) and their decomposition', 'reactions of $^{\bullet}OH$ and $X^{\bullet}$ with chlorine/bromine species and $XO^{\bullet}$ formation', 'reactions of $^{\bullet}OH$ with X^-', 'reactions of chlorine/bromine species with peroxyl radicals ($HO_2^{\bullet}$ and $O_2^{\bullet-}$)', 'reactions of $XO^{\bullet}$ and formation XO_3^-', 'reactions of reactive species with probe compounds', 'reactions of $^{\bullet}OH$ and $X^{\bullet}$ with *tert*-butanol' and 'equilibrium reactions of chlorine/bromine species, $^{\bullet}OH$, $HO_2^{\bullet}$, H_2O_2, and probe compounds'.

It has been shown that the photolysis of OCl^- also produces $O(^1D)$ ($OCl^- \xrightarrow{h\nu} Cl^- + O(^1D)$) and $O(^3P)$ ($OCl^- \xrightarrow{h\nu} Cl^- + O(^3P)$) with quantum yields of 0.133 and 0.074 at 254 nm.[30] $O(^1D)$ is very rapidly converted into H_2O_2 (and some $^{\bullet}OH$) in aqueous solution,[31] and the formed H_2O_2 (HO_2^-) is expected to react rapidly with HOCl, forming O_2 and Cl^- in the UV/chlorine system (Equations S7).[20]

$O(^3P)$ can react with O_2 to form O_3 or react with OCl^- to form ClO_2 or Cl^- and O_2.[32,33] O_3 can react with OCl^-, forming O_2 and Cl^- or O_2 and ClO_2^- via two separate pathways.[34] The O_3 formation in UVA photolysis of chlorine has been shown to enhance the degradation of O_3-reactive contaminants and the inactivation of protozoan microorganisms.[35,36] The inclusion of the $O(^1D)$ and $O(^3P)$ formation pathways in our UV/chlorine kinetics model had little effect on the predicted $^{\bullet}OH$ concentration and ClO_3^- formation; however, this could affect the chlorine decomposition rate, especially at basic pH

values. This is because the $O(^1D)$ and $O(^3P)$ are mainly converted into H_2O_2 and O_3, respectively, and the H_2O_2 and O_3 are mainly consumed by chlorine generating non-radical products such as Cl^- and O_2. The photolysis of ClO_2^- was also found to be unimportant for the fate of ClO_2^- due to the rapid oxidation of ClO_2^- by $ClO^•$.

The photolysis of OBr^- has been shown to produce negligible O_3 at pH below 10, indicating little $O(^3P)$ formation.[32] The O_3 formation from the photolysis of OBr^- at pH above 12 has been attributed to the formation of $O^{•-}$ as the primary radical product which subsequently reacts with O_2 forming $O_3^{•-}$. The reaction of $O_3^{•-}$ with $Br^•$, the latter as another primary radical product, produces O_3 and Br^-.[32] Our separate experiments also showed negligible O_3 formation from the photolysis (254 nm) of bromine species (140 μM) at pH 8 (5 mM phosphate buffer), in which the O_3 formation was checked by reacting the photolyzed bromine samples with cinnamic acid (50 μM) and quantifying the benzaldehyde formation, using the similar method reported in previous study.[36,37] Overall, our UV/bromine kinetics model did not include the oxygen atom formation from the photolysis of bromine species.

The UV/bromine system in this study contained some level of Cl^- (e.g., ~140 μM) as the bromine stock was prepared by reacting OCl^- with Br^- at ~1:1 stoichiometric ratio (i.e., $OCl^- + Br^- \rightarrow OBr^- + Cl^-$). In the presence of Cl^-, mixed halogen species such as $BrCl^{•-}$ can be formed in UV/bromine system from the reaction of $Br^•$ with Cl^- ($Br^• + Cl^- \rightarrow BrCl^{•-}$, $k = 1\times10^8$ $M^{-1}s^{-1}$ [38]). Nevertheless, the sensitivity analysis showed that the formation of $BrCl^{•-}$ and its further reaction pathways were insignificant in our UV/bromine system containing low level of Cl^- (140 μM). In addition, the kinetic modeling of UV/bromine system considering the formation and reactions of $BrCl^{•-}$ did not affect the bromine decomposition and BrO_3^- formation, indicating negligible role of $BrCl^{•-}$. Overall, the formation and reactions of $BrCl^{•-}$ were excluded from the final version of the UV/bromine kinetic model.

In the presence of *tert*-butanol (50 mM), $^{\bullet}OH$ and $^{\bullet}Cl$ formed from the UV photolysis of chlorine species and $^{\bullet}OH$ from the UV photolysis of bromine species can be fully scavenged by *tert*-butanol. However, $Br^{\bullet}$ formed from the photolysis of bromine species is not fully scavenged by *tert*-butanol due to the relative low reactivity of $Br^{\bullet}$ toward *tert*-butanol (Equation S4). Using the UV/bromine/*tert*-butanol kinetic model (Table S4), the % reaction pathways of $Br^{\bullet}$ could be assessed quantitatively. At pH 6, 46% of the $Br^{\bullet}$ was scavenged by *tert*-butanol (50 mM) and 41% of the $Br^{\bullet}$ was consumed by its reaction with bromine. The remaining 13% of the $Br^{\bullet}$ reacted with H_2O and OH^-, and was converted into $^{\bullet}OH$ and $Br^{\bullet}$ via $BrOH^{\bullet-}$ as an intermediate with a branching ratio of 89% ($BrOH^{\bullet-} \rightarrow Br^- + {}^{\bullet}OH$, $k = 3.3\times10^7\ s^{-1}$ [39]) and 11% ($BrOH^{\bullet-} \rightarrow Br^{\bullet} + OH^-$, $k = 4.0\times10^6\ s^{-1}$ [39]), respectively. The $^{\bullet}OH$ from the $BrOH^{\bullet-}$ intermediate could then be fully scavenged by *tert*-butanol, while the $Br^{\bullet}$ from the $BrOH^{\bullet-}$ intermediate followed again the reaction pathways described above. Overall, it was estimated that at pH 6, 58% of the $Br^{\bullet}$ was scavenged by *tert*-butanol directly or indirectly after its conversion to $^{\bullet}OH$, and 42% of the $Br^{\bullet}$ was consumed by bromine. At pH 10, 74% of the $Br^{\bullet}$ reacted with water due to the high reactivity of $Br^{\bullet}$ with OH^- ($Br^{\bullet} + OH^- \rightarrow BrOH^{\bullet-}$, $k = 1.3\times10^{10}\ M^{-1}s^{-1}$ [40]). Thus, significant fraction of the $Br^{\bullet}$ was converted into $^{\bullet}OH$ and then scavenged by *tert*-butanol, although direct scavenging of $Br^{\bullet}$ by *tert*-butanol was negligible at pH 10. Overall, it was estimated that 72% of the $Br^{\bullet}$ was scavenged indirectly by *tert*-butanol via $^{\bullet}OH$, and 28% of the $Br^{\bullet}$ was consumed by bromine at pH 10. Despite the incomplete scavenging of $Br^{\bullet}$ by *tert*-butanol, however, the UV/bromine/*tert*-butanol kinetic model could be used to determine the intrinsic quantum yields for bromine species as the model could consider all the reaction pathways of $Br^{\bullet}$ in this system.

SI-Text-7. Determination of *k* for the reaction of •OH with nitrobenzene

The second-order rate constant for the reaction of •OH with nitrobenzene ($k_{\bullet OH,NB}$) was determined by a competition kinetics method.[41] The second-order rate constant for the reaction of •OH with target ($k_{\bullet OH(tar)}$) and reference compounds ($k_{\bullet OH(ref)}$) are related as expressed in Equation S19.

$$k_{\bullet OH(tar)} = \frac{k'_{tar}}{k'_{ref}} \times k_{\bullet OH(ref)} = \frac{\ln([tar]/[tar]_0)}{\ln([ref]/[ref]_0)} \times k_{\bullet OH(ref)} \quad (S19)$$

Here, k'_{tar} and k'_{ref} are the apparent first-order degradation rate constants of the target and reference compounds for •OH. When using UV/H_2O_2 as a source of •OH, degradation of the target and reference compounds can also be achieved by direct UV photolysis. Thus, the degradation of target compounds by direct UV photolysis needs to be corrected using Equation S20. The same correction can also be applied to the reference compound.

$$k'_{tar} = k'_{UV/H_2O_2(tar)} - \left[\frac{E_{UV/H_2O_2}}{E_{UV}}\right] \times k'_{UV(tar)} \qquad k'_{ref} = k'_{UV/H_2O_2(ref)} - \left[\frac{E_{UV/H_2O_2}}{E_{UV}}\right] \times k'_{UV(ref)} \quad (S20)$$

Here, k'_{UV/H_2O_2} and k'_{UV} are the apparent first-order degradation rate constants in UV/H_2O_2 and UV systems, respectively, and E_{UV/H_2O_2} and E_{UV} represent the average UV fluence rates in UV/H_2O_2 and UV systems, respectively. Inserting Equation S20 for the target and reference compound into Equation S19 can result in Equation S21.

$$k_{\bullet OH(tar)} = \frac{k'_{obs(tar)} - \left[\frac{E_{UV/H_2O_2}}{E_{UV}}\right] \times k'_{UV(tar)}}{k'_{obs(ref)} - \left[\frac{E_{UV/H_2O_2}}{E_{UV}}\right] \times k'_{UV(ref)}} \times k_{\bullet OH(ref)} \quad (S21)$$

In this study, benzoic acid (BA) was used as the reference compound, as its reactivity toward •OH is well characterized ($k_{\bullet OH,BA} = 5.9\times10^9$ $M^{-1}s^{-1}$).[42] Figure S4 shows the results for BA and NB competition kinetics, from which the •OH reaction rate constant for NB was determined as $3.8(\pm0.2)\times10^9$ $M^{-1}s^{-1}$.

SI-Text-8. Determination of the rate constants for the reaction of •OH and Cl• with HOCl and OCl^-

The second-order rate constants for the reactions of •OH with HOCl and OCl^- were determined by a competition kinetics method with NB as the •OH probe and *tert*-butanol as the •OH scavenger. The kinetic equation for NB degradation was used for the competition kinetics plot, and its derivation is provided here. The apparent first-order degradation rate constant of NB by •OH in the UV/chlorine system (k'_{NB}) can be expressed as shown in Equation S22,

$$k'_{NB} = (k'_{NB,UV/chlorine} - k'_{NB,UV}) = k_{\bullet OH,NB}[\bullet OH]_{ss} \quad (S22)$$

where $k'_{NB,UV/chlorine}$ is the apparent first-order degradation rate constant of NB in UV/chlorine, $k'_{NB,UV}$ is the first-order degradation rate constant of NB in UV (i.e., the direct UV photolysis rate constant), and $k_{\bullet OH,NB}$ is the second-order rate constant for the reaction of •OH with NB. $[\bullet OH]_{ss}$ in Equation S22 can be expressed as Equation S23.

$$[\bullet OH]_{ss} = \frac{R^{form}_{\bullet OH}}{\Sigma k_{\bullet OH,Si}[S]_i}$$

$$= \frac{R^{form}_{\bullet OH}}{k_{\bullet OH,HOCl}[HOCl]+k_{\bullet OH,OCl^-}[OCl^-]+k_{\bullet OH,NB}[NB]+k_{\bullet OH,BA}[BA]+k_{\bullet OH,t\text{-}BuOH}[t\text{-}BuOH]} \quad (S23)$$

Here, $R^{form}_{\bullet OH}$ is the •OH formation rate from the chlorine photolysis (M s^{-1}) and $\Sigma k_{\bullet OH,Si}[S]_i$ is the sum of the •OH scavenging rates by the water matrix components in the system.

Substituting Equation S23 into S22 and inverting the resulting equation yields Equation S24, which shows that the inverse of k'_{NB} is linearly related to the concentration of *tert*-butanol (*t*-BuOH).

$$\frac{1}{k'_{NB}} = \frac{k_{\bullet OH,HOCl}[HOCl]+k_{\bullet OH,OCl^-}[OCl^-]+k_{\bullet OH,NB}[NB]+k_{\bullet OH,BA}[BA]}{R^{form}_{\bullet OH}k_{\bullet OH,NB}} + \frac{k_{\bullet OH,t\text{-}BuOH}[t\text{-}BuOH]}{R^{form}_{\bullet OH}k_{\bullet OH,NB}} \quad (S24)$$

The slope ($= \frac{k_{\bullet OH,t\text{-}BuOH}}{R^{form}_{\bullet OH}k_{\bullet OH,NB}}$) and y-intercept ($= \frac{k_{\bullet OH,HOCl}[HOCl]+k_{\bullet OH,OCl^-}[OCl^-]+k_{\bullet OH,NB}[NB]}{R^{form}_{\bullet OH}k_{\bullet OH,NB}}$) of Equation

S24 can be obtained from the experimental $\frac{1}{k'_{NB}}$ determined as a function of [*t*-BuOH]. The $R_{\bullet OH}^{form}$ value can then be calculated from the values of the slope, $k_{\bullet OH,NB}$ (= 3.8×10^9 $M^{-1}s^{-1}$), and $k_{\bullet OH,t\text{-}BuOH}$ (= 6×10^8 $M^{-1}s^{-1}$). In turn, from the y-intercept, $R_{\bullet OH}^{form}$, $k_{\bullet OH,NB}$, and $k_{\bullet OH,BA}$, the $^\bullet$OH consumption rate by chlorine species ($=k_{\bullet OH,HOCl}[HOCl]+k_{\bullet OH,OCl^-}[OCl^-]$) can be obtained.

Figure S7a shows the competition kinetics plot based on Equation S24 for the data obtained at pH 5, where HOCl is the dominant species. The original kinetic data are shown in Figure S5a. From the slope and *y*-intercept of the plot, the apparent rate constant for the reaction of $^\bullet$OH with chlorine species ($k_{\bullet OH,Chlorine}^{app}$) at pH 5 was determined as $1.4(\pm0.2)\times10^8$ $M^{-1}s^{-1}$. The same experiment was conducted at pH 6 (shown in Figure S6a), and a $k_{\bullet OH,Chlorine}^{app}$ value of $1.9(\pm0.3)\times10^8$ $M^{-1}s^{-1}$ was determined. The $k_{\bullet OH,Chlorine}^{app}$ value can be expressed as Equation S25, where α_{HOCl} is the fraction of HOCl at a given pH value ($[HOCl]/([HOCl]+[OCl^-]) = [H^+]/([H^+]+K_{a,HOCl})$). Although the fraction of OCl^- at pH 6 was only 3%, the $^\bullet$OH scavenging effect of OCl^- could not be ignored because its reactivity toward $^\bullet$OH is much higher than that of HOCl. At pH 6, HOCl and OCl^- accounted for 69% and 31% of the $^\bullet$OH scavenging rate, respectively.

$$k_{\bullet OH,Chlorine}^{app} = \alpha_{HOCl}k_{\bullet OH,HOCl} + (1-\alpha_{HOCl})k_{\bullet OH,OCl^-} \quad \text{(S25)}$$

Using Equation S25 and the $k_{\bullet OH,Chlorine}^{app}$ values at pH 5 and pH 6, the $k_{\bullet OH,HOCl}$ and $k_{\bullet OH,OCl^-}$ values for Equations S26 and S27 were determined as $1.4(\pm0.2)\times10^8$ and $2.0(\pm0.5)\times10^9$ $M^{-1}s^{-1}$, respectively.

$$^\bullet OH + HOCl \rightarrow ClO^\bullet + H_2O \qquad k_{\bullet OH,HOCl} = 1.4\times10^8\ M^{-1}s^{-1} \quad \text{(S26)}$$

$$^\bullet OH + OCl^- \rightarrow ClO^\bullet + OH^- \qquad k_{\bullet OH,OCl^-} = 2.0\times10^9\ M^{-1}s^{-1} \quad \text{(S27)}$$

The second-order rate constants for the reaction of $Cl^\bullet$ with HOCl and OCl^- were determined by a competition kinetics method, with BA as a probe for both $^\bullet$OH and $Cl^\bullet$. The kinetic equation for BA

degradation was used for the competition kinetics plot, and its derivation is provided here. The apparent first-order degradation rate constant of BA with •OH and Cl• in the UV/chlorine system (k'_{BA}) can be expressed as Equation S28,

$$k'_{BA} = (k'_{BA,UV/chlorine} - k'_{BA,UV}) = k_{•OH,BA}[•OH]_{ss} + k_{Cl•,BA}[Cl•]_{ss} \quad (S28)$$

where $k'_{BA,UV/chlorine}$ is the apparent first-order degradation rate constant of BA in UV/chlorine; $k'_{BA,UV}$ is the first-order degradation rate constant of BA in UV (i.e., the direct UV photolysis rate constant); and $k_{•OH,BA}$ and $k_{Cl•,BA}$ are the second-order rate constants for the reaction of •OH and Cl• with BA, respectively. $[Cl•]_{ss}$ can be expressed as Equation S29.

$$[Cl•]_{ss} = \frac{R^{form}_{Cl•}}{\Sigma k_{Cl•,Si}[S]_i} = \frac{R^{form}_{Cl•}}{k_{Cl•,HOCl}[HOCl]+k_{Cl•,OCl^-}[OCl^-]+k_{Cl•,BA}[BA]+k_{Cl•,t\text{-BuOH}}[t\text{-BuOH}]} \quad (S29)$$

Here, $R^{form}_{Cl•}$ is the Cl• formation rate from the chlorine photolysis (M s^{-1}) and $\Sigma k_{Cl•,Si}[S]_i$ is the sum of the Cl• scavenging rates by the water matrix components in the system.

Substituting Equation S29 into Equation S28 and inverting the resulting equation yields Equation S30, which shows that the inverse of $(k'_{BA} - k_{•OH,BA}[•OH]_{ss})$ is linearly related to the concentration of *tert*-butanol ([*t*-BuOH]). The slope and y-intercept of Equation S30 can be determined from the experimental kinetics data of NB and BA in the UV/chlorine system. From the slope and y-intercept of the plot, the •Cl consumption rate by chlorine species ($=k_{Cl•,HOCl}[HOCl]+k_{Cl•,OCl^-}[OCl^-]$) can be obtained.

$$\frac{1}{k'_{BA} - k_{•OH,BA}[•OH]_{ss}} = \frac{k_{Cl•,HOCl}[HOCl]+k_{Cl•,OCl^-}[OCl^-]+k_{Cl•,BA}[BA]}{R^{form}_{Cl•}k_{Cl•,BA}} + \frac{k_{Cl•,t\text{-BuOH}}[t\text{-BuOH}]}{R^{form}_{Cl•}k_{Cl•,BA}} \quad (S30)$$

in which k'_{BA} is the apparent first-order degradation rate constant of BA by •OH and Cl•.

Figure S7b shows the competition kinetics plot based on Equation S30 for the data obtained at pH 5 (shown in Figure S5b) and pH 6 (shown in Figure S6b). From the slope and y-intercept of the plots, the apparent rate constants for the reaction of Cl• with chlorine species ($k^{app}_{Cl•,Chlorine}$) were determined

as 3.0(±0.2)×10^9 M^{-1}s^{-1} and 3.2(±0.1)×10^9 M^{-1}s^{-1} at pH 5 and pH 6, respectively. Finally, the $k_{Cl^\bullet,HOCl}$ and $k_{Cl^\bullet,OCl^-}$ values for Equations S31 and S32 were determined as 3.0(±0.3)×10^9 and 1.0(±0.5)×10^{10} M^{-1}s^{-1}, respectively, using Equation S33 and the obtained $k^{app}_{Cl^\bullet,Chlorine}$ values.

$$Cl^\bullet + HOCl \rightarrow ClO^\bullet + H^+ + Cl^- \qquad k_{Cl^\bullet,HOCl} = 3.0\times10^9\ M^{-1}s^{-1} \tag{S31}$$

$$Cl^\bullet + OCl^- \rightarrow ClO^\bullet + Cl^- \qquad k_{Cl^\bullet,OCl^-} = 1.0\times10^{10}\ M^{-1}s^{-1} \tag{S32}$$

$$k^{app}_{Cl^\bullet,Chlorine} = \alpha_{HOCl}k_{Cl^\bullet,HOCl} + (1-\alpha_{HOCl})k_{Cl^\bullet,OCl^-} \tag{S33}$$

SI-Text-9. Chemistry of $ClO^\bullet$ leading to ClO_3^- formation in the UV/chlorine system

The fate of $ClO^\bullet$ in the UV/chlorine system was investigated by measuring the evolution of HOCl/OCl^-, Cl^-, ClO_2^-, and ClO_3^-. In the organic compound-free system, Cl^- and ClO_3^- were the major products from decomposition of HOCl/OCl^- (Figure S11a and S11b). Formation of ClO_2^- was negligible and below 1% of the initial chlorine concentration. This result was expected considering that the fast reactions of ClO_2^- with radicals such as $^\bullet$OH and $ClO^\bullet$ led to ClO_3^- formation. ClO_4^- was not detected, indicating that further oxidation of ClO_3^- was negligible.

$ClO^\bullet$ is known to dimerize and form Cl_2O_2 as a transient intermediate (Equation S34).[40] Cl_2O_2 quickly decomposed to OCl^- and ClO_2^- (Equation S35)[43] or Cl^-, OCl^-, and O_2 (Equation S36).[30] The former pathway is the only one that generates ClO_2^- for further oxidation to $ClO_2^\bullet$ and then ClO_3^-. The ratio between the reaction rate constants for the formation of ClO_2^- and Cl^- from the decomposition of Cl_2O_2 was calculated to be 1.93 ± 0.24 by Buxton and Subhani.[30] Using this ratio, the rate constant for Equation S36 was calculated as 5.18×10^3 s^{-1} ($k_{36} = k_{35}/1.93$). ClO_2^- in the UV/chlorine system can be oxidized by several oxidizing species such as $^\bullet$OH, $Cl^\bullet$, and $ClO^\bullet$. Our kinetic model showed that $ClO^\bullet$ was mainly responsible for the oxidation of ClO_2^- (Equation S37),[44] and the contributions of $^\bullet$OH and $Cl^\bullet$ to ClO_2^- oxidation were negligible (Equations S38 and S39). Despite the high reaction rates

for Equations S38 and S39,[45,46] the concentrations of $^{\bullet}OH$ and $Cl^{\bullet}$ were too low to compete with $ClO^{\bullet}$ for reaction with ClO_2^- (see Table S9). Similar to ClO_2^-, $ClO_2^{\bullet}$ can be oxidized by $^{\bullet}OH$, $Cl^{\bullet}$, and $ClO^{\bullet}$. However, the oxidation of $ClO_2^{\bullet}$ by $ClO^{\bullet}$ has not been considered in previous UV/chlorine kinetic models found in the literature.[37,45,47-51] The reaction of $ClO_2^{\bullet}$ with $ClO^{\bullet}$ to form ClO_3^- and OCl^- via Cl_2O_3 as a transient intermediate (Equations S40 and S41) has been proposed in an earlier study, but the rate constants for these reactions are unknown.[43] In a later study,[52] rate constants for these reactions were estimated to be $7.4\times10^9\ M^{-1}s^{-1}$ for Equation S40 and $10^4\ s^{-1}$ for Equation S41. When Equations S40 and S41 were included, the UV/chlorine kinetics model gave a good simulation of the ClO_3^- experimental data (Figure S12). The simulation showed that as long as the k of Equation S40 was larger than $1\times10^9\ M^{-1}s^{-1}$ and the k of Equation S41 was larger than $0.1\ s^{-1}$, the predicted ClO_3^- formation showed little difference. In the final version of the UV/chlorine kinetics model, k values of $7.4\times10^9\ M^{-1}s^{-1}$ and $10^4\ s^{-1}$ were used for Equations S40 and S41, respectively. Finally, the oxidation of $ClO_2^{\bullet}$ by $^{\bullet}OH$ and $Cl^{\bullet}$ was negligible according to the model sensitivity analysis.

$$2ClO^{\bullet} \rightarrow Cl_2O_2 \qquad k = 2.5\times10^9\ M^{-1}s^{-1}\ [40] \qquad \text{(S34)}$$

$$Cl_2O_2 + H_2O \rightarrow OCl^- + ClO_2^- + 2H^+ \qquad k = 1.0\times10^4\ s^{-1}\ [43] \qquad \text{(S35)}$$

$$Cl_2O_2 + H_2O \rightarrow Cl^- + O_2 + OCl^- + 2H^+ \qquad k = 5.18\times10^3\ s^{-1}\ [30,43] \qquad \text{(S36)}$$

$$ClO_2^- + ClO^{\bullet} \rightarrow ClO_2^{\bullet} + OCl^- \qquad k = 9.4\times10^8\ M^{-1}s^{-1}\ [44] \qquad \text{(S37)}$$

$$ClO_2^- + {}^{\bullet}OH \rightarrow ClO_2^{\bullet} + OH^- \qquad k = 7.0\times10^9\ M^{-1}s^{-1}\ [46] \qquad \text{(S38)}$$

$$ClO_2^- + Cl^{\bullet} \rightarrow ClO_2^{\bullet} + Cl^- \qquad k = 7.0\times10^9\ M^{-1}s^{-1}\ [45] \qquad \text{(S39)}$$

$$ClO_2^{\bullet} + ClO^{\bullet} \rightarrow Cl_2O_3 \qquad k = 7.4\times10^9\ M^{-1}s^{-1}\ [52] \qquad \text{(S40)}$$

$$Cl_2O_3 + H_2O \rightarrow ClO_3^- + OCl^- + 2H^+ \qquad k = 10^4\ s^{-1}\ [52] \qquad \text{(S41)}$$

SI-Text-10. Chemistry of $BrO^{\bullet}$ leading to BrO_3^- formation in the UV/bromine system

In the proposed formation pathway of BrO_3^- in this study, $BrO^{\bullet}$ can be dimerized and form OBr^- and BrO_2^- (Equation S42)[42] in a similar manner to ClO_2^- formation in the UV/chlorine system. BrO_2^- can be further oxidized by several oxidizing species such as $^{\bullet}OH$ and $BrO^{\bullet}$. Our kinetic model showed that $BrO^{\bullet}$ was mainly responsible for the oxidation of BrO_2^- (Equation S43),[42] and the contributions of $^{\bullet}OH$ to BrO_2^- oxidation were negligible (Equations S44).[42] Despite the high reaction rates for Equation S44, the concentrations of $^{\bullet}OH$ were too low to compete with $BrO^{\bullet}$ for reaction with BrO_2^- (see Table S9). The $BrO_2^{\bullet}$ can be dimerized and form Br_2O_4 as a transient intermediate (Equation S45).[53] Br_2O_4 quickly decomposed to BrO_3^- and BrO_2^- (Equation S46).[53] Because of the rapid dimerization of $BrO_2^{\bullet}$, the contributions of $^{\bullet}OH$ and $BrO^{\bullet}$ to the oxidation of $BrO_2^{\bullet}$ were negligible. This was different from the case for $ClO_2^{\bullet}$ where $ClO^{\bullet}$ was mainly responsible for the oxidation of $ClO_2^{\bullet}$ (Equation S40).

$$2BrO^{\bullet} + H_2O \rightarrow OBr^- + BrO_2^- + 2H^+ \qquad k = 5.0\times10^9\ M^{-1}s^{-1}\ [42] \qquad \text{(S42)}$$

$$BrO_2^- + BrO^{\bullet} \rightarrow BrO_2^{\bullet} + OBr^- \qquad k = 3.4\times10^8\ M^{-1}s^{-1}\ [42] \qquad \text{(S43)}$$

$$BrO_2^- + {}^{\bullet}OH \rightarrow BrO_2^{\bullet} + OH^- \qquad k = 1.9\times10^9\ M^{-1}s^{-1}\ [42] \qquad \text{(S44)}$$

$$BrO_2^{\bullet} + BrO_2^{\bullet} \rightarrow Br_2O_4 \qquad k = 1.4\times10^9\ M^{-1}s^{-1}\ [53] \qquad \text{(S45)}$$

$$Br_2O_4 + H_2O \rightarrow BrO_3^- + BrO_2^- + 2H^+ \qquad k = 2.2\times10^3\ s^{-1}\ [53] \qquad \text{(S46)}$$

SI-Text-11. Analysis of violation of the principle of detailed balancing in the UV/chlorine models

Different versions of UV/chlorine kinetic models have been developed and presented in literature. Table S7 summarizes the UV/chlorine kinetic models from this study and the literature, and individual reactions used in these models. It has been shown elsewhere that large kinetic models containing high numbers of individual reactions occasionally violate the principle of detailed balancing.[54-56] These

violations can occur in three ways: 1) disagreement of the ratio of the forward and reverse rate equations of an individual reaction step with the equilibrium expression, 2) disagreement of the equilibrium constants within a series of reversible steps (called a loop) based on the linear combination of the constants (loop violation), and 3) inclusion of irreversible steps in the loop that are unopposed by other irreversible steps (illegal loop). Here, we tried to check the different UV/chlorine models in terms of the violation of the principle of detailed balancing. For this purpose, DETBAL,[54] a software code that can automatically report reversible and illegal reaction loops based on the principle of detailed balancing[56] was applied. The following seven UV/chlorine models were checked with DETBAL, namely, the Bulman-model,[37] Chuang-model,[45] Fang-model,[47] Guo-model,[48] Li-model,[49] Sun-model,[50] and Wu-model.[51] At least one illegal loop was detected in each of the tested models. Eight, three, and two illegal loops were detected in the Bulman-, Sun-, and Guo-models, respectively. One illegal loop was detected in each of the Chuang-, Fang-, Li-, and Wu-models. The detected illegal loops (A–K) are describe further below.

Illegal loop A: Equation S47 + Equation S49 = Equation S48

$$Cl^{\bullet} + Cl^{-} \rightleftharpoons Cl_2^{\bullet -} \quad \text{(S47)}$$

$$Cl^{\bullet} + OH^{-} \rightarrow ClOH^{\bullet -} \quad \text{(S48)}$$

$$Cl_2^{\bullet -} + OH^{-} \rightleftharpoons ClOH^{\bullet -} + Cl^{-} \quad \text{(S49)}$$

Loop A was illegal because it contained a single irreversible reaction (Equation S48). This loop was found in six models (Bulman-, Chuang-, Fang-, Guo-, Li-, and Wu-models). The value for the reverse rate constant k_{S48r} could be calculated from the relationship $K_{S47}K_{S49} = k_{S48f}/k_{S48r}$. The result showed k_{S48r} values of 2.0×10^{1}, 3.0×10^{1}, 6.8×10^{2}, 2.8×10^{2}, 2.8×10^{1}, and 6.8×10^{2} s^{-1}, respectively. The reverse rate constant k_{S48r} has been reported in literature as 23 s^{-1}.[40]

Illegal loop B: Equation S50 + Equation S51 + Equation S52 = Equation S47 + Equation S49

$$HOCl + Cl^{-} + H^{+} \rightleftharpoons Cl_2 + H_2O \quad \text{(S50)}$$

$$Cl_2 + OH^- \rightarrow HOCl + Cl^- \quad \text{(S51)}$$

$$Cl^\bullet + H_2O \rightleftharpoons ClOH^{\bullet-} + H_+ \quad \text{(S52)}$$

$$Cl^\bullet + Cl^- \rightleftharpoons Cl_2^{\bullet-} \quad \text{(S47)}$$

$$Cl_2^{\bullet-} + OH^- \rightleftharpoons ClOH^{\bullet-} + Cl^- \quad \text{(S49)}$$

Loop B was illegal as it contained a single irreversible reaction (Equation S51), which was similar to the case of loop A. Illegal loop B was found in the Bulman- and Guo-models. The value for the reverse rate constant k_{S51r} could be calculated from the relationship $K_{S50}(k_{S51f}/k_{S51r})K_{S52} = K_{S47}K_{S49}$. As a result, $k_{S51r} = 1.1\times10^{-8}$ and 2.2×10^{-6} $M^{-1}s^{-1}$ were obtained.

Illegal loop C: Equation S53 + Equation S47 + Equation S49 = Equation S54

$$^\bullet OH + Cl^- \rightarrow Cl^\bullet + OH^- \quad \text{(S53)}$$

$$^\bullet OH + Cl^- \rightleftharpoons ClOH^{\bullet-} \quad \text{(S54)}$$

$$Cl^\bullet + Cl^- \rightleftharpoons Cl_2^{\bullet-} \quad \text{(S47)}$$

$$Cl_2^{\bullet-} + OH^- \rightleftharpoons ClOH^{\bullet-} + Cl^- \quad \text{(S49)}$$

Loop C was illegal because it contained a single irreversible reaction (Equation S53). Illegal loop C was found in the Bulman-model. The reverse rate constant, k_{S53r}, could be calculated from the relationship $(k_{S53f}/k_{S53r})K_{S47}K_{S49} = K_{S54}$, which yielded a k_{S53r} of 1.63×10^{18} $M^{-1}s^{-1}$. However, the obtained value far exceeded the diffusion-controlled reaction limit in aqueous solution (~10^{11} $M^{-1}s^{-1}$), indicating that the k_{S53r} value of 1.63×10^{18} $M^{-1}s^{-1}$ is impossible. Therefore, the loop C could not be repaired by applying the calculated reverse rate constant, k_{S53r}. This loop could be repaired by removing Equation S53.

Illegal loop D: Equation S55 + Equation S56 = Equation S57 + Equation S58 + Equation S59 + Equation S60

$$^\bullet OH + H_2 \rightleftharpoons H_2O + H^\bullet \quad \text{(S55)}$$

$HO_2^\bullet \rightleftharpoons H^+ + O_2^{\bullet-}$ (S56)

$HO_2^\bullet + H_2 \rightarrow H_2O_2 + H^\bullet$ (S57)

$^\bullet OH + H_3PO_4 \rightleftharpoons H_2PO_4^\bullet + H_2O$ (S58)

$H_2O_2 + H_2PO_4^\bullet \rightarrow H_2PO_4^- + 2H^+ + O_2^{\bullet-}$ (S59)

$H_2PO_4^- + H^+ \rightleftharpoons H_3PO_4$ (S60)

Loop D was illegal because it contained two irreversible reactions (Equations S57 and S59). Loop D was found in the Bulman-model. This loop could not be repaired since both the reverse rate constants k_{S57r} and k_{S59r} from the relationship $K_{S55}K_{S56} = (k_{S57f}/k_{S57r})K_{S58}(k_{S59f}/k_{S59r})K_{S60}$ have not been reported.

Illegal loop E: Equation S61 + Equation S52 + Equation S63 = Equation S47 + Equation S49 + Equation S62

$^\bullet OH + OH^- \rightleftharpoons H_2O + O^{\bullet-}$ (S61)

$Cl^\bullet + H_2O \rightleftharpoons ClOH^{\bullet-} + H_+$ (S52)

$Cl^\bullet + Cl^- \rightleftharpoons Cl_2^{\bullet-}$ (S47)

$Cl_2^{\bullet-} + OH^- \rightleftharpoons ClOH^{\bullet-} + Cl^-$ (S49)

$O_3^{\bullet-} \rightleftharpoons O_2 + O^{\bullet-}$ (S62)

$O_3^{\bullet-} + H^+ \rightarrow O_2 + {}^\bullet OH$ (S63)

Loop E was illegal because it contained one irreversible reaction (Equation S63). Illegal loop E was found in the Bulman-model. The value for the reverse rate constant k_{S63r} could be calculated from the relationship $K_{S61}K_{S52}(k_{S63f}/k_{S63r}) = K_{S47}K_{S49}K_{S62}$. As the result, $k_{S63r} = 1.1\times10^5$ $M^{-1}s^{-1}$ was obtained.

Illegal loop F: Equation S54 = Equation S52 + Equation S58 + Equation S64 + Equation S60

$^\bullet OH + Cl^- \rightleftharpoons ClOH^{\bullet-}$ (S54)

$Cl^\bullet + H_2O \rightleftharpoons ClOH^{\bullet-} + H_+$ (S52)

$^\bullet OH + H_3PO_4 \rightleftharpoons H_2PO_4^\bullet + H_2O$ (S58)

$$Cl^- + H_2PO_4^\bullet \rightarrow H_2PO_4^- + Cl^\bullet \quad \text{(S64)}$$

$$H_2PO_4^- + H^+ \rightleftharpoons H_3PO_4 \quad \text{(S60)}$$

Loop F was illegal because it contained one irreversible reaction (Equation S64). Illegal loop F was found in the Bulman-model. The value for the reverse rate constant k_{S64r} could be calculated from the relationship $K_{S54} = K_{S52}K_{S58}(k_{S64f}/k_{S64r})K_{S60}$. As a result, $k_{S64r} = 4.9\times10^4$ $M^{-1}s^{-1}$ was obtained.

Illegal loop G: Equation S54 = Equation S52 + Equation S58 + Equation S65

$$^\bullet OH + Cl^- \rightleftharpoons ClOH^{\bullet-} \quad \text{(S54)}$$

$$Cl^\bullet + H_2O \rightleftharpoons ClOH^{\bullet-} + H_+ \quad \text{(S52)}$$

$$^\bullet OH + H_3PO_4 \rightleftharpoons H_2PO_4^\bullet + H_2O \quad \text{(S58)}$$

$$H_2PO_4^\bullet + Cl^- + H^+ \rightarrow H_3PO_4 + Cl^\bullet \quad \text{(S65)}$$

Loop G was illegal because it contained one irreversible reaction (Equation S65). Illegal loop G was found in the Bulman-model. The value for the reverse rate constant k_{S65r} could be calculated from the relationship $K_{S54} = K_{S52}K_{S58}(k_{S65f}/k_{S65r})$. As the result, $k_{S65r} = 3.4\times10^5$ $M^{-1}s^{-1}$ was obtained.

Illegal loop H: Equation S55 + Equation S66 = Equation S58

$$^\bullet OH + H_2 \rightleftharpoons H_2O + H^\bullet \quad \text{(S55)}$$

$$^\bullet OH + H_3PO_4 \rightleftharpoons H_2PO_4^\bullet + H_2O \quad \text{(S58)}$$

$$H^\bullet + H_3PO_4 \rightarrow H_2PO_4^\bullet + H_2 \quad \text{(S66)}$$

Loop H was illegal because it contained one irreversible reaction (Equation S66). Illegal loop H was found in the Bulman-model. The value for reverse rate constant k_{S66r} could be calculated from the relationship $K_{S55}(k_{S66f}/k_{S66r}) = K_{S58}$, which yielded a k_{S66r} of 4.6×10^{11} $M^{-1}s^{-1}$, which was an impossible value because it exceeded the diffusion-controlled limit. Therefore, loop H could not be repaired by applying the calculated reverse rate constant, k_{S66r}. This loop could be repaired by removing Equation S66.

Illegal loop I: Equation S67 + Equation S54 = Equation S52 + Equation S53

$$H_2O \rightleftharpoons H^+ + OH^- \quad \text{(S67)}$$

$$Cl^\bullet + H_2O \rightleftharpoons ClOH^{\bullet-} + H_+ \quad \text{(S52)}$$

$$^\bullet OH + Cl^- \rightarrow Cl^\bullet + OH^- \quad \text{(S53)}$$

$$^\bullet OH + Cl^- \rightleftharpoons ClOH^{\bullet-} \quad \text{(S54)}$$

Illegal loop I was analogous to loop C in that it contained the irreversible Equation S53 and reversible Equation S54. Illegal loop I was found in the Sun-model. The value for the reverse rate constant, k_{S53r}, could be calculated from the relationship $K_{S67}K_{S54} = K_{S52}(k_{S53f}/k_{S53r})$ as 1.3×10^{17} $M^{-1}s^{-1}$, which was impossible as it greatly exceeded the diffusion-controlled limit. Therefore, loop I could not be repaired by applying the calculated reverse rate constant, k_{S53r}. This loop could be repaired by removing Equation S53.

Illegal loop J: Equation S52 = Equation S67 + Equation S48

$$H_2O \rightleftharpoons H^+ + OH^- \quad \text{(S67)}$$

$$Cl^\bullet + H_2O \rightleftharpoons ClOH^{\bullet-} + H_+ \quad \text{(S52)}$$

$$Cl^\bullet + OH^- \rightarrow ClOH^{\bullet-} \quad \text{(S48)}$$

Illegal loop J was analogous to loop A in that it contained irreversible Equation S48. Illegal loop I was found in the Sun-model. The value for the reverse rate constant, k_{S48r}, could be calculated from the relationship $K_{S52} = K_{S67}(k_{S48f}/k_{S48r})$ as 8.4×10^2 s^{-1}. The reverse rate constant k_{S48r} has been reported in the literature as 23 s^{-1}.[40]

Illegal loop K: Equation S52 = Equation S67 + Equation S47 + Equation S49

$$H_2O \rightleftharpoons H^+ + OH^- \quad \text{(S67)}$$

$$Cl^\bullet + H_2O \rightleftharpoons ClOH^{\bullet-} + H_+ \quad \text{(S52)}$$

$$Cl^\bullet + Cl^- \rightleftharpoons Cl_2^{\bullet-} \quad \text{(S47)}$$

$$Cl_2^{\bullet-} + OH^- \rightarrow ClOH^{\bullet-} + Cl^- \quad \text{(S49)}$$

Loop K was illegal since it contained a single irreversible reaction (Equation S49). Illegal loop K was found in the Sun-model. The value for the reverse rate constant k_{S49r} was calculated from the relationship $K_{S52} = K_{S67}K_{S47}(k_{S49f}/k_{S49r})$ as 3.0×10^6 $M^{-1}s^{-1}$. The Bulman-, Chuang-, and Li-models used a k_{S49r} value of 1.0×10^4 $M^{-1}s^{-1}$, and the Fang-, Guo-, and Wu-models used a k_{S49r} value of 1.0×10^5 $M^{-1}s^{-1}$.

All of the illegal loops except for loops C, D, I, and H could be repaired by applying the calculated reverse rate constants for the irreversible reactions. Loops C and I could be repaired by removing Equation S53. Loop D could not be repaired by calculating the reverse rate constants because this loop has two irreversible reaction steps. Loop H could be repaired by removing Equation S66.

We checked how the illegal loop corrections mentioned above affected the UV/chlorine model predictions. For this, the fluence-based decomposition rate constant of chlorine ($k_{chlorine}$) and the steady-state $^{\bullet}OH$ concentration ($[^{\bullet}OH]_{ss}$) in the UV/chlorine system ($[chlorine]_0 = 140$ μM, UV fluence rate = 3.7 mW cm^{-2}) were predicted using the UV/chlorine models before and after the illegal loop corrections. As the result, only the Bulman-model and Sun-model showed different model predictions after the illegal loop corrections, and the other models were not affected. Specifically, the correction of the illegal loops C and I by removal of Equation S53 showed significant changes in the model predictions. Figure S18 shows the model predictions for the $k_{chlorine}$ and $[^{\bullet}OH]_{ss}$ as a function of pH before and after the illegal loop corrections in the Bulman- and Sun-models. In the Bulman-model, both the $k_{chlorine}$ and $[^{\bullet}OH]_{ss}$ increased after the model corrections. In the Sun-model, the $k_{chlorine}$ did not change but the $[^{\bullet}OH]_{ss}$ increased after the model corrections. Overall, the previous UV/chlorine models contained some violations of the principle of detailed balancing, some of which could have led to erroneous results in model predictions.

SI-Text-12. Modeling of the relative contributions of reactive halogen species to BA degradation.

The kinetic model was applied to assess the relative contributions of individual RCS ($Cl^{\bullet}$, $ClO^{\bullet}$, and $Cl_2^{\bullet-}$) or RBS ($Br^{\bullet}$, $BrO^{\bullet}$, and $Br_2^{\bullet-}$) to the degradation of BA. The contribution of each reactive halogen species (RHS) could be calculated using the apparent first-order degradation rate of BA by each radical species ($k'_{BA,RHS}$), which could be obtained from the bimolecular rate constant $k_{RHS,BA}$ and the $[RHS]_{ss}$ using $k'_{BA,RHS} = k_{RHS,BA} \times [RHS]_{ss}$. For the UV/chlorine system, the k for the reaction of BA with $Cl^{\bullet}$ ($k_{Cl^{\bullet},BA} = 1.8\times10^{10}$ $M^{-1}s^{-1}$)[57] and $Cl_2^{\bullet-}$ ($k_{Cl_2^{\bullet-},BA} = 2\times10^{6}$ $M^{-1}s^{-1}$)[58] were used. The k for the reaction of $ClO^{\bullet}$ could be estimated by comparing the UV/chlorine kinetic model predictions versus the experimentally determined degradation of BA & relative contributions of RCS ($Cl^{\bullet}$, $Cl_2^{\bullet-}$, and $ClO^{\bullet}$) to the BA degradation (i.e., 25% at pH 6 and 53% at pH 10). As the result, a k value of 5×10^{5} $M^{-1}s^{-1}$ was obtained for the reaction of $ClO^{\bullet}$ with BA. Our value is within the k of $<3\times10^{6}$ $M^{-1}s^{-1}$ estimated by Alfassi et al.,[44] while smaller than the k value reported by Zhou et al. ($\sim1\times10^{6}$ $M^{-1}s^{-1}$).[59] For the UV/bromine system, the k for the reaction of BA with $Br^{\bullet}$ ($k_{Br^{\bullet},BA}$) was newly obtained to be 6.1×10^{8} $M^{-1}s^{-1}$ using a competition kinetics method with UV/HOBr/*tert*-butanol as the source of $Br^{\bullet}$ and formate as the competitor as described below. Rate constants for the reaction of BA with $BrO^{\bullet}$ and $Br_2^{\bullet-}$ are currently unknown. For these reactions, the k values of BA with $ClO^{\bullet}$ and $Cl_2^{\bullet-}$ could be used as an upper limit (i.e., $k_{BrO^{\bullet},BA} \approx 5\times10^{5}$ $M^{-1}s^{-1}$, $k_{Br_2^{\bullet-},BA} \approx 2\times10^{6}$ $M^{-1}s^{-1}$), considering the typical lower reactivity of Br radicals compared with the corresponding Cl radicals.[29]

Determination of the rate constant for the reaction of $Br^{\bullet}$ with BA. The second-order rate constant for the reaction of $Br^{\bullet}$ with BA was determined by a competition kinetics method using the UV/bromine system at pH 6 with *tert*-butanol as a source of $Br^{\bullet}$. Although this system can produce both $^{\bullet}OH$ and $Br^{\bullet}$ (Equation S68), $Br^{\bullet}$ can exist as the dominant radical species because of the rapid scavenging of $^{\bullet}OH$ by *tert*-butanol (Equation S69).[42] By contrast, the scavenging of $Br^{\bullet}$ by *tert*-butanol

592 is approximately four orders of magnitude slower than that of •OH (Equation S70).

593 $$HOBr \xrightarrow{h\nu} {}^{\bullet}OH + Br^{\bullet} \quad (S68)$$

594 $$^{\bullet}OH + (CH_3)_3COH \rightarrow H_2O + {}^{\bullet}CH_2(CH_3)_2COH \qquad k = 6\times10^8\ M^{-1}s^{-1}\ [42] \quad (S69)$$

595 $$Br^{\bullet} + (CH_3)_3COH \rightarrow Br^- + {}^{\bullet}CH_2(CH_3)_2COH \qquad k = 1.4\times10^4\ M^{-1}s^{-1}\ [17] \quad (S70)$$

596 To demonstrate the dominance of Br•, the degradation of NB and BA by UV alone, UV/bromine,
597 and UV/bromine with *tert*-butanol (7 mM) at pH 6 was investigated. The results (Figure S19a) showed
598 that the degradation rate of NB in UV/bromine (k = 5.9×10^{-4} cm^2 mJ^{-1}) was significantly decreased
599 upon the addition of *tert*-butanol (k = 1.2×10^{-4} cm^2 mJ^{-1}) and became similar to that in UV alone (k =
600 9.8×10^{-5} cm^2 mJ^{-1}). This result can be understood because the degradation of NB was solely achieved
601 by •OH and UV (but not by Br•), and •OH was nearly completely scavenged by *tert*-butanol. The
602 degradation behavior of BA (Figure S19b) was different from that of NB. Upon the addition of *tert*-
603 butanol, the degradation rate of BA was decreased (from 1.3×10^{-3} to 2.7×10^{-4} cm^2 mJ^{-1}) but was still
604 much larger than that in UV alone (k = 3.7×10^{-5} cm^2 mJ^{-1}). The result indicates that the degradation
605 of BA in the UV/bromine/*tert*-butanol system was achieved by its reaction with Br•, which was much
606 less scavenged by *tert*-butanol compared to •OH. Overall, our data show that UV/bromine/*tert*-butanol
607 (7 mM) can be used as a Br•-generation system by the selective scavenging of •OH by *tert*-butanol.
608 As a next step, BA and formate were treated by UV/bromine/*tert*-butanol (7 mM) at pH 6. Formate
609 was used as the competitor because its reactivity with Br• is known ($k_{Br^{\bullet},HCO_2^-}$ = 4.6×10^8 M^{-1}s^{-1}).[17]
610 Figure S20 shows the competition kinetics plot of the degradation of BA and formate by Br•. From the
611 slope of the kinetics plot, the second-order rate constant for the reaction of Br• with BA was determined
612 as 6.1(±0.1)×10^8 M^{-1}s^{-1}.
613

SI-Text-13. Application of the UV/chlorine model to predict micropollutant elimination and ClO_3^- formation during UV photolysis of chlorine

The kinetic model for the UV/chlorine system can be used to optimize the operation conditions, such as the chlorine dose and UV fluence, for achieving micropollutant elimination under the control of ClO_3^- formation. Model predictions were made for the percentage abatement of micropollutant and ClO_3^- formation in the UV/chlorine system at different chlorine doses (0 – 10 $mgCl_2\ L^{-1}$), DOC concentrations (0.5 and 3 $mgC\ L^{-1}$), and UV fluence values (500, 1000, 1500, and 2000 $mJ\ cm^{-2}$) at pH values of 6 and 10. A hypothetical compound reacting with $^{\bullet}OH$ at a k of $5\times10^9\ M^{-1}s^{-1}$ was considered in the modeling as an organic micropollutant (OMP) exhibiting moderate reactivity toward $^{\bullet}OH$. It was assumed that UV and RCS did not degrade this OMP. The results (Figure S23) showed that the percentage elimination of the OMP and ClO_3^- generally increased with increasing chlorine dose and UV fluence, but the extent and behavior differed depending on the DOC concentration and pH. With certain operational and water quality parameters for the process, the percentage elimination of OMP varied more significantly than that of ClO_3^- formation.

With 0.5 $mgC\ L^{-1}$ DOC and pH 6, the elimination efficiency of OMP was high. More than 80% elimination of OMP could be achieved with a chlorine dose of ≥ 5.1 $mgCl_2\ L^{-1}$ and UV fluence of 500 $mJ\ cm^{-2}$, chlorine dose of ≥ 1.8 $mgCl_2\ L^{-1}$ and UV fluence of 1000 $mJ\ cm^{-2}$, chlorine dose of ≥ 1.1 $mgCl_2\ L^{-1}$ and UV fluence of 1500 $mJ\ cm^{-2}$, and chlorine dose of ≥ 0.9 $mgCl_2\ L^{-1}$ and UV fluence of 2000 $mJ\ cm^{-2}$. It was notable that the percentage OMP elimination increased rapidly with the chlorine dose in the low chlorine dose range (0–2 $mgCl_2\ L^{-1}$) but did not show further increases at the higher chlorine dose range (> 2 $mgCl_2\ L^{-1}$). By contrast, ClO_3^- formation continued increasing throughout the chlorine dose range. Thus, to achieve more than 80% OMP elimination while keeping ClO_3^- formation below 0.25 $mg\ L^{-1}$ (the guideline value), the optimum chlorine doses were 1.8–5.6 $mgCl_2\ L^{-1}$ at a UV fluence of 1000 $mJ\ cm^{-2}$ or 0.9–3.9 $mgCl_2\ L^{-1}$ at a UV fluence of 2000 $mJ\ cm^{-2}$.

When the DOC concentration was increased to 3 mgC L^{-1} at pH 6, the percentage elimination of OMP decreased, and increased more gradually with increasing chlorine dose than at 0.5 mgC L^{-1} DOC. The ClO_3^- formation also decreased at the higher DOC level but the extent of the ClO_3^- formation decrease was less than the extent of decrease in the percentage OMP elimination. In the presence of 3 mgC L^{-1} DOC, 80% OMP elimination with less than 0.25 mg L^{-1} of ClO_3^- formation could be achieved only at chlorine doses of 5.1–5.6 mgCl_2 L^{-1} and a UV fluence of 2000 mJ cm^{-2}. At other chlorine doses or UV fluence values, either the OMP elimination was lower than 80% or the ClO_3^- formation exceeded 0.25 mg L^{-1}.

At pH 10, the percentage elimination of OMP was relatively low compared with that at pH 6. The percentage OMP elimination increased with increasing UV fluence to 2000 mJ cm^{-2}. With the DOC concentration at 0.5 mgC L^{-1} and UV fluence at 2000 mJ cm^{-2}, chlorine doses of 2.9–3.5 mgCl_2 L^{-1} could achieve 58% OMP elimination and ClO_3^- formation below 0.25 mg L^{-1}.

SI-Tables

Table S1. Summary of kinetics parameters for the decomposition of chlorine and bromine during UV photolysis in the absence and in the presence of organic substrate.

	pH [a]	Organic substrate	k_{OX}, $cm^2\ mJ^{-1}$	Φ_{OX}^{app}, mol $Einsein^{-1}$ [b]	Ratio of k_{OX} [c]
Chlorine	6 (HOCl)	none	$4.9(\pm0.2)\times10^{-4}$	1.58±0.06	-
		tert-butanol	$5.0(\pm0.6)\times10^{-4}$	1.60±0.18	1.0
		methanol	$3.3(\pm0.3)\times10^{-2}$	106.1±10.2	67.2
	10 (OCl^-)	none	$4.0(\pm0.1)\times10^{-4}$	1.45±0.05	-
		tert-butanol	$4.1(\pm0.2)\times10^{-4}$	1.51±0.07	1.0
		methanol	$6.3(\pm0.5)\times10^{-4}$	2.32±0.17	1.6
Bromine	6 (HOBr)	none	$2.3(\pm0.02)\times10^{-4}$	0.55±0.01	-
		tert-butanol	$4.6(\pm0.6)\times10^{-4}$	1.12±0.14	2.0
		methanol	$2.3(\pm0.04)\times10^{-3}$	5.64±0.09	10.3
	10 (OBr^-)	none	$7.2(\pm0.5)\times10^{-5}$	0.74±0.05	-
		tert-butanol	$1.3(\pm0.1)\times10^{-4}$	1.36±0.08	1.8
		methanol	$6.5(\pm0.3)\times10^{-3}$	66.6±3.1	90.0

[a]Parentheses represent the major oxidant species at the given pH, [b]Apparent quantum yield for the oxidant decomposition, [c]Ratio =(k_{OX} with organics) / (k_{OX} without organics).

Table S2. Summary of kinetics parameters for the decomposition of chlorine and bromine species and the formation of radicals in the UV/chlorine and UV/bromine systems.

pH	ε_{254}, $M^{-1}cm^{-1}$	Φ_{Ox}^{app}, mol Einstein^{-1} [b]	Φ_{Ox}^{app} from literature, mol Einstein^{-1}	Φ_{Ox}^{int}, mol Einstein^{-1} [c]	Φ_{Ox}^{int} from literature, mol Einstein^{-1}
6 (HOCl)[a]	64	1.58±0.06	1.0-2.8[11,47,60-62]	0.61	0.55[63], 0.62[45]
10 (OCl^-)[a]	56	1.45±0.05	0.85-2.4[11,30,47,60-62]	0.45	0.41[11], 0.55[45]
6 (HOBr)[a]	84 (77)[d]	0.55±0.01	0.69[10], 4.4[11]	0.32	0.43 (0.39)[10] [e]
10 (OBr^-)[a]	20 (28)[d]	0.74±0.05	0.37–0.55[10]	0.43	0.26 (0.36)[10] [e]

[a]Parentheses represent the major oxidant species at the given pH, [b]Apparent quantum yields for the oxidant decomposition. [c]Intrinsic quantum yields for the radical generation, determined from the formaldehyde formation in the presence of excess *tert*-butanol and kinetics modeling, [d]The values in parentheses indicate the ε_{254} used in Guo et al.,[10] [e]The values in parentheses indicate the recalculated Φ_{Ox}^{int} values of Guo et al.[10] using the ε_{254} values from this study (i.e., 84 $M^{-1}cm^{-1}$ HOBr and 20 $M^{-1}cm^{-1}$ for OBr^-).

665 **Table S3.** Reactions used for the kinetic modeling of UV/chlorine (UV/chlorine/*tert*-butanol) system.

	Reaction	Rate constant, s^{-1} or $M^{-1}s^{-1}$	Reference
Photolysis of chlorine species and ozone [a]			
1	$HOCl \xrightarrow{h\nu} {}^{\bullet}OH + Cl^{\bullet}$	Φ^{int} = 0.61, ε_{254} = 64 $M^{-1}cm^{-1}$	This study
2	$OCl^- \xrightarrow{h\nu} {}^{\bullet}O^- + Cl^{\bullet}$	Φ^{int} = 0.45, ε_{254} = 56 $M^{-1}cm^{-1}$	This study
3	$OCl^- \xrightarrow{h\nu} O(^1D) + Cl^-$	Φ^{int} = 0.13, ε_{254} = 56 $M^{-1}cm^{-1}$	30
4	$OCl^- \xrightarrow{h\nu} O(^3P) + Cl^-$	Φ^{int} = 0.07, ε_{254} = 56 $M^{-1}cm^{-1}$	30
5	$O_3 \xrightarrow{h\nu} 0.91O(^1D) + 0.09O(^3P) + O_2$	Φ^{int} = 0.5, ε_{254} = 3300 $M^{-1}cm^{-1}$	14,64
Reactions of oxygen atoms ($O(^1D)$ and $O(^3P)$)			
6	$O(^1D) + H_2O \rightarrow H_2O_2$ (hot) $\rightarrow 0.9H_2O_2 + 0.2{}^{\bullet}OH$	1.8×10^{10}	14,31
7	$O(^3P) + O_2 \rightarrow O_3$	4.0×10^{9}	32,33
Reactions of ozone			
8	$OCl^- + O_3 \rightarrow 2O_2 + Cl^-$	1.1×10^{2}	34
9	$OCl^- + O_3 \rightarrow O_2 + ClO_2^-$	30	34
Reactions of ${}^{\bullet}OH$ and $Cl^{\bullet}$ with chlorine species and $ClO^{\bullet}$ formation			
10	$HOCl + {}^{\bullet}OH \rightarrow ClO^{\bullet} + H_2O$	1.4×10^{8}	This study
11	$OCl^- + {}^{\bullet}OH \rightarrow ClO^{\bullet} + OH^-$	2.0×10^{9}	This study
12	$HOCl + {}^{\bullet}Cl \rightarrow ClO^{\bullet} + H^+ + Cl^-$	3.0×10^{9}	This study
13	$OCl^- + {}^{\bullet}Cl \rightarrow ClO^{\bullet} + Cl^-$	1.0×10^{10}	This study
14	$OCl^- + Cl_2^{\bullet-} \rightarrow ClO^{\bullet} + 2Cl^-$	2.9×10^{8}	65
Reactions of ${}^{\bullet}OH$ with Cl^-			
15	${}^{\bullet}OH + Cl^- \rightarrow ClOH^{\bullet-}$	4.3×10^{9}	40
16	$Cl^{\bullet} + OH^- \rightarrow ClOH^{\bullet-}$	1.8×10^{10}	40
17	$Cl^{\bullet} + H_2O \rightarrow ClOH^{\bullet-} + H^+$	2.5×10^{5}	66
18	$ClOH^{\bullet-} \rightarrow {}^{\bullet}OH + Cl^-$	6.1×10^{9}	40
19	$ClOH^{\bullet-} \rightarrow OH^- + Cl^{\bullet}$	23	40
20	$ClOH^{\bullet-} + H^+ \rightarrow Cl^{\bullet} + H_2O$	2.1×10^{10}	40
Reactions of $Cl_2^{\bullet-}$			
21	$Cl^{\bullet} + Cl^- \rightarrow Cl_2^{\bullet-}$	6.5×10^{9}	67
22	$Cl_2^{\bullet-} \rightarrow Cl^{\bullet} + Cl^-$	1.1×10^{5}	67
23	$Cl_2^{\bullet-} + OH^- \rightarrow ClOH^{\bullet-} + Cl^-$	4.5×10^{7}	68
24	$ClOH^{\bullet-} + Cl^- \rightarrow OH^- + Cl_2^{\bullet-}$	1.0×10^{4}	68
25	$2Cl_2^{\bullet-} \rightarrow Cl_2 + 2Cl^-$	9.0×10^{8}	69
26	$2Cl_2^{\bullet-} \rightarrow Cl_3^- + Cl^-$	4.1×10^{9}	70-85
Reactions of chlorine species with H_2O_2 and peroxyl radicals ($HO_2^{\bullet}$ and $O_2^{\bullet-}$)			
27	$HOCl + H_2O_2 \rightarrow O_2 + H_2O + Cl^- + H^+$	1.1×10^{4}	86,87
28	$HOCl + O_2^{\bullet-} \rightarrow {}^{\bullet}OH + O_2 + Cl^-$	7.5×10^{6}	23
29	$HOCl + O_2^{\bullet-} \rightarrow {}^{\bullet}Cl + O_2 + OH^-$	7.5×10^{6}	23,38,86
30	$HOCl + HO_2^- \rightarrow O_2 + H_2O + Cl^-$	4.4×10^{7}	20
31	$HOCl + HO_2^{\bullet} \rightarrow Cl^{\bullet} + OH^- + O_2$	7.5×10^{6}	38,86
32	$OCl^- + H_2O_2 \rightarrow O_2 + H_2O + Cl^-$	1.7×10^{5}	86,87
33	$OCl^- + O_2^{\bullet-} + H_2O \rightarrow Cl^{\bullet} + O_2 + 2OH^-$	2.0×10^{8}	38,86

Reactions of $ClO^{\bullet}$ and formation of ClO_3^-			
34	$2ClO^{\bullet} \rightarrow Cl_2O_2$	2.5×10^9	40
35	$Cl_2O_2 + H_2O \rightarrow OCl^- + ClO_2^- + 2H^+$	1.0×10^4	88
36	$Cl_2O_2 + H_2O \rightarrow Cl^- + O_2 + OCl^- + 2H^+$	5.2×10^3	30
37	$ClO_2^- + ClO^{\bullet} \rightarrow ClO_2^{\bullet} + OCl^-$	9.4×10^8	44
38	$ClO_2^{\bullet} + ClO^{\bullet} \rightarrow Cl_2O_3$	7.4×10^9	52
39	$Cl_2O_3 + H_2O \rightarrow ClO_3^- + OCl^- + 2H^+$	1.0×10^4	52
Reactions of reactive species with probe compounds			
40	$^{\bullet}OH + C_6H_5NO_2$ (NB) → product	3.8×10^9	This study
41	$^{\bullet}OH + C_6H_5COO^-$ (BA) → product	5.9×10^9	42
42	$Cl^{\bullet} + C_6H_5COO^-$ (BA) → product	1.8×10^{10}	89
43	$ClO^{\bullet} + C_6H_5COO^-$ (BA) → product	5×10^5	Estimated
44	$Cl_2^{\bullet-} + C_6H_5COO^-$ (BA) → product	2.0×10^6	58
Reactions of $^{\bullet}OH$ and $Cl^{\bullet}$ with tert-butanol			
45	$^{\bullet}OH + (CH_3)_3COH \rightarrow H_2O + {}^{\bullet}CH_2C(CH_3)_2OH$	6.0×10^8	42
46	$^{\bullet}O^- + (CH_3)_3COH \rightarrow OH^- + {}^{\bullet}CH_2C(CH_3)_2OH$	5.0×10^8	90
47	$Cl^{\bullet} + (CH_3)_3COH \rightarrow H^+ + Cl^- + {}^{\bullet}CH_2C(CH_3)_2OH$	1.5×10^9	16
48	$Cl^{\bullet} + (CH_3)_3COH \rightarrow H^+ + Cl^- + (CH_3)_3CO^{\bullet}$	7.0×10^8	16
49	$^{\bullet}CH_2C(CH_3)_2OH + O_2 \rightarrow {}^{\bullet}OOCH_2C(CH_3)_2OH$	1.4×10^9	14,91
50	$2{}^{\bullet}OOCH_2C(CH_3)_2OH \rightarrow O_2 + HOC(CH_3)_2CH_2OH + HOC(CH_3)_2CHO$	8.0×10^7	14,18
51	$2{}^{\bullet}OOCH_2C(CH_3)_2OH \rightarrow H_2O_2 + 2HOC(CH_3)_2CHO$	1.2×10^8	14,18
52	$2{}^{\bullet}OOCH_2C(CH_3)_2OH \rightarrow O_2 + 2CH_2O + 2{}^{\bullet}C(CH_3)_2OH$	1.0×10^8	14,18
53	$2{}^{\bullet}OOCH_2C(CH_3)_2OH \rightarrow O_2 + HO(CH_3)_2CCH_2OOCH_2C(CH_3)_2OH$	1.0×10^8	14,18
54	$^{\bullet}C(CH_3)_2OH + O_2 \rightarrow {}^{\bullet}OOC(CH_3)_2OH$	2.0×10^9	14
55	$^{\bullet}OOC(CH_3)_2OH \rightarrow (CH_3)_2CO + HO_2^{\bullet}$	6.0×10^2	14,92
Equilibrium reactions of chlorine species, $^{\bullet}OH$, $HO_2^{\bullet}$, H_2O_2, and probe compounds			
56	$H^+ + OCl^- \rightarrow HOCl$	1.0×10^{11}	Assumed
57	$HOCl \rightarrow H^+ + OCl^-$	3.8×10^4	Calculated ($pK_a = 7.5$)[93]
58	$^{\bullet}O^- + H^+ \rightarrow {}^{\bullet}OH$	1.0×10^{11}	Assumed
59	$^{\bullet}OH \rightarrow {}^{\bullet}O^- + H^+$	1.3×10^{-1}	Calculated ($pK_a = 11.9$)[42]
60	$^{\bullet}OH + OH^- \rightarrow O^{\bullet-} + H_2O$	1.2×10^{10}	42
61	$^{\bullet}O^- + H_2O \rightarrow {}^{\bullet}OH + OH^-$	9.3×10^7	94
62	$O_2^{\bullet-} + H^+ \rightarrow HO_2^{\bullet}$	1.0×10^{11}	Assumed
63	$HO_2^{\bullet} \rightarrow O_2^{\bullet-} + H^+$	2.0×10^6	Calculated ($pK_a = 4.7$)[95]
64	$HO_2^- + H^+ \rightarrow H_2O_2$	1.0×10^{11}	Assumed
65	$H_2O_2 \rightarrow HO_2^- + H^+$	2.5×10^{-1}	Calculated ($pK_a = 11.6$)[96]
66	$C_6H_5COO^- + H^+ \rightarrow C_6H_5COOH$	1.0×10^{11}	Assumed
67	$C_6H_5COOH \rightarrow C_6H_5COO^- + H^+$	6.3×10^6	Calculated[97]

[a]The photolysis rate for each reaction were calculated using following equation. $\frac{dC}{dt} = \frac{E_P^0[1-10^{-\varepsilon C d}]\cdot\Phi}{d}$; C: concentration of oxidant (M), E_P^0 : photon flux at 254 nm (mEinstein $s^{-1}cm^{-2}$), ε_{254}: molar extinction coefficient ($M^{-1}cm^{-1}$), Φ^{int}: intrinsic quantum yield (mol $Einstein^{-1}$), *d*: pathlength (cm)

669 **Table S4.** Reactions used for the kinetic modeling of UV/bromine (UV/bromine/*tert*-butanol) system.

	Reaction	Rate constant, s^{-1} or $M^{-1}s^{-1}$	Reference
Photolysis of bromine species [a]			
1	$HOBr \xrightarrow{h\nu} {}^{\bullet}OH + Br^{\bullet}$	Φ^{int} = 0.32, ε_{254} = 84 $M^{-1}cm^{-1}$	This study
2	$OBr^{-} \xrightarrow{h\nu} {}^{\bullet}O^{-} + Br^{\bullet}$	Φ^{int} = 0.43, ε_{254} = 20 $M^{-1}cm^{-1}$	This study
Reactions of $^{\bullet}OH$ and $Br^{\bullet}$ with bromine species and $BrO^{\bullet}$ formation			
3	$HOBr + {}^{\bullet}OH \rightarrow BrO^{\bullet} + H_2O$	1.0×10^{9}	Estimated
4	$OBr^{-} + {}^{\bullet}OH \rightarrow BrO^{\bullet} + OH^{-}$	4.2×10^{9}	98
5	$HOBr + Br^{\bullet} \rightarrow BrO^{\bullet} + H^{+} + Br^{-}$	$<1.0\times10^{6}$	Estimated
6	$OBr^{-} + Br^{\bullet} \rightarrow BrO^{\bullet} + Br^{-}$	4.1×10^{9}	40
Reaction of $^{\bullet}OH$ with Br^{-}			
7	$^{\bullet}OH + Br^{-} \rightarrow BrOH^{\bullet-}$	1.0×10^{10}	39
8	$Br^{\bullet} + OH^{-} \rightarrow BrOH^{\bullet-}$	1.3×10^{10}	40
9	$Br^{\bullet} + H_2O \rightarrow BrOH^{\bullet-} + H^{+}$	1.36	40
10	$BrOH^{\bullet-} + H^{+} \rightarrow Br^{\bullet} + H_2O$	4.4×10^{10}	39
11	$BrOH^{\bullet-} \rightarrow Br^{-} + {}^{\bullet}OH$	3.3×10^{7}	39
12	$BrOH^{\bullet-} \rightarrow Br^{\bullet} + OH^{-}$	4.0×10^{6}	39
Reactions of bromine species with H_2O_2 and peroxyl radicals ($HO_2^{\bullet}$ and $O_2^{\bullet-}$)			
13	$HOBr + O_2^{\bullet-} \rightarrow BrOH^{\bullet-} + O_2$	3.5×10^{9}	21
14	$HOBr + HO_2^{\bullet} \rightarrow BrOH^{\bullet-} + H^{+}$	3.5×10^{9}	38
15	$HOBr + HO_2^{-} \rightarrow Br^{-} + O_2 + H_2O$	7.6×10^{8}	21
16	$OBr^{-} + O_2^{\bullet-} + H_2O \rightarrow Br^{\bullet} + 2OH^{-} + O_2$	2.0×10^{8}	38
Reactions of $BrO^{\bullet}$ and formation of BrO_3^{-}			
17	$2BrO^{\bullet} + H_2O \rightarrow BrO_2^{-} + OBr^{-} + 2H^{+}$	2.8×10^{9}	40
18	$BrO_2^{-} + BrO^{\bullet} \rightarrow OBr^{-} + BrO_2^{\bullet}$	4.0×10^{8}	99
19	$2BrO_2^{\bullet} \rightarrow Br_2O_4$	1.4×10^{9}	53
20	$Br_2O_4 \rightarrow 2BrO_2^{\bullet}$	7.4×10^{4}	53
21	$Br_2O_4 + H_2O \rightarrow BrO_3^{-} + BrO_2^{-} + 2H^{+}$	2.2×10^{3}	53
Reactions of reactive species with probe compounds			
22	$^{\bullet}OH + C_6H_5NO_2$ (NB) → product	3.8×10^{9}	This study
23	$^{\bullet}OH + C_6H_5COO^{-}$ (BA) → product	5.9×10^{9}	42
24	$Br^{\bullet} + C_6H_5COO^{-}$ (BA) → product	6.1×10^{8}	This study
25	$BrO^{\bullet} + C_6H_5COO^{-}$ (BA) → product	$< 5\times10^{5}$	Assumed
Reactions of $^{\bullet}OH$ and $Br^{\bullet}$ with tert-butanol			
26	$^{\bullet}OH + (CH_3)_3COH \rightarrow H_2O + {}^{\bullet}CH_2C(CH_3)_2OH$	6.0×10^{8}	42
27	$^{\bullet}O^{-} + (CH_3)_3COH \rightarrow OH^{-} + {}^{\bullet}CH_2C(CH_3)_2OH$	5.0×10^{8}	90
28	$Br^{\bullet} + (CH_3)_3COH \rightarrow H^{+} + Br^{-} + {}^{\bullet}CH_2C(CH_3)_2OH$	1.4×10^{4}	17
29	$^{\bullet}CH_2C(CH_3)_2OH + O_2 \rightarrow {}^{\bullet}OOCH_2C(CH_3)_2OH$	1.4×10^{9}	14,91
30	$2{}^{\bullet}OOCH_2C(CH_3)_2OH \rightarrow O_2 + HOC(CH_3)_2CH_2OH + HOC(CH_3)_2CHO$	8.0×10^{7}	14,18
31	$2{}^{\bullet}OOCH_2C(CH_3)_2OH \rightarrow H_2O_2 + 2HOC(CH_3)_2CHO$	1.2×10^{8}	14,18

32	$2^{\bullet}OOCH_2C(CH_3)_2OH \rightarrow O_2 + 2CH_2O + 2^{\bullet}C(CH_3)_2OH$	1.0×10^{8}	14,18
33	$2^{\bullet}OOCH_2C(CH_3)_2OH \rightarrow O_2 + HO(CH_3)_2CCH_2OOCH_2C(CH_3)_2OH$	1.0×10^{8}	14,18
34	$^{\bullet}C(CH_3)_2OH + O_2 \rightarrow {}^{\bullet}OOC(CH_3)_2OH$	2.0×10^{9}	14
35	$^{\bullet}OOC(CH_3)_2OH \rightarrow (CH_3)_2CO + HO_2^{\bullet}$	6.0×10^{2}	14,92
	Equilibrium reactions of bromine species, $^{\bullet}OH$, $HO_2^{\bullet}$, and H_2O_2		
36	$OBr^- + H^+ \rightarrow HOBr$	1.0×10^{11}	Assumed
37	$HOBr \rightarrow OBr^- + H^+$	158	Calculated ($pK_a = 8.8$)
38	$^{\bullet}O^- + H^+ \rightarrow {}^{\bullet}OH$	1.0×10^{11}	Assumed
39	$^{\bullet}OH \rightarrow {}^{\bullet}O^- + H^+$	1.3×10^{-1}	Calculated ($pK_a = 11.9$)[42]
40	$^{\bullet}OH + OH^- \rightarrow {}^{\bullet}O^- + H_2O$	1.2×10^{10}	42
41	$^{\bullet}O^- + H_2O \rightarrow {}^{\bullet}OH + OH^-$	9.3×10^{7}	94
42	$O_2^{\bullet-} + H^+ \rightarrow HO_2^{\bullet}$	1.0×10^{11}	Assumed
43	$HO_2^{\bullet} \rightarrow O_2^{\bullet-} + H^+$	2.0×10^{6}	Calculated ($pK_a = 4.7$)[95]
44	$HO_2^- + H^+ \rightarrow H_2O_2$	1.0×10^{11}	Assumed
45	$H_2O_2 \rightarrow HO_2^- + H^+$	2.5×10^{-1}	Calculated ($pK_a = 11.6$)[96]
46	$C_6H_5COO^- + H^+ \rightarrow C_6H_5COOH$	1.0×10^{11}	Assumed
47	$C_6H_5COOH \rightarrow C_6H_5COO^- + H^+$	6.3×10^{6}	Calculated[97]

[a]The photolysis rate for each reaction were calculated using following equation. $\frac{dC}{dt} = \frac{E_P^0[1-10^{-\varepsilon Cd}]\cdot\Phi}{d}$; C: concentration of oxidant (M), E_P^0 : photon flux at 254 nm (mEinstein $s^{-1}cm^{-2}$), ε_{254}: molar extinction coefficient ($M^{-1}cm^{-1}$), Φ^{int}: intrinsic quantum yield (mol $Einstein^{-1}$), *d*: pathlength (cm)

673 **Table S5.** Reactions not included in the kinetic models (Tables S2 and S3) based on the sensitivity
674 analysis model.

	Reaction	Rate constant, s^{-1} or $M^{-1}s^{-1}$	Reference
Photolysis of chlorite [a]			
1	$ClO_2^- \xrightarrow{h\nu} OCl^- + O(^1D)$	Φ^{int} = 0.11, ε_{254} = 130 $M^{-1}cm^{-1}$	33,100
2	$ClO_2^- \xrightarrow{h\nu} ClO^\bullet + {}^\bullet O^-$	Φ^{int} = 0.08, ε_{254} = 130 $M^{-1}cm^{-1}$	33,100
3	$ClO_2^- + ClO_2^- \xrightarrow{h\nu} ClO_2^\bullet + OCl^- + {}^\bullet O^-$	Φ^{int} = 0.08, ε_{254} = 130 $M^{-1}cm^{-1}$	33,100
Reactions of chlorine and reactive species			
4	$OCl^- + {}^\bullet O^- + H^+ \rightarrow ClO^\bullet + OH^-$	2.4×10^8	101
5	$OCl^- + O(^3P) \rightarrow ClO_2^-$	9.4×10^9	32,33
Reactions of ozone			
6	$O_3 + H_2O_2 \rightarrow O_2 + {}^\bullet OH + HO_2^\bullet$	6.5×10^{-2}	102
7	$O_3 + {}^\bullet OH \rightarrow HO_2^\bullet + O_2$	1.1×10^8	103
8	$O_3 + O_2^{\bullet-} \rightarrow O_3^{\bullet-} + O_2$	1.6×10^9	104
9	$O_3 + HO_2^\bullet \rightarrow {}^\bullet OH + 2O_2$	1.2×10^6	105
10	$O_3^{\bullet-} \rightarrow O_2 + O^{\bullet-}$	2.6×10^3	106
11	$O_3^{\bullet-} + H^+ \rightarrow {}^\bullet OH + O_2$	9.0×10^{10}	107
12	$O_3 + ClO_2^\bullet \rightarrow O_2 + ClO_3^\bullet$	1.4×10^3	108
13	$O_3 + ClO_2^- \rightarrow O_3^{\bullet-} + ClO_2^\bullet$	4.0×10^6	109
Reactions of HO_x			
14	$2\,{}^\bullet OH \rightarrow H_2O_2$	5.5×10^9	42
15	$^\bullet OH + H_2O_2 \rightarrow HO_2^\bullet + H_2O$	2.7×10^7	42
16	$^\bullet OH + HO_2^- \rightarrow HO_2^\bullet + OH^-$	7.5×10^9	110
17	$^\bullet OH + HO_2^\bullet \rightarrow O_2 + H_2O$	6.6×10^9	110
18	$^\bullet OH + O_2^{\bullet-} \rightarrow O_2 + OH^-$	7.0×10^9	110
19	$H_2O_2 + HO_2^\bullet \rightarrow {}^\bullet OH + H_2O + O_2$	3.0	110
20	$H_2O_2 + O_2^{\bullet-} \rightarrow {}^\bullet OH + O_2 + OH^-$	1.3×10^{-1}	110
21	$2\,HO_2^\bullet \rightarrow H_2O_2 + O_2$	8.3×10^5	110
22	$HO_2^\bullet + O_2^{\bullet-} \rightarrow HO_2^- + O_2$	9.7×10^7	110
Reactions of Cl_xO_x			
23	$Cl_2O_2 + ClO_2^- \rightarrow ClO_3^- + Cl_2O$	7.7×10^{-2}	30
24	$Cl_2O + H_2O \rightarrow 2HOCl$	1.0×10^4	Assumed
25	$ClO_2^- + {}^\bullet OH \rightarrow ClO_2^\bullet + OH^-$	7.0×10^9	46
26	$ClO_2^- + {}^\bullet O^- \rightarrow ClO_2^\bullet + O_2^{\bullet-}$	1.9×10^8	101
27	$ClO_2^- + Cl^\bullet \rightarrow ClO_2^\bullet + Cl^-$	7.0×10^9	Assumed[45]
28	$ClO_2^\bullet + O \rightarrow ClO_3$	8.8×10^9	52
29	$ClO_2^\bullet + {}^\bullet OH \rightarrow HOCl + O_2$	2.6×10^9	52
30	$ClO_2^\bullet + {}^\bullet OH \rightarrow ClO_3^- + H^+$	4.0×10^9	109
31	$ClO_2^\bullet + {}^\bullet O^- \rightarrow ClO_3^-$	2.7×10^9	109
32	$ClO_2^\bullet + Cl^\bullet \rightarrow Cl_2O_2$	7.8×10^9	52
33	$ClO_2^\bullet + Cl_2^{\bullet-} \rightarrow Cl_2O_2 + Cl^-$	1.0×10^9	88
34	$ClO_2^\bullet + ClO_3 \rightarrow Cl_2O_5$	7.5×10^9	52
35	$ClO_3 + ClO^\bullet \rightarrow Cl_2O_4$	7.5×10^9	52
36	$ClO_3 + ClO_3 \rightarrow Cl_2O_6$	3.7×10^9	52
37	$Cl_2O_5 + H_2O \rightarrow 2ClO_3^- + 2H^+$	1.0×10^4	52

38	$Cl_2O_4 + H_2O \rightarrow HOCl + ClO4^- + H^+$	1.0×10^4	52
39	$Cl_2O_6 + H_2O \rightarrow ClO_3^- + ClO4^- + 2H^+$	1.0×10^4	52
	Reactions of bromine species and reactive bromine species (RBS)		
40	$HOBr + H^+ + Br^- \rightarrow Br_2 + H_2O$	1.6×10^{10}	111
41	$OBr^- + {}^\bullet O^- \rightarrow BrO^\bullet + OH$-	2.9×10^9	112
42	$Br^\bullet + Br^- \rightarrow Br_2^{\bullet-}$	1.0×10^{10}	39
43	$Br_2^{\bullet-} \rightarrow Br^\bullet + Br^-$	1.0×10^5	39
44	$Br_3^- \rightarrow Br_2 + Br^-$	8.3×10^8	111
45	$Br_2 + Br^- \rightarrow Br_3^-$	1.0×10^{10}	111
46	$Br^\bullet + Br^\bullet \rightarrow Br_2$	1.0×10^9	38
47	$Br^\bullet + H_2O_2 \rightarrow HO_2^\bullet + Br^-$	4.0×10^9	38
48	$Br^\bullet + HO_2^\bullet \rightarrow H^+ + O_2 + Br^-$	1.6×10^8	38
49	$Br_2^{\bullet-} + Br_2^{\bullet-} \rightarrow Br_3^- + Br^-$	2.4×10^9	70
50	$Br_2^{\bullet-} + OBr^- \rightarrow BrO^\bullet + 2Br^-$	8.0×10^7	42
51	$Br_2^{\bullet-} + HO_2^\bullet \rightarrow O_2 + 2Br^- + H^+$	1.0×10^8	113
52	$Br_2^{\bullet-} + HO_2^\bullet \rightarrow HO_2^- + Br_2$	4.4×10^9	114
53	$Br_2^{\bullet-} + O_2^{\bullet-} \rightarrow O_2 + 2Br^-$	1.7×10^8	113
54	$Br_2^{\bullet-} + {}^\bullet OH \rightarrow HOBr + Br^-$	1.0×10^9	113
55	$Br_2^{\bullet-} + OH^- \rightarrow BrOH^{\bullet-} + Br^-$	2.7×10^6	115
56	$Br_2 + H_2O \rightarrow HOBr + H^+ + Br^-$	5.4×10^3	111
57	$Br_2 + HO_2^\bullet \rightarrow Br_2^{\bullet-} + O_2 + H^+$	1.1×10^8	38
58	$Br_2 + O_2^{\bullet-} \rightarrow Br_2^{\bullet-} + O_2$	5.6×10^9	38
59	$Br_2 + H_2O_2 \rightarrow 2Br^- + O_2 + 2H^+$	1.3×10^3	113
60	$Br_3^- + HO_2^\bullet \rightarrow Br_2^{\bullet-} + Br^- + H^+ + O_2$	1.0×10^7	38
61	$Br_3^- + O_2^{\bullet-} \rightarrow Br_2^{\bullet-} + Br^- + O_2$	3.8×10^9	38
62	$BrOH^{\bullet-} + Br^- \rightarrow Br_2^{\bullet-} + OH^-$	2.0×10^8	115
	Reactions of BrO_x		
63	$BrO_2^- + {}^\bullet OH \rightarrow BrO_2^\bullet + OH^-$	1.9×10^9	42
64	$BrO_2^- + Br_2^{\bullet-} \rightarrow OBr^- + BrO^\bullet + Br^-$	8.0×10^7	42
65	$BrO_2^\bullet + {}^\bullet OH \rightarrow BrO_3^- + H^+$	2.0×10^9	116
	Reactions of mixed-halogen species		
66	$HOBr + Cl^- \rightarrow BrCl + OH^-$	5.6×10^2	117
67	$HOCl + Br^- \rightarrow BrCl + OH^-$	1.3×10^{-1}	117
68	$BrCl + H_2O \rightarrow HOBr + Cl^- + H^+$	1.8×10^3	38
69	$BrCl + Cl^- \rightarrow BrCl_2^-$	1.0×10^6	118
70	$BrCl_2^- \rightarrow BrCl + Cl^-$	1.2×10^6	118
71	$BrCl + Br^- \rightarrow Br_2Cl^-$	3.0×10^8	38
72	$Br_2Cl^- \rightarrow BrCl + Br^-$	1.7×10^4	38
73	$Br_2 + Cl^- \rightarrow Br_2Cl^-$	5.0×10^4	38
74	$Br_2Cl^- \rightarrow Br_2 + Cl^-$	3.8×10^4	38
75	$Cl_2 + Br^- \rightarrow BrCl_2^-$	6.0×10^9	118
76	$BrCl_2^- \rightarrow Cl_2 + Br^-$	9.0×10^3	118
77	$Br_2Cl^- + Cl^- \rightarrow BrCl_2^- + Br^-$	1.0×10^5	38
78	$BrCl_2^- + Br^- \rightarrow Br_2Cl^- + Cl^-$	3.0×10^8	118
79	$BrOH^{\bullet-} + Cl^- \rightarrow BrCl^{\bullet-} + OH^-$	1.9×10^8	38
80	$Br^\bullet + Cl^- \rightarrow BrCl^{\bullet-}$	1.0×10^8	38
81	$BrCl^{\bullet-} + {}^\bullet OH \rightarrow BrCl + OH^-$	1.0×10^9	38
82	$BrCl^{\bullet-} + OH^- \rightarrow ClOH^{\bullet-} + Br^-$	3.0×10^6	38
83	$BrCl^{\bullet-} + OH^- \rightarrow BrOH^{\bullet-} + Cl^-$	2.0×10^7	38
84	$BrCl^{\bullet-} + BrCl^{\bullet-} \rightarrow Br^- + Cl^- + BrCl$	4.7×10^9	38

85	$BrCl^{\bullet-} \rightarrow Cl^{\bullet} + Br^{-}$	2.0×10^{3}	119
86	$BrCl^{\bullet-} \rightarrow Br^{\bullet} + Cl^{-}$	6.1×10^{4}	119
	Reactions of reactive species with probe compounds		
87	$^{\bullet}O^{-} + C_6H_5COO^{-} \rightarrow$ product	4.0×10^{7}	120
	Reactions with phosphate buffer		
88	$^{\bullet}OH + HPO_4^{2-} \rightarrow HPO_4^{\bullet-} + OH^{-}$	1.5×10^{5}	86,110
89	$^{\bullet}OH + H_2PO_4^{-} \rightarrow HPO_4^{\bullet-} + H_2O$	2.0×10^{4}	110
90	$^{\bullet}OH + H_3PO_4 \rightarrow H_2PO_4^{\bullet} + H_2O$	1.4×10^{6}	121,122
91	$H_2PO_4^{-} + H^{+} \rightarrow H_3PO_4$	5.0×10^{10}	86
92	$H_3PO_4 \rightarrow H^{+} + H_2PO_4^{-}$	4.0×10^{8}	86
93	$HPO_4^{2-} + H^{+} \rightarrow H_2PO_4^{-}$	5.0×10^{10}	86
94	$H_2PO_4^{-} \rightarrow HPO_4^{\bullet-} + H^{+}$	3.2×10^{3}	86
95	$PO_4^{3-} + H^{+} \rightarrow HPO_4^{2-}$	5.0×10^{10}	86
96	$HPO_4^{2-} \rightarrow PO_4^{3-} + H^{+}$	2.5×10^{-2}	86

[a]The photolysis rate for each reaction were calculated using following equation. $\frac{dC}{dt} = \frac{E_P^0[1\text{-}10^{-\varepsilon Cd}]\cdot\Phi}{d}$; C: concentration of oxidant (M), E_P^0 : photon flux at 254 nm (mEinstein $s^{-1}cm^{-2}$), ε_{254}: molar extinction coefficient ($M^{-1}cm^{-1}$), Φ^{int}: intrinsic quantum yield (mol $Einstein^{-1}$), *d*: pathlength (cm)

Table S6. Summary of *k* values for the reactions of •OH, Cl•, and Br• with chlorine and bromine species.

Reaction	*k* from this study, $M^{-1}s^{-1}$	*k* from literature, $M^{-1}s^{-1}$	Reference
•OH + HOCl	$1.4(\pm0.2)\times10^{8}$ [a]	$(1.1–1.4)\times10^{8}$	(Zuo et al. 1997)[123]
		2.0×10^{9}	(Matthew and Anastasio 2006)[38]
		8.5×10^{4}	(Watts and Linden 2007)[60]
		5.0×10^{8}	(Chuang et al. 2017)[45]
		1.2×10^{9}	(Bulman et al. 2019)[37]
•OH + OCl^-	$2.0(\pm0.5)\times10^{9}$ [a]	9.0×10^{9}	(Buxton and Subhani 1972)[101]
		9.8×10^{9}	(Buxton and Subhani 1972)[30]
		8×10^{9}	(Nowell and Hoigné 1992)[124]
		2.7×10^{9}	(Zuo et al. 1997)[123]
		1.9×10^{9}	(Chuang et al. 2017)[45]
		6.4×10^{9}	(Bulman et al. 2019)[37]
Cl• + HOCl	$3.0(\pm0.3)\times10^{9}$ [b]	3.0×10^{9}	(Kläning and Wolff 1985)[40]
Cl• + OCl^-	$1.0(\pm0.5)\times10^{10}$ [b]	8.2×10^{9}	(Kläning and Wolff 1985)[40]
•OH + HOBr	1.0×10^{9} [c]	2.0×10^{9}	(Buxton et al. 1988)[42]
•OH + OBr^-	ND [d]	4.5×10^{9}	(Buxton and Dainton 1968)[98]
Br• + HOBr	$<1.0\times10^{6}$ [c]	no apparent reactivity	(Kläning and Wolff 1985)[40]
Br• + OBr^-	ND [d]	4.1×10^{9}	(Kläning and Wolff 1985)[40]

[a]Determined by a competition kinetics method with NB and *tert*-butanol (SI-Text-8 and Figure S7a). [b]Determined by a competition kinetics method with BA and *tert*-butanol (SI-Text-8 and Figure S7b). [c]Estimated by fitting the NB and BA degradation data at pH 6 in the UV/bromine system with the kinetics model prediction (Figure S14). [d]Not determined in this study.

685 **Table S7.** Reactions used for kinetic modeling of the UV/chlorine system in this study and previous studies.

	Reaction and rate constants (Unit : $M^{-1}s^{-1}$ or s^{-1})	This study [a]	Bulman et al., 2019 [37]	Chuang et al., 2017 [45]	Fang et al., 2014 [47]	Guo et al., 2017 [48]	Li et al., 2017 [49]	Sun et al., 2016 [50]	Wu et al., 2016 [51]
Photolysis of chlorine species and ozone [b]									
1	$HOCl \xrightarrow{h\nu} {}^{\bullet}OH + Cl^{\bullet}$	$\frac{dC}{dt} = \frac{E_P^0[1\text{-}10^{-\varepsilon C d}]\cdot\Phi}{d}$							
2	$OCl^- \xrightarrow{h\nu} {}^{\bullet}O^- + Cl^{\bullet}$	C: concentration of oxidant (M)							
3	$OCl^- \xrightarrow{h\nu} O(^1D) + Cl^-$	E_P^0 : photon flux at 254 nm (mEinstein $s^{-1}cm^{-2}$)							
4	$OCl^- \xrightarrow{h\nu} O(^3P) + Cl^-$	ε_{254}: molar extinction coefficient ($M^{-1}cm^{-1}$)							
		Φ: quantum yield (mol $Einstein^{-1}$)							
		d: pathlength (cm)							
5	$O_3 \xrightarrow{h\nu} 0.91O(^1D) + 0.09O(^3P) + O_2$								
Reactions of oxygen atoms ($O(^1D)$ and $O(^3P)$)									
6	$O(^1D) + H_2O \rightarrow H_2O_2$ (hot) $\rightarrow 0.9H_2O_2 + 0.2{}^{\bullet}OH$	1.8×10^{10}							
7	$O(^3P) + O_2 \rightarrow O_3$	4.0×10^{9}	4.0×10^{9}						
Reactions of ozone									
8	$O_3 + OCl^- \rightarrow 2O_2 + Cl^-$	1.1×10^{2}	1.1×10^{2}						
9	$O_3 + OCl^- \rightarrow O_2 + ClO_2^-$	30	30						
Reactions of ${}^{\bullet}OH$ and $Cl^{\bullet}$ with chlorine species and $ClO^{\bullet}$ formation									
10	$HOCl + {}^{\bullet}OH \rightarrow ClO^{\bullet} + H_2O$	1.4×10^{8}	1.2×10^{9}	5.0×10^{8}	2.0×10^{9}	2.0×10^{9}	2.0×10^{9}	2.0×10^{9}	2.0×10^{9}
11	$OCl^- + {}^{\bullet}OH \rightarrow ClO^{\bullet} + OH^-$	2.0×10^{9}	6.4×10^{9}	1.9×10^{9}	8.8×10^{9}	8.8×10^{9}	8.8×10^{9}	8.8×10^{9}	8.8×10^{9}
12	$HOCl + {}^{\bullet}Cl \rightarrow ClO^{\bullet} + H^+ + Cl^-$	3.0×10^{9}	3.0×10^{9}	3.0×10^{9}	3.0×10^{9}	3.0×10^{9}	3.0×10^{9}	3.0×10^{9}	3.0×10^{9}
13	$OCl^- + {}^{\bullet}Cl \rightarrow ClO^{\bullet} + Cl^-$	1.0×10^{10}	8.3×10^{9}	8.3×10^{9}	8.2×10^{9}	8.3×10^{9}	8.3×10^{9}	8.3×10^{9}	8.2×10^{9}
14	$OCl^- + Cl_2^{\bullet-} \rightarrow ClO^{\bullet} + 2Cl^-$	2.9×10^{8}	2.9×10^{8}						
Reactions of ${}^{\bullet}OH$ with Cl^-									
15	$^{\bullet}OH + Cl^- \rightarrow ClOH^{\bullet-}$	4.3×10^{9}	3.7×10^{9}	4.3×10^{9}	4.3×10^{9}	4.3×10^{9}	4.3×10^{9}	4.3×10^{9}	
16	$Cl^{\bullet} + OH^- \rightarrow ClOH^{\bullet-}$	1.8×10^{10}	1.8×10^{10}	1.8×10^{10}	1.8×10^{10}	1.8×10^{10}	1.8×10^{10}	1.8×10^{10}	1.8×10^{10}
17	$Cl^{\bullet} + H_2O \rightarrow ClOH^{\bullet-} + H^+$	2.5×10^{5}	2.1×10^{5}	2.5×10^{5}		4.5×10^{3}	2.5×10^{5}	4.5×10^{3}	2.5×10^{5}
18	$ClOH^{\bullet-} \rightarrow {}^{\bullet}OH + Cl^-$	6.1×10^{9}	6.1×10^{9}	6.1×10^{9}	6.1×10^{9}	6.1×10^{9}	6.1×10^{9}	6.1×10^{9}	6.1×10^{9}
19	$ClOH^{\bullet-} \rightarrow OH^- + Cl^{\bullet}$	23							
20	$ClOH^{\bullet-} + H^+ \rightarrow Cl^{\bullet} + H_2O$	2.1×10^{10}	2.1×10^{10}	2.1×10^{10}	2.1×10^{10}	2.1×10^{10}	2.1×10^{10}	2.1×10^{10}	2.1×10^{10}

Reactions of $Cl_2^{\bullet-}$									
21	$Cl^\bullet + Cl^- \rightarrow Cl_2^{\bullet-}$	6.5×10^9	1.2×10^{10}	8.0×10^9	6.5×10^9	8.5×10^9	8.5×10^9	8.5×10^9	6.5×10^9
22	$Cl_2^{\bullet-} \rightarrow Cl^\bullet + Cl^-$	1.1×10^5	6.0×10^4	6.0×10^4	1.1×10^5	6.0×10^4	6.0×10^4	6.0×10^4	1.1×10^5
23	$Cl_2^{\bullet-} + OH^- \rightarrow ClOH^{\bullet-} + Cl^-$	4.5×10^7	4.5×10^7	4.5×10^7	4.5×10^7	4.5×10^7	4.5×10^7	4.5×10^7	4.5×10^7
24	$ClOH^{\bullet-} + Cl^- \rightarrow OH^- + Cl_2^{\bullet-}$	1.0×10^4	1.0×10^4	1.0×10^4	1.0×10^5	1.0×10^5	1.0×10^4		1.0×10^5
25	$2Cl_2^{\bullet-} \rightarrow Cl_2 + 2Cl^-$	9.0×10^8	9.0×10^8	9.0×10^8		8.3×10^8	9.0×10^8	9.0×10^8	
26	$2Cl_2^{\bullet-} \rightarrow Cl_3^- + Cl^-$	4.1×10^9	4.1×10^9						2.0×10^9
Reactions of chlorine species with H_2O_2 and peroxyl radicals ($HO_2^\bullet$ and $O_2^{\bullet-}$)									
27	$HOCl + H_2O_2 \rightarrow O_2 + H_2O + Cl^- + H^+$	1.1×10^4	1.1×10^4	1.1×10^4		1.1×10^4	1.1×10^4	1.1×10^4	
28	$HOCl + O_2^{\bullet-} \rightarrow {}^\bullet OH + O_2 + Cl^-$	7.5×10^6	7.5×10^6						
29	$HOCl + O_2^{\bullet-} \rightarrow {}^\bullet Cl + O_2 + OH^-$	7.5×10^6	7.5×10^6	7.5×10^6		7.5×10^6	7.5×10^6	7.5×10^6	
30	$HOCl + HO_2^- \rightarrow O_2 + H_2O + Cl^-$	4.4×10^7							
31	$HOCl + HO_2^\bullet \rightarrow Cl^\bullet + OH^- + O_2$	7.5×10^6	7.5×10^6	7.5×10^6		7.5×10^6	7.5×10^6	7.5×10^6	
32	$OCl^- + H_2O_2 \rightarrow O_2 + H_2O + Cl^-$	1.7×10^5	1.7×10^5	1.7×10^5		1.7×10^5	1.7×10^5	1.7×10^5	
33	$OCl^- + O_2^{\bullet-} + H_2O \rightarrow Cl^\bullet + O_2 + 2OH^-$	2.0×10^8	2.0×10^8	2.0×10^8		2.0×10^8	2.0×10^8	2.0×10^8	
Reactions of $ClO^\bullet$ and formation of ClO_3^-									
34	$2ClO^\bullet \rightarrow Cl_2O_2$	2.5×10^9	5.0×10^9	2.5×10^9		2.5×10^9		2.5×10^9	2.5×10^9
35	$Cl_2O_2 + H_2O \rightarrow OCl^- + ClO_2^- + 2H^+$	1.0×10^4	1.0×10^4	1.0×10^4					
36	$Cl_2O_2 + H_2O \rightarrow Cl^- + O_2 + OCl^- + 2H^+$	5.2×10^3							
37	$ClO_2^- + ClO^\bullet \rightarrow ClO_2^\bullet + OCl^-$	9.4×10^8	9.4×10^8	9.4×10^8		9.4×10^8			
38	$ClO_2^\bullet + ClO^\bullet \rightarrow Cl_2O_3$	7.4×10^9							
39	$Cl_2O_3 + H_2O \rightarrow ClO_3^- + OCl^- + 2H^+$	1.0×10^4							
Reactions of reactive species with probe compounds									
40	${}^\bullet OH + C_6H_5NO_2$ (NB) $\rightarrow$ product	3.8×10^9	4.6×10^9		3.9×10^9				
41	${}^\bullet OH + C_6H_5COO^-$ (BA) $\rightarrow$ product	5.9×10^9	5.3×10^9	5.9×10^9	5.9×10^9				
42	$Cl^\bullet + C_6H_5COO^-$ (BA) $\rightarrow$ product	1.8×10^{10}	1.8×10^{10}	1.8×10^{10}	1.8×10^{10}				
43	$ClO^\bullet + C_6H_5COO^-$ (BA) $\rightarrow$ product	5×10^5	3.0×10^6						
44	$Cl_2^{\bullet-} + C_6H_5COO^-$ (BA) $\rightarrow$ product	2.0×10^6	2.0×10^6	2.0×10^6	2.0×10^6				
Reactions of ${}^\bullet OH$ and $Cl^\bullet$ with tert-butanol									
45	${}^\bullet OH + (CH_3)_3COH \rightarrow H_2O + {}^\bullet CH_2C(CH_3)_2OH$	6.0×10^8							
46	${}^\bullet O^- + (CH_3)_3COH \rightarrow OH^- + {}^\bullet CH_2C(CH_3)_2OH$	5.0×10^8							

47	$Cl^{\bullet} + (CH_3)_3COH \rightarrow H^+ + Cl^- + {}^{\bullet}CH_2C(CH_3)_2OH$	1.5×10^9							
48	$Cl^{\bullet} + (CH_3)_3COH \rightarrow H^+ + Cl^- + (CH_3)_3CO^{\bullet}$	7.0×10^8							
49	${}^{\bullet}CH_2C(CH_3)_2OH + O_2 \rightarrow {}^{\bullet}OOCH_2C(CH_3)_2OH$	1.4×10^9							
50	$2{}^{\bullet}OOCH_2C(CH_3)_2OH \rightarrow O_2 + HOC(CH_3)_2CH_2OH + HOC(CH_3)_2CHO$	8.0×10^7							
51	$2{}^{\bullet}OOCH_2C(CH_3)_2OH \rightarrow H_2O_2 + 2HOC(CH_3)_2CHO$	1.2×10^8							
52	$2{}^{\bullet}OOCH_2C(CH_3)_2OH \rightarrow O_2 + 2CH_2O + 2{}^{\bullet}C(CH_3)_2OH$	1.0×10^8							
53	$2{}^{\bullet}OOCH_2C(CH_3)_2OH \rightarrow O_2 + HO(CH_3)_2CCH_2OOCH_2C(CH_3)_2OH$	1.0×10^8							
54	${}^{\bullet}C(CH_3)_2OH + O_2 \rightarrow {}^{\bullet}OOC(CH_3)_2OH$	2.0×10^9							
55	${}^{\bullet}OOC(CH_3)_2OH \rightarrow (CH_3)_2CO + HO_2{}^{\bullet}$	6.0×10^2							
Equilibrium reactions of chlorine species, ${}^{\bullet}OH$, $HO_2{}^{\bullet}$, and H_2O_2									
56	$H^+ + OCl^- \rightarrow HOCl$	1.0×10^{11}	5.0×10^{10}	5.0×10^{10}	5.0×10^{10}	5.0×10^{10}		5.0×10^{10}	5.0×10^{10}
57	$HOCl \rightarrow H^+ + OCl^-$	3.8×10^4	1.4×10^3	1.4×10^3	1.4×10^3	1.6×10^3		1.4×10^3	1.6×10^3
58	${}^{\bullet}O^- + H^+ \rightarrow {}^{\bullet}OH$	1.0×10^{11}							
59	${}^{\bullet}OH \rightarrow {}^{\bullet}O^- + H^+$	1.3×10^{-1}							
60	${}^{\bullet}OH + OH^- \rightarrow O^{\bullet-} + H_2O$	1.2×10^{10}	1.3×10^{10}	1.2×10^{10}	1.3×10^{10}		1.2×10^{10}		
61	${}^{\bullet}O^- + H_2O \rightarrow {}^{\bullet}OH + OH^-$	9.3×10^7	9.4×10^7		1.8×10^6	1.8×10^6	1.8×10^5	1.8×10^6	1.8×10^6
62	$O_2{}^{\bullet-} + H^+ \rightarrow HO_2{}^{\bullet}$	1.0×10^{11}	1.6×10^5			7.0×10^5	1.6×10^5	7.9×10^5	
63	$HO_2{}^{\bullet} \rightarrow O_2{}^{\bullet-} + H^+$	2.0×10^6	5.0×10^{10}	5.0×10^{10}		5.0×10^{10}	5.0×10^{10}	5.0×10^{10}	
64	$HO_2^- + H^+ \rightarrow H_2O_2$	1.0×10^{11}	1.3×10^{-1}	1.3×10^{-1}		1.3×10^{-1}	1.3×10^{-1}	1.3×10^{-1}	
65	$H_2O_2 \rightarrow HO_2^- + H^+$	2.5×10^{-1}							
66	$C_6H_5COO^- + H^+ \rightarrow C_6H_5COOH$	1.00×10^{11}							
67	$C_6H_5COOH \rightarrow C_6H_5COO^- + H^+$	6.31×10^6							

Photolysis reactions

68	$H_2O_2 \xrightarrow{h\nu} {}^{\bullet}OH + {}^{\bullet}OH$	$\frac{dC}{dt} = \frac{E_P^0[1\text{-}10^{-\varepsilon C d}]\cdot\Phi}{d}$ C: concentration of oxidant (M) E_P^0 : photon flux at 254 nm (mEinstein $s^{-1}cm^{-2}$) ε_{254}: molar extinction coefficient ($M^{-1}cm^{-1}$) Φ: quantum yield (mol $Einstein^{-1}$) d: pathlength (cm)
69	$HO_2^- \xrightarrow{h\nu} {}^{\bullet}OH + {}^{\bullet}O^-$	
70	$O_3 \xrightarrow{h\nu} O(^1D) + O_2$	

Reactions of chlorine and reactive chlorine species (RCS)							
71	$HOCl + Cl^- + H^+ \rightarrow Cl_2 + H_2O$	2.1×10^{-2}		1.8×10^{-1}		1.8×10^{-1}	4.3×10^{4}
72	$HOCl + Cl^- \rightarrow Cl_2OH^-$	1.5×10^{4}			1.5×10^{4}		
73	$Cl_2 + H_2O \rightarrow HOCl + Cl^- + H^+$	2.2×10	1.5×10	2.7×10^{-1}	2.2	2.7×10^{-1}	2.2×10
74	$Cl_2 + OH^- \rightarrow HOCl + Cl^-$	1.0×10^{9}		1.0×10^{9}			
75	$^{\bullet}OH + Cl_2^{\bullet-} \rightarrow HOCl + Cl^-$	1.0×10^{9}	1.0×10^{9}		1.0×10^{9}		
76	$^{\bullet}OH + Cl_2 \rightarrow HOCl + Cl^-$					1.0×10^{9}	
77	$^{\bullet}OH + Cl^- \rightarrow Cl^{\bullet} + OH^-$	1.1×10^{9}				4.3×10^{9}	
78	$Cl^{\bullet} + H_2O_2 \rightarrow HO_2^{\bullet} + Cl^- + H^+$	2.0×10^{9}	2.0×10^{9}	2.0×10^{9}	2.0×10^{9}	2.0×10^{9}	
79	$Cl^{\bullet} + Cl_2^{\bullet-} \rightarrow Cl_2 + Cl^-$	2.1×10^{9}	2.1×10^{9}	2.1×10^{9}	2.1×10^{9}	2.1×10^{9}	
80	$Cl^{\bullet} + Cl_2 \rightarrow Cl_3^{\bullet}$	5.3×10^{8}			5.3×10^{8}		
81	$Cl^{\bullet} + Cl^{\bullet} \rightarrow Cl_2$	8.8×10^{7}	8.8×10^{7}	8.8×10^{7}	8.8×10^{7}	8.8×10^{7}	1.2×10^{10}
82	$Cl_2^{\bullet-} + H_2O_2 \rightarrow HO_2^{\bullet} + 2Cl^- + H^+$	1.4×10^{5}	1.4×10^{5}	1.4×10^{5}	1.4×10^{5}	1.4×10^{5}	
83	$Cl_2^{\bullet-} + H_2O \rightarrow H_2OCl + Cl^-$	1.3×10^{3}			1.3×10^{3}		
84	$Cl_2^{\bullet-} + H_2O \rightarrow Cl^- + ClOH^{\bullet-}$		1.3×10^{3}	2.3×10			
85	$Cl_2^{\bullet-} + HO_2^{\bullet} \rightarrow O_2 + 2Cl^- + H^+$	2.8×10^{9}	3.0×10^{9}	3.0×10^{9}	3.1×10^{9}	3.0×10^{9}	
86	$Cl_2^{\bullet-} + HO_2^{\bullet} \rightarrow Cl^- + H_2OCl$					2.3×10	
87	$Cl_2^{\bullet-} + O_2^{\bullet-} \rightarrow O_2 + 2Cl^-$	2.0×10^{9}	2.0×10^{9}	1.0×10^{9}	2.0×10^{9}	2.0×10^{9}	
88	$H_2O_2 + Cl_2 \rightarrow 2Cl^- + 2H^+ + O_2$	1.3×10^{4}	1.3×10^{4}	1.3×10^{4}	1.3×10^{4}	1.3×10^{4}	
89	$HO_2^{\bullet} + Cl_3^- \rightarrow Cl_2^{\bullet-} + HCl + O_2$	1.0×10^{9}	1.0×10^{9}	1.0×10^{9}	1.0×10^{9}	1.0×10^{9}	
90	$HO_2^{\bullet} + Cl_2 \rightarrow Cl_2^{\bullet-} + H^+ + O_2$	1.0×10^{9}	1.0×10^{9}	1.0×10^{9}	1.0×10^{9}	1.0×10^{9}	
91	$O_2^{\bullet-} + Cl_3^- \rightarrow Cl_2^{\bullet-} + Cl^- + O_2$	3.8×10^{9}	3.8×10^{9}	3.8×10^{9}	3.8×10^{9}	3.8×10^{9}	
92	$O_2^{\bullet-} + Cl_2 \rightarrow Cl_2^{\bullet-} + O_2$	1.0×10^{9}	1.0×10^{9}	1.0×10^{9}	1.0×10^{9}	1.0×10^{9}	
93	$O_2^{\bullet-} + Cl^- \rightarrow$ products	1.4×10^{2}					
94	$^{\bullet}O^- + OCl^- + H_2O \rightarrow ClO^{\bullet} + 2OH^-$	2.3×10^{8}					
95	$Cl_2 + Cl^- \rightarrow Cl_3^-$	2.0×10^{4}	2.0×10^{4}	2.0×10^{4}	2.0×10^{4}	2.0×10^{4}	
96	$H_2ClO^{\bullet} \rightarrow ClOH^{\bullet-} + H^+$	1.0×10^{8}	1.0×10^{8}	1.0×10^{8}	1.0×10^{8}	1.0×10^{8}	
97	$H_2ClO^{\bullet} + Cl^- \rightarrow Cl_2^{\bullet-} + H_2O$	5.0×10^{9}		5.0×10^{9}	5.0×10^{9}	5.0×10^{9}	
98	$H_2ClO^{\bullet} \rightarrow Cl^{\bullet} + H_2O$	1.0×10^{2}		1.0×10^{2}	1.0×10^{2}	1.0×10^{2}	
99	$Cl_2OH^- \rightarrow HOCl + Cl^-$	5.5×10^{9}			5.5×10^{9}		
100	$Cl_3^- \rightarrow Cl_2 + Cl^-$	1.1×10^{5}	1.1×10^{5}	1.1×10^{5}	1.1×10^{5}	1.1×10^{5}	
Reactions of reactive oxygen species and ozone							
101	$O(^1D) + H_2O \rightarrow 2^{\bullet}OH$	1.2×10^{11}					
102	$O(^3P) + OCl^- \rightarrow ClO_2^-$	9.4×10^{9}					

103	$O(^3P) + H_2O_2 \rightarrow {}^\bullet OH + HO_2^\bullet$	1.6×10^{9}						
104	$O(^3P) + HO_2^- \rightarrow {}^\bullet OH + O_2^{\bullet-}$	5.3×10^{9}						
105	$O(^3P) + ClO_4^- \rightarrow$ products	6.0×10^{5}						
106	$O(^3P) + OH^- \rightarrow HO_2^-$	4.2×10^{8}						
107	$O_3 \rightarrow O_2 + O(^3P)$	4.5×10^{-6}						
108	$O_3 + OH^- \rightarrow O_2 + HO_2^-$	7.0×10						
109	$O_3 + HO_2^- \rightarrow O_3^{\bullet-} + HO_2^\bullet$	5.5×10^{6}						
110	$O_3 + HO_2^\bullet \rightarrow H^+ + O_2 + O_3^{\bullet-}$	1.6×10^{9}						
111	$O_3 + Cl^- \rightarrow O_2 + OCl^-$	1.6×10^{-3}						
112	$O_3 + H_2O_2 \rightarrow O_2 + {}^\bullet OH + HO_2^\bullet$	2.7×10^{-2}						
113	$O_3 + HO_2^- \rightarrow O_2 + {}^\bullet OH + O_2^{\bullet-}$	5.5×10^{6}						
114	$O_3 + Cl_2^{\bullet-} \rightarrow$ products	9.0×10^{7}						
115	$O_3 + O_2^{\bullet-} \rightarrow O_2 + O_3^{\bullet-}$	1.6×10^{9}						
116	$O_3 + ClO_2^\bullet \rightarrow O_2 + ClO_3^\bullet$	1.2×10^{3}						
117	$O_3 + ClO_2^- \rightarrow O_3^{\bullet-} + ClO_2^\bullet$	2.0×10^{6}						
118	$O_3 + ClO_3^- \rightarrow$ products	1.0×10^{-4}						
119	$O_3 + ClO_4^- \rightarrow$ products	2.0×10^{-5}						
120	$O_3 + H^+ \rightarrow$ products	4.0×10^{-4}						
121	$O_3^{\bullet-} \rightarrow O_2 + {}^\bullet O^-$	4.3×10^{3}				3.2×10^{3}		
122	$O_3^{\bullet-} + ClO^\bullet \rightarrow OCl^- + O_3$	1.0×10^{9}						
123	$O_3^{\bullet-} + H^+ \rightarrow O_2 + {}^\bullet OH$	9.0×10^{10}						
124	$O_3^{\bullet-} + {}^\bullet O^- \rightarrow O_4^{2-}$	7.0×10^{8}						
125	$O_3^{\bullet-} + {}^\bullet O^- \rightarrow 2O_2^{\bullet-}$	7.0×10^{8}						
126	$O_3^{\bullet-} + ClO_2^\bullet \rightarrow O_2 + ClO_3^-$	1.8×10^{5}						
127	$O_3^{\bullet-} + H^+ \rightarrow HO_3^\bullet$	5.2×10^{10}						
128	$O_3^{\bullet-} + O_3^{\bullet-} \rightarrow$ products	9.0×10^{8}						
129	$O_3^{\bullet-} + ClO_2^\bullet \rightarrow ClO_2^- + O_3$	3.2×10^{9}						
	Reactions of HO_x							
130	${}^\bullet OH + {}^\bullet OH \rightarrow H_2O_2$	5.5×10^{9}	5.5×10^{9}	5.5×10^{9}	5.5×10^{9}	3.6×10^{9}	5.5×10^{9}	5.5×10^{9}
131	${}^\bullet OH + H_2O_2 \rightarrow HO_2^\bullet + H_2O$	2.7×10^{7}	2.7×10^{7}		2.7×10^{7}	2.7×10^{7}	2.7×10^{7}	
132	${}^\bullet OH + O_2^{\bullet-} \rightarrow O_2 + OH^-$	8.5×10^{9}	7.0×10^{9}		1.0×10^{10}	7.0×10^{9}	7.0×10^{9}	
133	${}^\bullet OH + HO_2^\bullet \rightarrow O_2 + H_2O$	7.5×10^{9}	6.6×10^{9}		7.1×10^{9}	6.6×10^{9}	6.6×10^{9}	
134	${}^\bullet OH + HO_2^- \rightarrow H_2O + O_2^{\bullet-}$	7.1×10^{9}						
135	${}^\bullet OH + HO_2^- \rightarrow HO_2^\bullet + OH^-$		7.5×10^{9}		7.5×10^{9}	7.5×10^{9}	7.5×10^{9}	

136	$^{\bullet}OH + {}^{\bullet}O^{-} \rightarrow HO_2^{-}$	2.0×10^{10}			1.0×10^{10}	
137	$^{\bullet}OH + H_2 \rightarrow H_2O + H^{\bullet}$	4.6×10^{7}				
138	$^{\bullet}OH + O_3^{\bullet-} \rightarrow HO_2 + O_2^{\bullet-}$	8.5×10^{9}				
139	$^{\bullet}OH + H_2O_2 + \rightarrow O_2 + H^{+} + H_2O$	1.2×10^{10}				
140	$^{\bullet}OH + O_3 \rightarrow O_2 + HO_2^{\bullet}$	1.1×10^{8}				
141	$H_2O_2 + HO_2^{\bullet} \rightarrow O_2 + {}^{\bullet}OH + H_2O$	3.0	3.0	3.0	3.0	3.0
142	$H_2O_2 + {}^{\bullet}O^{-} \rightarrow O_2^{\bullet-} + H_2O$	4.0×10^{8}			4.0×10^{8}	
143	$H_2O_2 + O_2^{\bullet-} \rightarrow O_2 + {}^{\bullet}OH + OH^{-}$	6.7×10^{-1}	1.3×10^{-1}	1.3×10^{-1}	1.3×10^{-1}	1.3×10^{-1}
144	$HO_2^{-} + {}^{\bullet}O^{-} + H_2O \rightarrow HO_2^{\bullet} + 2OH^{-}$	5.0×10^{8}				
145	$HO_2^{-} + {}^{\bullet}O^{-} \rightarrow {}^{\bullet}OH + O_2^{\bullet-}$	4.0×10^{8}			4.0×10^{8}	
146	$HO_2^{-} + O_2^{\bullet-} \rightarrow O_2 + H_2O_2$	2.0				9.7×10^{7}
147	$HO_2^{\bullet} + H_2 \rightarrow H_2O_2 + H^{\bullet}$	1.0				
148	$HO_2^{\bullet} + O_2^{\bullet-} + H_2O \rightarrow H_2O_2 + O_2 + OH^{-}$	9.7×10^{7}				
149	$HO_2^{\bullet} + O_2^{\bullet-} \rightarrow HO_2^{-} + O_2$		9.7×10^{7}	9.7×10^{7}	9.7×10^{7}	
150	$HO_2^{\bullet} + HO_2^{\bullet} \rightarrow H_2O_2 + O_2$	1.2×10^{7}	8.3×10^{5}	8.3×10^{9}	8.3×10^{5}	8.3×10^{9}
151	$O_2^{\bullet-} + {}^{\bullet}O^{-} + H_2O \rightarrow O_2 + 2OH^{-}$	6.0×10^{8}				
152	$O_2^{\bullet-} + {}^{\bullet}O^{-} + H^{+} \rightarrow OH^{-} + O_2$				6.0×10^{8}	
153	$^{\bullet}O^{-} + O_2 \rightarrow O_3^{\bullet-}$	3.5×10^{9}			3.6×10^{9}	
154	$^{\bullet}O^{-} + {}^{\bullet}O^{-} \rightarrow O_2^{2-}$	4.7×10^{9}				
	Reactions of Cl_xO_x					
155	$ClO^{\bullet} + {}^{\bullet}OH \rightarrow ClO_2^{-} + H^{+}$	1.0×10^{9}		1.0×10^{9}		
156	$ClO^{\bullet} + ClO^{\bullet} + H_2O + OH^{-} \rightarrow HOCl + HClO_2$	2.5×10^{9}		2.5×10^{9}		
157	$ClO^{\bullet} + ClO^{\bullet} + H_2O \rightarrow HOCl + H^{+} + ClO_2^{-}$	2.5×10^{9}		2.5×10^{9}		
158	$ClO_2^{-} + {}^{\bullet}OH \rightarrow OH^{-} + ClO_2^{\bullet}$	4.5×10^{9}	7.0×10^{9}	6.3×10^{9}		
159	$ClO_2^{-} + Cl^{\bullet} \rightarrow ClO_2^{\bullet} + Cl^{-}$	7.0×10^{9}	7.0×10^{9}			
160	$ClO_2^{-} + O_2^{\bullet-} \rightarrow$ products	4.0×10				
161	$ClO_2^{-} + {}^{\bullet}O^{-} \rightarrow OH^{-} + ClO_2^{\bullet}$	2.0×10^{8}				
162	$ClO_2^{\bullet} + {}^{\bullet}OH \rightarrow ClO_3^{-} + H^{+}$	4.0×10^{9}	4.0×10^{9}	4.0×10^{9}		
163	$ClO_2^{\bullet} + Cl^{\bullet} \rightarrow$ products	1.0×10^{9}	1.0×10^{9}			
164	$ClO_2^{\bullet} + Cl_2^{\bullet-} \rightarrow$ products	1.0×10^{9}		1.3×10^{8}		
165	$ClO_2^{\bullet} + HO_2^{-} \rightarrow HO_2^{\bullet} + ClO_2^{-}$	9.6×10^{4}				
166	$ClO_2^{\bullet} + HO_2^{\bullet} \rightarrow$ products	1.0×10^{6}				
167	$ClO_2^{\bullet} + O_2^{\bullet-} \rightarrow O_2 + ClO_2^{-}$	3.2×10^{9}				
168	$ClO_2^{\bullet} + {}^{\bullet}O^{-} \rightarrow ClO_3^{-}$	2.7×10^{9}				
169	$ClO_2^{\bullet} \rightarrow O_2 + Cl^{\bullet}$	6.7×10^{9}				

170	$ClO_3^- + {}^\bullet OH \rightarrow$ products	1.0×10^{6}	1.0×10^{6}			
171	$ClO_3^- + Cl^\bullet \rightarrow$ products	1.0×10^{6}	1.0×10^{6}			
172	$ClO_3^- + O_2^{\bullet-} \rightarrow$ products	3.0×10^{-3}			3.2×10^{3}	
	Reactions of reactive species with probe compounds					
173	$H^\bullet + C_6H_5NO_2 \rightarrow$ products	1.7×10^{9}				
174	$O_3 + C_6H_5NO_2 \rightarrow$ products	9.0×10^{-2}				
175	$Cl^\bullet + C_6H_5COOH \rightarrow$ products	1.8×10^{10}	1.8×10^{10}	1.8×10^{10}		
176	${}^\bullet OH + C_6H_5COOH \rightarrow$ products	3.3×10^{9}	4.3×10^{9}			
177	$Cl_2^{\bullet-} + C_6H_5COOH \rightarrow$ products		1.5×10^{6}			
178	$H^\bullet + C_6H_5COOH \rightarrow$ products	9.2×10^{8}				
179	${}^\bullet O^- + C_6H_5COO^- \rightarrow$ products	4.0×10^{7}	4.0×10^{7}	4.0×10^{7}		
180	$H^\bullet + C_6H_5COO^- \rightarrow$ products	1.1×10^{9}				
181	$O_3 + C_6H_5COO^- \rightarrow$ products	1.2				
182	O_3 + cinnamic acid → benzaldehyde + glyoxylic acid + H_2O_2	3.8×10^{5}				
	Reactions of hydrogen atom					
183	$H^\bullet + {}^\bullet OH \rightarrow H_2O$	7.0×10^{9}				
184	$H^\bullet + Cl_2^{\bullet-} \rightarrow 2Cl^- + H^+$	7.5×10^{9}				
185	$H^\bullet + H_2O_2 \rightarrow H_2O + {}^\bullet OH$	5.9×10^{7}				
186	$H^\bullet + HO_2^- \rightarrow {}^\bullet OH + OH^-$	1.2×10^{9}				
187	$H^\bullet + HO_2^\bullet \rightarrow H_2O_2$	1.5×10^{10}				
188	$H^\bullet + Cl^- \rightarrow$ products	1.0×10^{5}				
189	$H^\bullet + Cl_3^{\bullet-} \rightarrow Cl^- + Cl_2^{\bullet-} + H^+$	3.0×10^{10}				
190	$H^\bullet + HOCl \rightarrow H_2O + Cl^\bullet$	5.0×10^{-12}				
191	$H^\bullet + H_2O \rightarrow {}^\bullet OH + H_2$	5.5×10^{2}				
192	$H^\bullet + O_2 \rightarrow HO_2^\bullet$	1.4×10^{10}				
193	$H^\bullet + H^\bullet \rightarrow H_2$	7.8×10^{9}				
194	$H^\bullet + O_3 \rightarrow O_2 + {}^\bullet OH$	2.2×10^{10}				
	Equilibrium reactions					
195	$H_2O \rightarrow H^+ + OH^-$	1.0×10^{-3}	1.0×10^{-3}		1.0×10^{-3}	1.0×10^{-3}	1.0×10^{-3}
196	$H^+ + OH^- \rightarrow H_2O$	1.0×10^{11}	1.0×10^{11}		1.0×10^{11}	1.0×10^{11}	1.0×10^{11}
197	$HCl \rightarrow H^+ + Cl^-$	8.6×10^{16}	8.6×10^{16}		8.6×10^{16}	8.6×10^{16}	8.6×10^{16}
198	$H^+ + Cl^- \rightarrow HCl$	5.0×10^{10}	5.0×10^{10}		5.0×10^{10}	5.0×10^{10}	5.0×10^{10}

Reactions with buffers [c]					
199	$^{\bullet}OH + HPO_4^{2-} \rightarrow HPO_4^{\bullet-} + OH^-$	1.5×10^5	1.5×10^5	1.5×10^5	1.5×10^5
200	$^{\bullet}OH + H_2PO_4^- \rightarrow HPO_4^{\bullet-} + H_2O$	2.0×10^4	2.0×10^4	2.0×10^4	2.0×10^4
201	$^{\bullet}OH + H_3PO_4 \rightarrow H_2PO_4^{\bullet} + H_2O$	1.4×10^6			
202	$H_2O_2 + HPO_4^{\bullet-} \rightarrow H_2PO_4^- + HO_2^{\bullet}$	2.7×10^7	2.7×10^7	2.7×10^7	2.7×10^7
203	$H_2O_2 + H_2PO_4^{\bullet} \rightarrow H_2PO_4^- + H^+ + H^+ + O_2^{\bullet-}$	5.5×10^7			
204	$^{\bullet}O^- + HPO_4^{2-} \rightarrow$ products	3.5×10^6			
205	$O_3 + H_2PO_4^- \rightarrow$ products	2.0×10^{-4}			
206	$H_3PO_4 + O_3 \rightarrow$ products	2.0×10^{-2}			
207	$O_3^- + H_2PO_4^- \rightarrow HPO_4^{2-} + HO_3$	9.1×10^7			
208	$H_2O + H_2PO_4^{\bullet} \rightarrow H_3PO_4 + {}^{\bullet}OH$	1.3×10^5			
209	$Cl^- + H_2PO_4^{\bullet} \rightarrow H_2PO_4^- + Cl^{\bullet}$	2.2×10^6			
210	$H_2PO_4^{\bullet} + Cl^- + H^+ \rightarrow H_3PO_4 + Cl^{\bullet}$	1.9×10^9			
211	$Cl^- + HPO_4^{\bullet-} \rightarrow$ products	1.0×10^4			
212	$H^{\bullet} + H_3PO_4 \rightarrow H_2PO_4^{\bullet} + H_2$	5.0×10^5			
213	$H^{\bullet} + H_2PO_4^- \rightarrow HPO_4^{\bullet-} + H_2$	5.0×10^5			
214	$H^{\bullet} + HPO_4^{2-} \rightarrow PO_4^{2-\bullet} + H_2$	5.0×10^4			
215	$HPO_4^{\bullet-} + HPO_4^{\bullet-} \rightarrow P_2O_8^{4-} + 2H^+$	3.0×10^8			
216	$H_2PO_4^{\bullet} + C_6H_5COOH \rightarrow$ products	2.4×10^8			
217	$H_2PO_4^- + H^+ \rightarrow H_3PO_4$	5.0×10^{10}		5.0×10^{10}	5.0×10^{10}
218	$H_3PO_4 \rightarrow H^+ + H_2PO_4^-$	4.0×10^8		3.9×10^8	4.0×10^8
219	$HPO_4^{2-} + H^+ \rightarrow H_2PO_4^-$	5.0×10^{10}		5.0×10^{10}	5.0×10^{10}
220	$H_2PO_4^- \rightarrow HPO_4^{--} + H^+$	3.2×10^3		3.2×10^3	3.2×10^3
221	$PO_4^{3-} + H^+ \rightarrow HPO_4^{2-}$	5.0×10^{10}		5.0×10^{10}	5.0×10^{10}
222	$HPO_4^{2-} \rightarrow PO_4^{3-} + H^+$	2.5×10^{-2}		2.5×10^{-2}	2.5×10^{-2}
223	$^{\bullet}OH + H_3BO_3 \rightarrow H_2BO_3^{\bullet} + H_2O$	5.0×10^4			
224	$O_3 + H_2BO_3^- \rightarrow$ products	4.0×10^{-3}			
225	$HBO_3^{2-} + O_3 \rightarrow$ products	6.0×10^{-2}			

[a]The reactions listed here (1 – 67) are the same as those in Table S3. The reactions (68 – 225) were not included in the kinetic model of this study, but used in the other models reported in literature. [b]Each photolysis rate was calculated using the photolysis parameters shown in Table S8. [c]Reactions with buffers were not added in Kintecus® since the pH could be controlled and fixed using the *'Constant File'* option.

Table S8. Summary of the molar absorption coefficients and quantum yields of chlorine species used in the kinetic modeling of the UV/chlorine system in this study and the previous studies.

		$HOCl \xrightarrow{h\nu} {}^{\bullet}OH + Cl^{\bullet}$	$OCl^{-} \xrightarrow{h\nu} {}^{\bullet}O^{-} + Cl^{\bullet}$
This study	ε_{254}	64	56
	Φ_{Ox}^{int}	0.61	0.45
Bulman et al., 2019 [37]	ε_{254}	62	60
	Φ_{Ox}^{int}	0.6–1.4[a]	0.278
Chuang et al., 2017 [45]	ε_{254}	62	60
	Φ_{Ox}^{int}	0.62	0.55
Fang et al., 2014 [47]	ε_{254}	59	66
	Φ_{Ox}^{int}	1.45	0.97
Guo et al., 2017 [48]	ε_{254}	59	66
	Φ_{Ox}^{int}	1.45	0.97
Li et al., 2017 [49]	ε_{254}	62	60
	Φ_{Ox}^{int}	0.7	0.52
Sun et al., 2016 [50]	ε_{254}	50	50
	Φ_{Ox}^{int}	1.08	1.08
Wu et al., 2016 [51]	ε_{254}	59	66
	Φ_{Ox}^{int}	1.45	0.97

[a]A value of 1.0 was used for Φ_{Ox}^{int} in the kinetic model comparison as it is the average value of reported quantum yields (range of 0.6–1.4).

Table S9. Average radical concentrations modeled for the corresponding reaction times of the UV/chlorine and UV/bromine systems using the oxidant at 140 μM.

		Modeled, mol L^{-1} [a]					
		[$^{\bullet}$OH]	[$Cl^{\bullet}$]	[$Cl_2^{\bullet-}$]	[$ClO^{\bullet}$]	[$Br^{\bullet}$]	[$BrO^{\bullet}$]
UV/Chlorine	pH 6.0	4.4×10^{-12}	1.2×10^{-13}	1.8×10^{-12}	4.3×10^{-9}	-	-
	pH 10.0	3.7×10^{-13}	1.4×10^{-14}	1.7×10^{-13}	3.6×10^{-9}	-	-
UV/Bromine	pH 6.0	5.7×10^{-13}	-		-	7.3×10^{-12}	2.9×10^{-9}
	pH 10.0	9.1×10^{-14}	-		-	1.8×10^{-14}	1.7×10^{-9}

[a]Average radical concentration during corresponding UV irradiation time with experimental data for probe compound degradation (e.g., 0–300 mJ cm^{-2} for UV/chlorine at pH 6, 0–500 mJ cm^{-2} for UV/bromine at pH 6, and 0–1250 mJ cm^{-2} for both UV/chlorine and UV/bromine at pH 10, as shown in Figure 2 in the main text).

SI-Figures

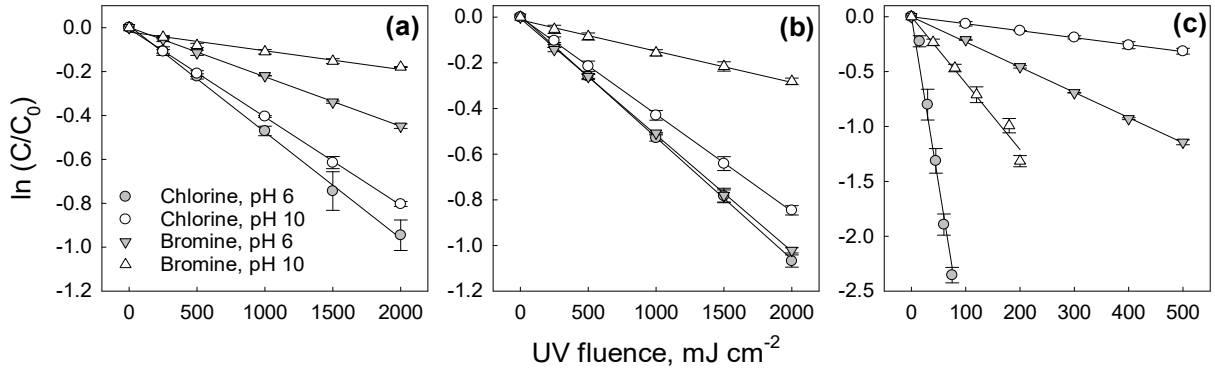

Figure S1. Logarithmic plots of the decomposition of chlorine and bromine (initial concentration = 140 μM for each) as a function of UV fluence during UV photolysis at pH 6 and pH 10 in (a) an organic-free solution and in the presence of (b) *tert*-butanol (50 mM) and (c) methanol (50 mM). The symbols show the measured data and error bars indicate one-standard deviation from triplicate measurements. Lines represent the linear regression of the data.

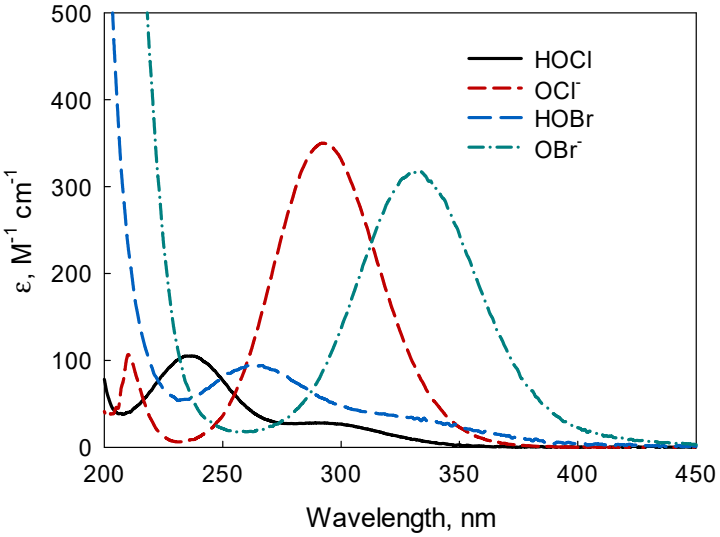

Figure S2. Wavelength-dependent molar absorption coefficients of free chlorine and bromine species in water. The following oxidant concentrations and solution pH values were used to obtain the light absorption spectra: 1.8 mM of NaOCl at pH 6 (5 mM of phosphate buffer) for HOCl, 2.0 mM of NaOCl at pH 10 (5 mM of borate buffer) for OCl^-, 0.94 mM of NaOBr at pH 6 (5 mM of phosphate buffer) for HOBr, and 0.94 mM of NaOBr at pH 11 (adjusted with NaOH) for OBr^-.

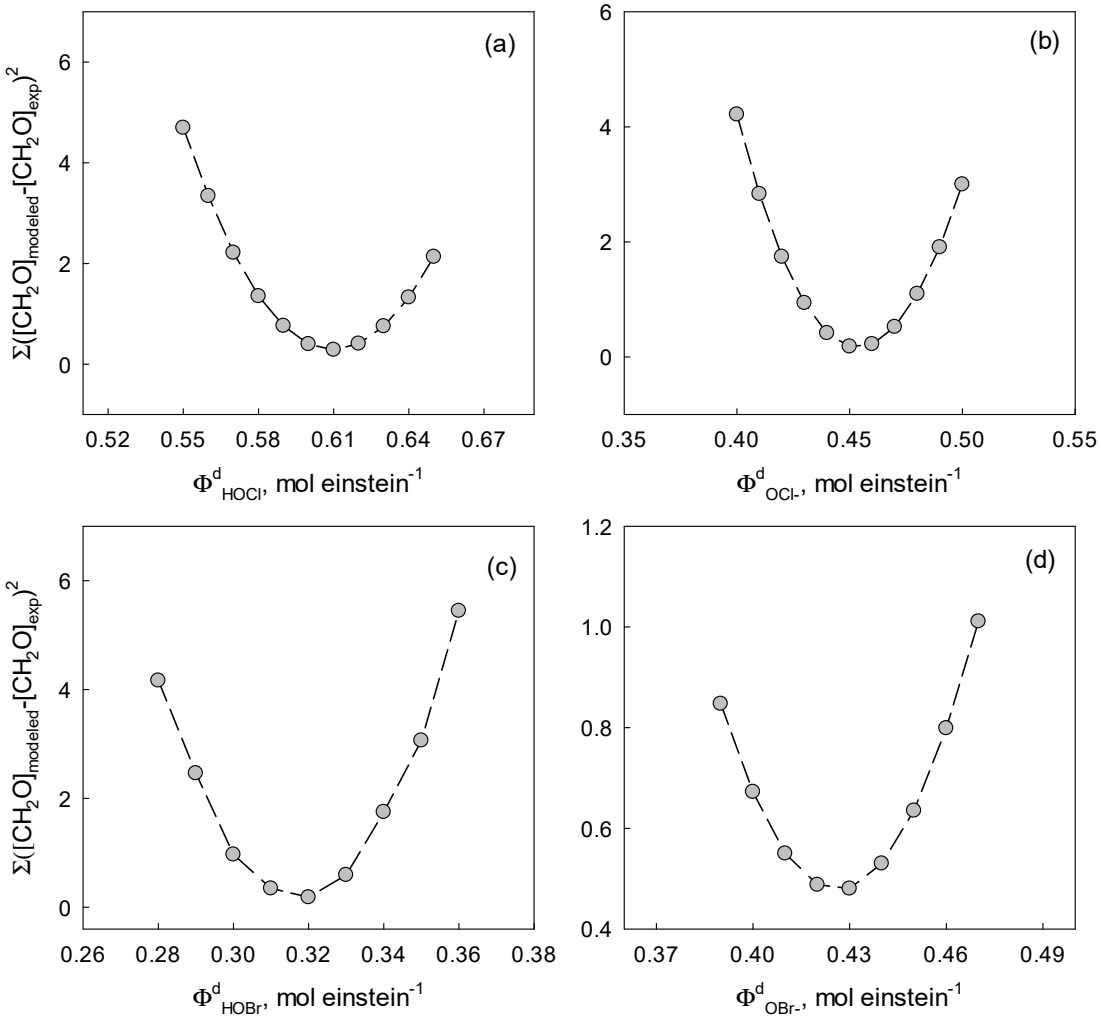

715

716 **Figure S3.** Sum of the squared errors (SSE) for the experimental and predicted values of
717 formaldehyde formation (= $\Sigma([CH_2O]_{exp} - [CH_2O]_{model})^2$) for (a) UV/chlorine at pH 6 (HOCl), (b)
718 UV/chlorine at pH 10 (OCl^-), (c) UV/bromine at pH 6 (HOBr) and (d) UV/bromine at pH 10 (OBr^-)
719 using a range of intrinsic quantum yield (Φ_{Ox}^{int}) values for each oxidant. The experimental CH_2O
720 data are also shown in Figure 1 in the main text. The optimized values of Φ_{Ox}^{int} were 0.61, 0.45,
721 0.32, and 0.43 mol einstein^{-1} for HOCl, OCl^-, HOBr and OBr^-, respectively.

722

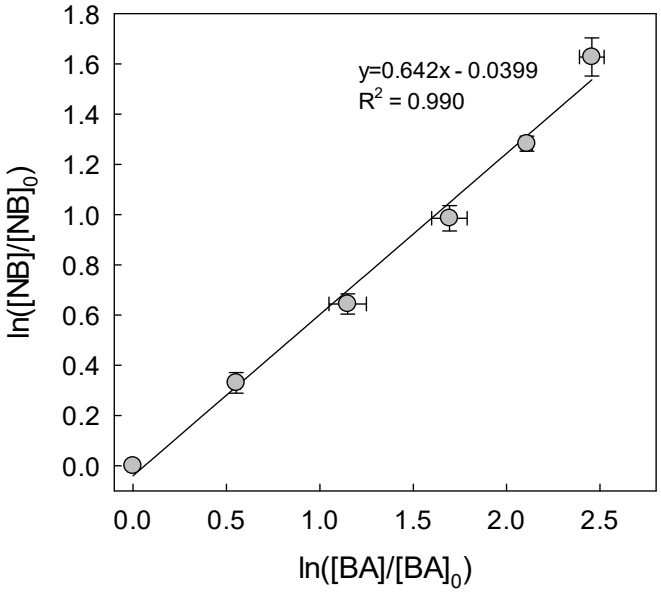

723

724 **Figure S4.** Competition kinetics plot of the logarithmic relative residual concentrations of NB
725 versus BA in UV/H_2O_2 (10 mg L^{-1}) at pH 6. The initial concentration of NB and BA were 1 μM.
726 The direct UV photolysis of NB and BA was subtracted from their degradation in UV/H_2O_2 to
727 determine the degradation of NB and BA by •OH using Equation S21. The symbols show the
728 measured data and error bars indicate one-standard deviation from triplicate measurements. The
729 line represents the linear regression of the data.

730

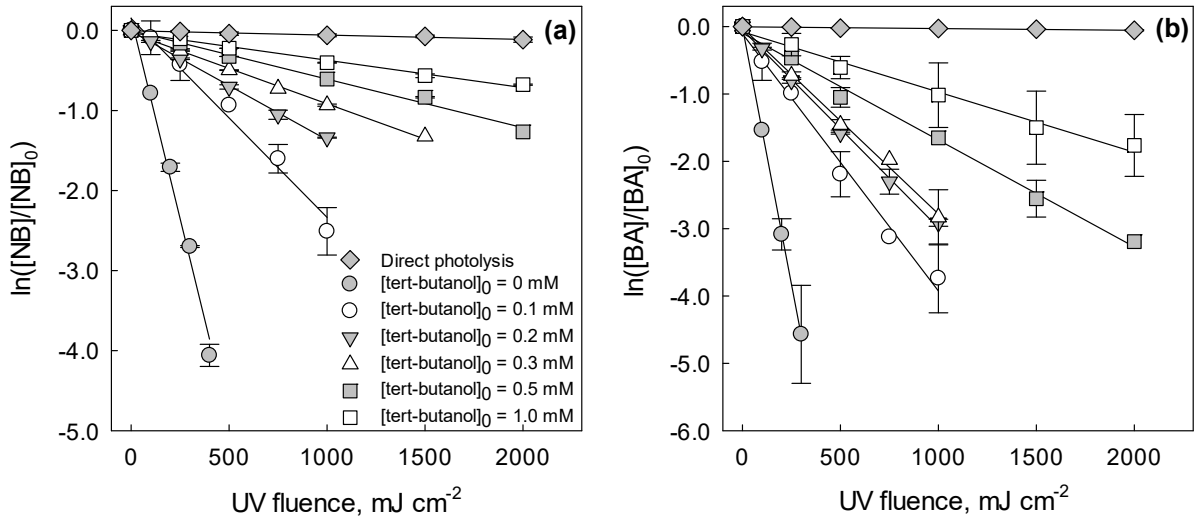

731

732 **Figure S5.** Logarithmic relative residual concentrations of (a) NB and (b) BA as a function of UV
733 fluence during treatment with UV alone and UV/chlorine (140 μM) at pH 5 (5 mM of phosphate
734 buffer) with different concentrations of *tert*-butanol (0 − 1.0 mM). NB and BA were spiked as a
735 mixture at 0.5 μM each. The symbols show the measured data and error bars indicate one-standard
736 deviation from triplicate measurements. Lines represents the linear regression of the data.

737

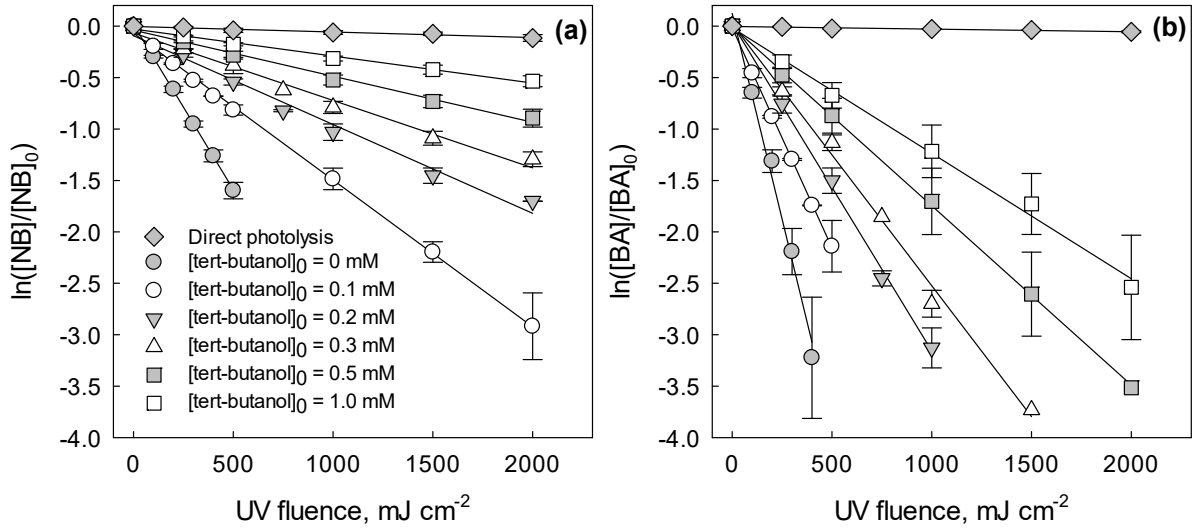

738

739 **Figure S6.** Logarithmic relative residual concentrations of (a) NB and (b) BA as a function of UV
740 fluence during treatment with UV alone and UV/chlorine (140 μM) at pH 6 (5 mM of phosphate
741 buffer) with different concentrations of tert-butanol (0 − 1.0 mM). NB and BA were spiked as a
742 mixture at 0.5 μM each. The symbols show the measured data and error bars indicate one-standard
743 deviation from triplicate measurements. Lines represents the linear regression of the data.

744

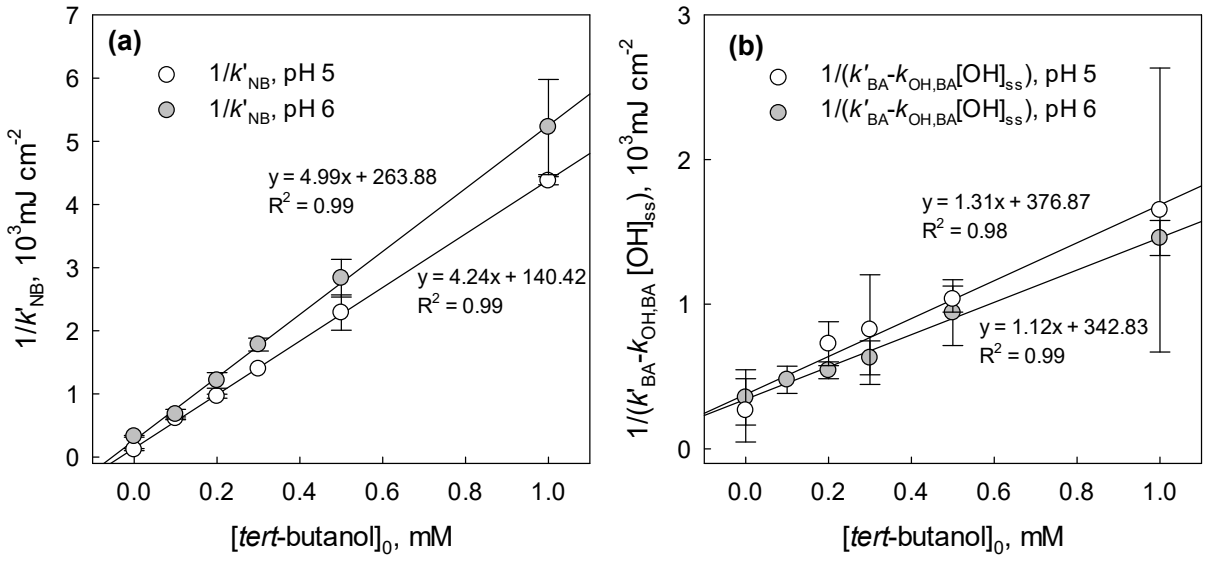

745

746 **Figure S7.** Inverse of the fluence-based first-order rate constant of (a) nitrobenzene (NB) and (b)
747 benzoic acid (BA) in the UV/chlorine system at pH 5 and 6 as a function of the initial concentration
748 of *tert*-butanol (0–1 mM). The solutions containing both NB and BA (initial concentration of 0.5
749 μM each) were treated with UV/chlorine (140 μM). Lines represent the linear regression of the
750 data. The NB and BA degradation kinetics data are shown in Figure S5 (pH 5) and Figure S6 (pH
751 6).

752

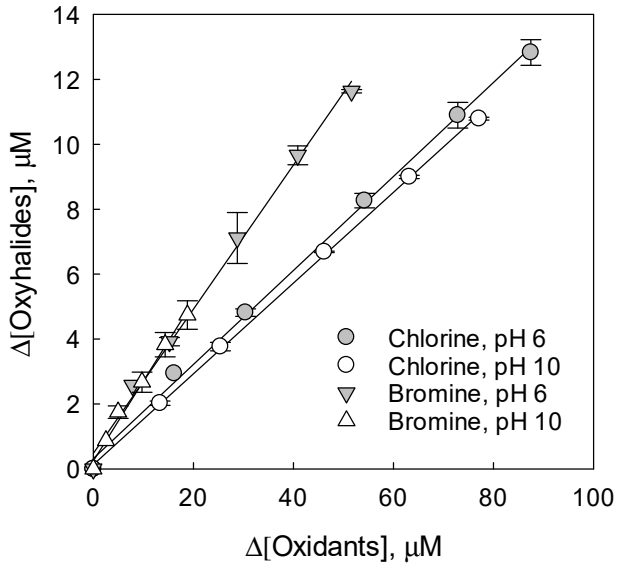

753

754 **Figure S8.** The linear regression of Δ[Oxyhalides] versus Δ[Oxidants]. The symbols show the
755 measured data and error bars indicate one-standard deviation from triplicate measurements. Lines
756 represents the linear regression of the data.

757

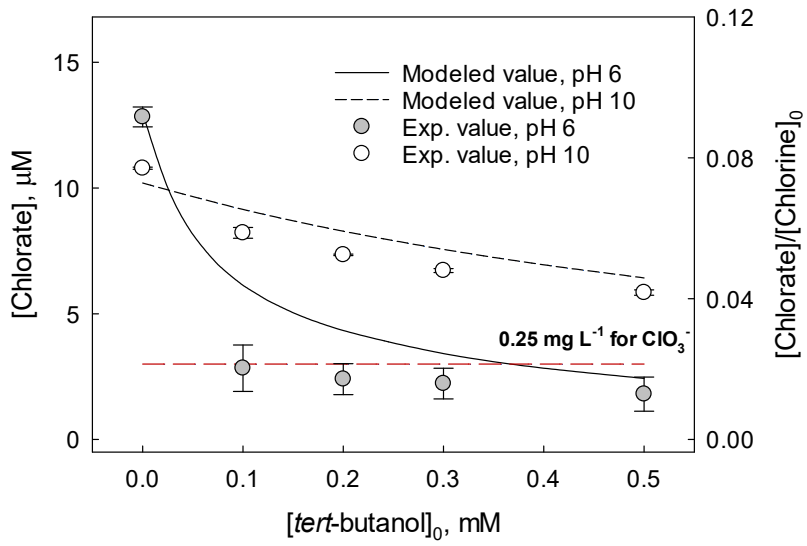

758

759 **Figure S9.** Formation of chlorate (ClO_3^-) during UV photolysis of chlorine (initial concentration
760 = 140 µM) at a UV fluence of 2000 mJ cm^{-2} at pH 6 and pH 10 in the presence of different initial
761 concentrations of *tert*-butanol (0–0.5 mM). The symbols show the measured data and the error bars
762 indicate one-standard deviation from triplicate measurements. Black lines represent the model
763 predictions. The red line represents the guideline value (0.25 mg L^{-1}).

764

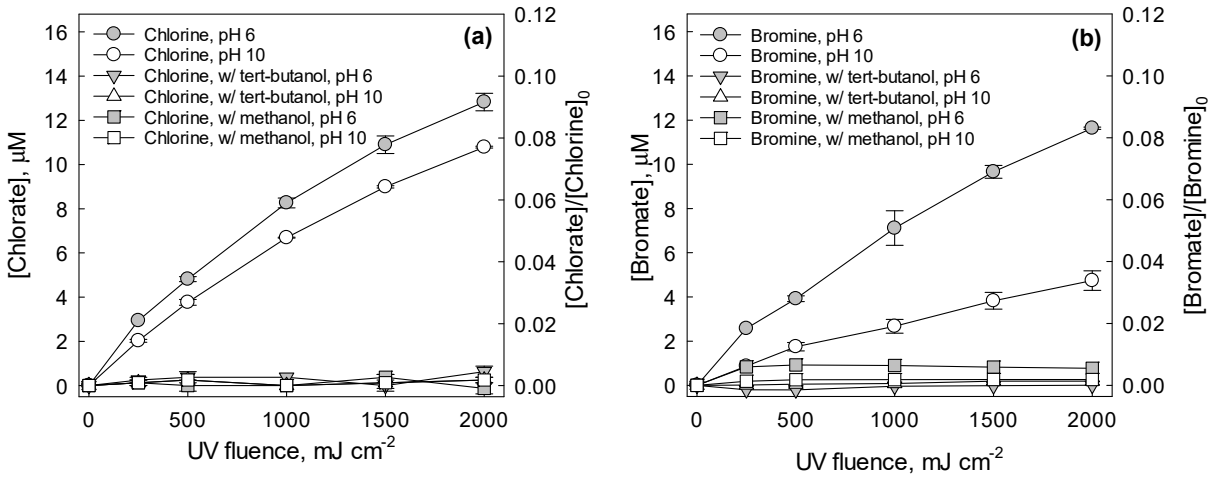

765

766 **Figure S10.** Formation of oxyhalides, (a) ClO_3^- from UV/chlorine and (b) BrO_3^- from UV/bromine,
767 as a function of UV fluence at pH 6 and pH 10 in an organic-free solution and in the presence of
768 *tert*-butanol (50 mM) and methanol (50 mM). The initial oxidant concentrations were 140 μM. The
769 data in an organic-free solution are the same as those shown in Figure 3 in the main text.

770

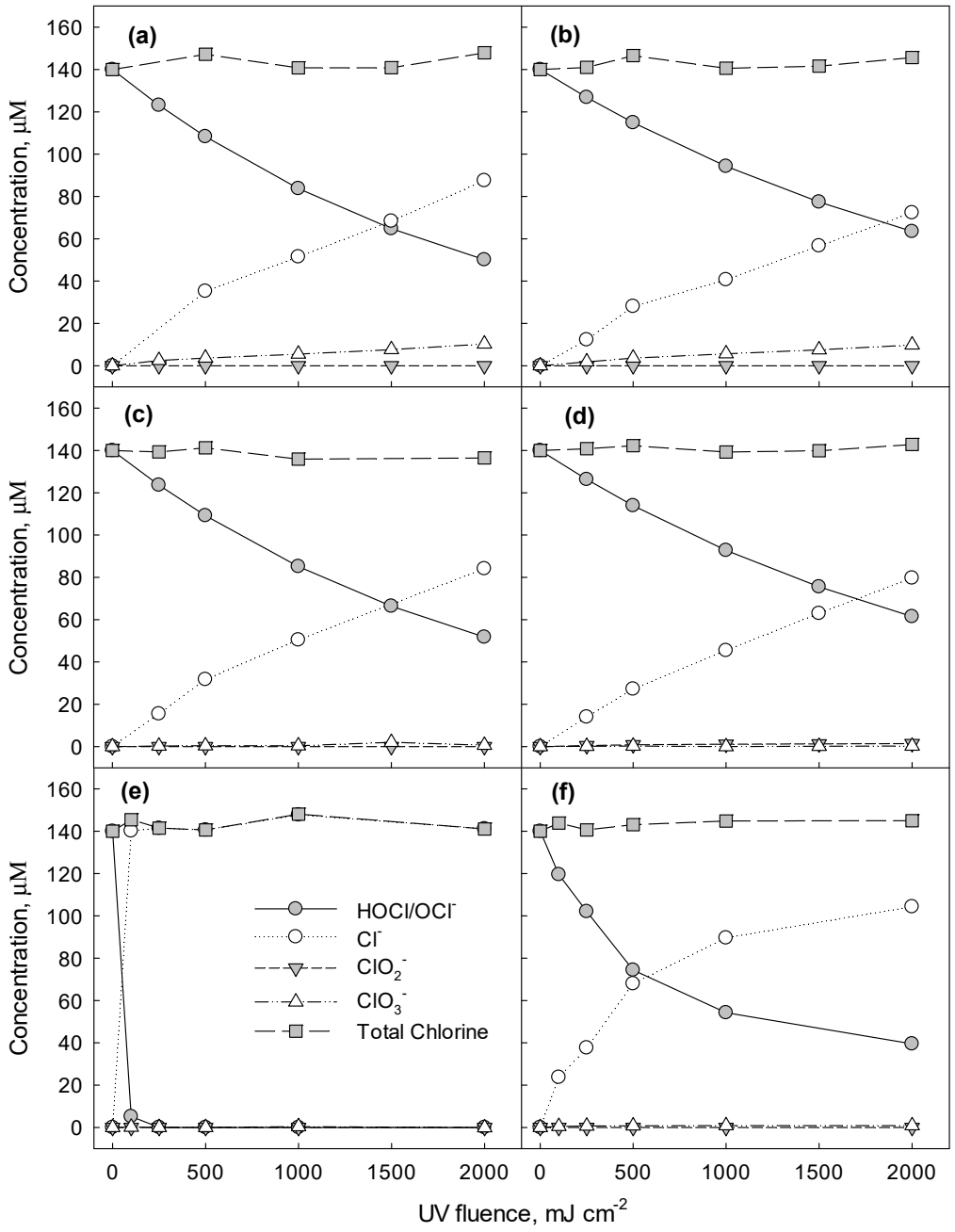

771

772 **Figure S11.** Variation of chlorine species ($HOCl/OCl^-$, Cl^-, ClO_2^-, and ClO_3^-) during UV
773 photolysis of chlorine (140 μM) (a) w/o a radical scavenger at pH 6, (b) w/o a radical scavenger at
774 pH 10, (c) w/ *tert*-butanol (50 mM) at pH 6, (d) w/ *tert*-butanol (50 mM) at pH 10, (e) w/ methanol
775 (50 mM) at pH 6, and (f) w/ methanol (50 mM) at pH 10. The symbols show the measured data.
776 Lines are used to guide the data.

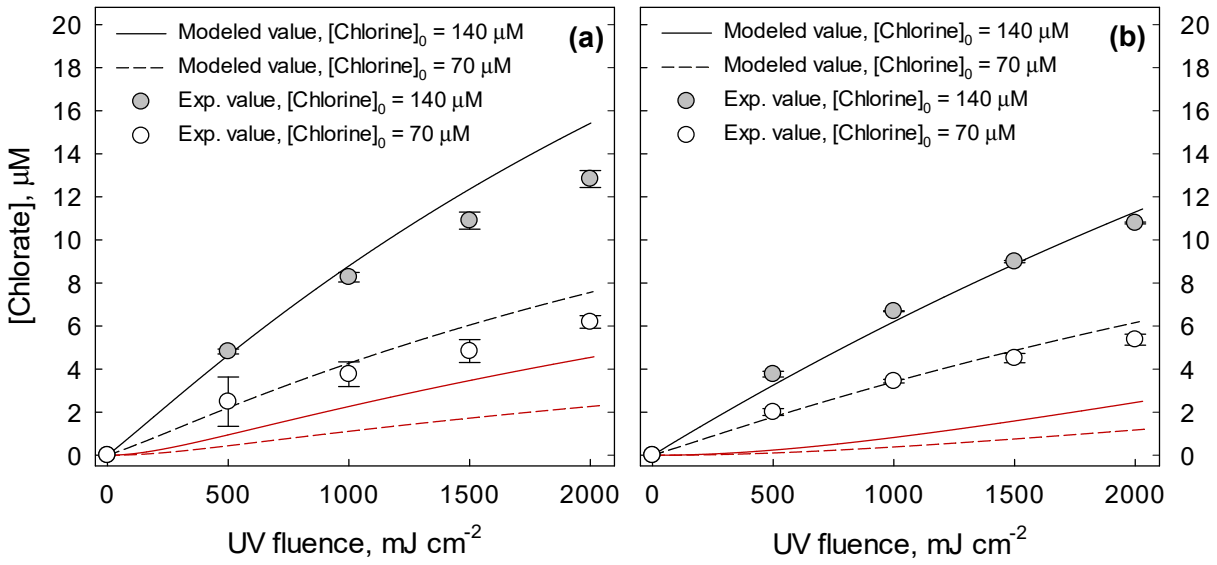

Figure S12. Model predictions of the formation of chlorate during UV photolysis of chlorine at (a) pH 6 and (b) pH 10. The initial chlorine concentrations were 70 μM (open circles) and 140 μM (filled circles). The experimental data from the initial 140 μM chlorine are the same as those shown in Figure 3 in the main text. Red lines represent the model predictions without considering Equation 19 ($ClO_2^{\bullet} + ClO^{\bullet} \rightarrow Cl_2O_3$, $k = 7.4\times10^9$ $M^{-1}s^{-1}$) and Equation 20 ($Cl_2O_3 + H_2O \rightarrow ClO_3^- + OCl^- + 2H^+$, $k = 10^4$ s^{-1}) in the main text. Black lines represent the model predictions after considering Equations 19 and 20.

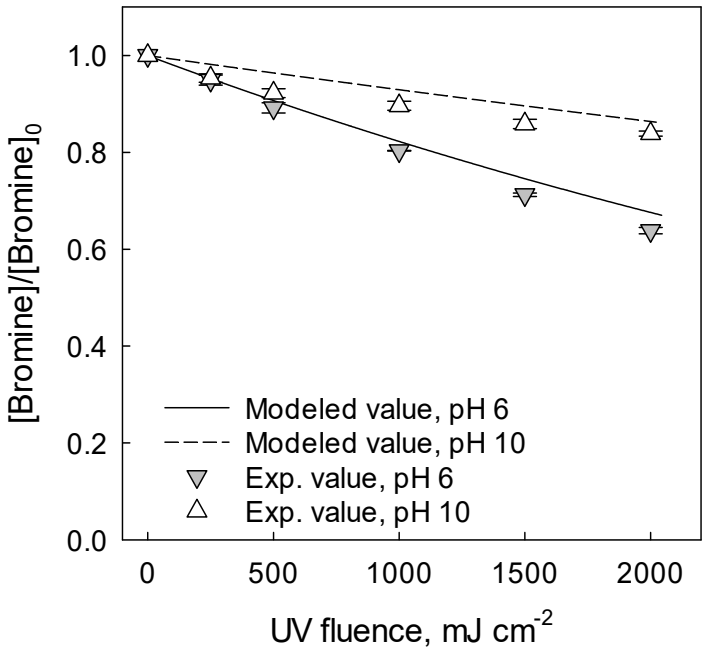

786

787 **Figure S13** Model predictions of bromine decomposition during UV photolysis of bromine (initial
788 concentration = 140 μM) at pH 6 and 10. The experimental data are the same as those shown in
789 Figure S1a.

790

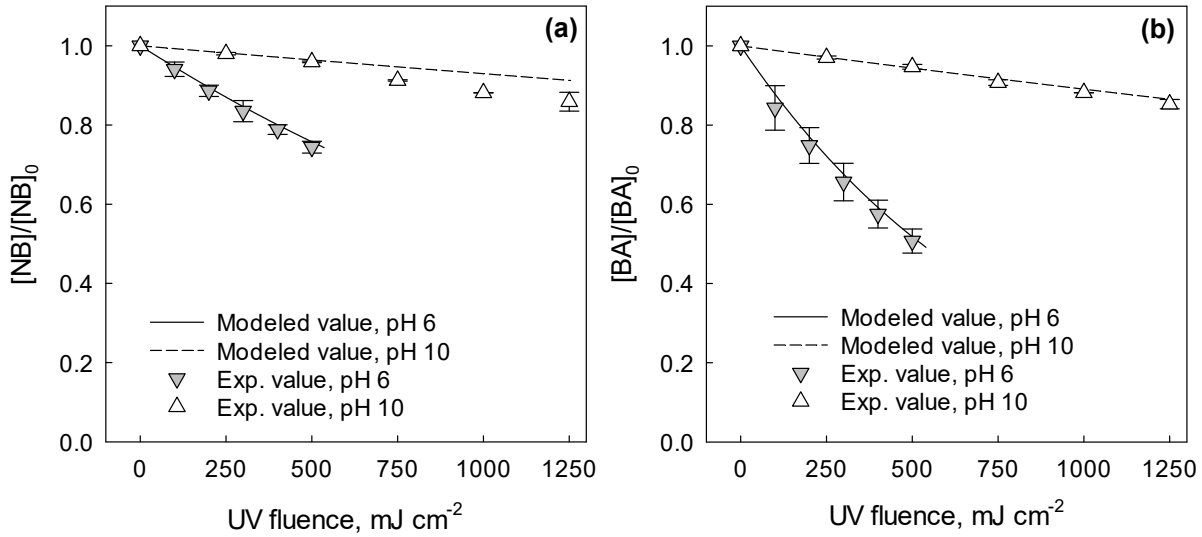

791

792 **Figure S14.** Model predictions of the degradation of (a) nitrobenzene (NB) and (b) benzoic acid
793 (NB) during UV photolysis of bromine (initial concentration = 140 μM) at pH 6 and 10. The
794 experimental data are the same as those shown in Figure 2 in the main text.

795

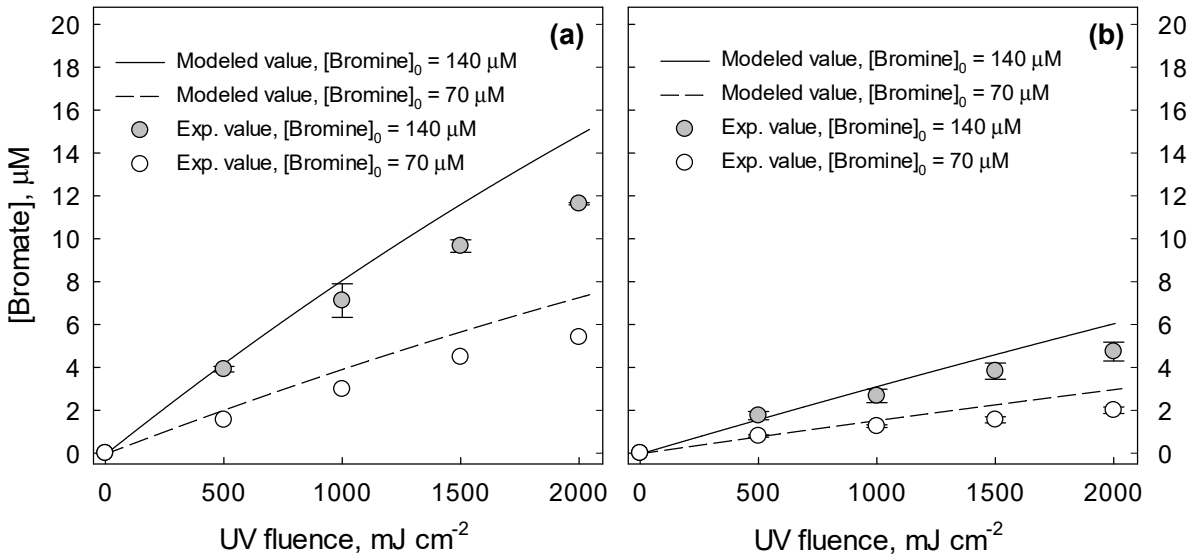

796

797 **Figure S15.** Model predictions of bromate formation during UV photolysis of bromine at (a) pH 6
798 and (b) pH 10. The initial bromine concentrations were 70 μM (open circles) and 140 μM (filled
799 circles). The experimental data from the initial 140 μM of bromine are the same as those shown in
800 Figure 3 in the main text.

801

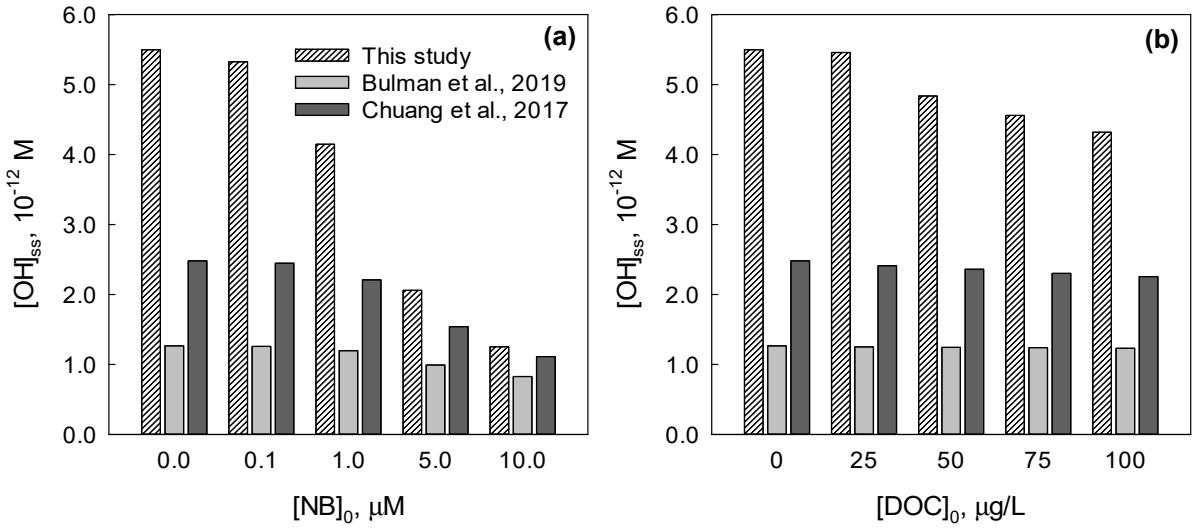

802

803 **Figure S16.** Modeled value for the $[^{\bullet}OH]_{ss}$ with different initial concentrations of (a) NB and (b)

804 DOC (a hypothetical dissolved organic impurity with a $k_{^{\bullet}OH}$ of 4×10^{8} $M^{-1}s^{-1}$) during UV

805 photolysis (UV fluence rate = 3.7 mW cm^{-2}) of chlorine (initial concentration = 56 μM).

806

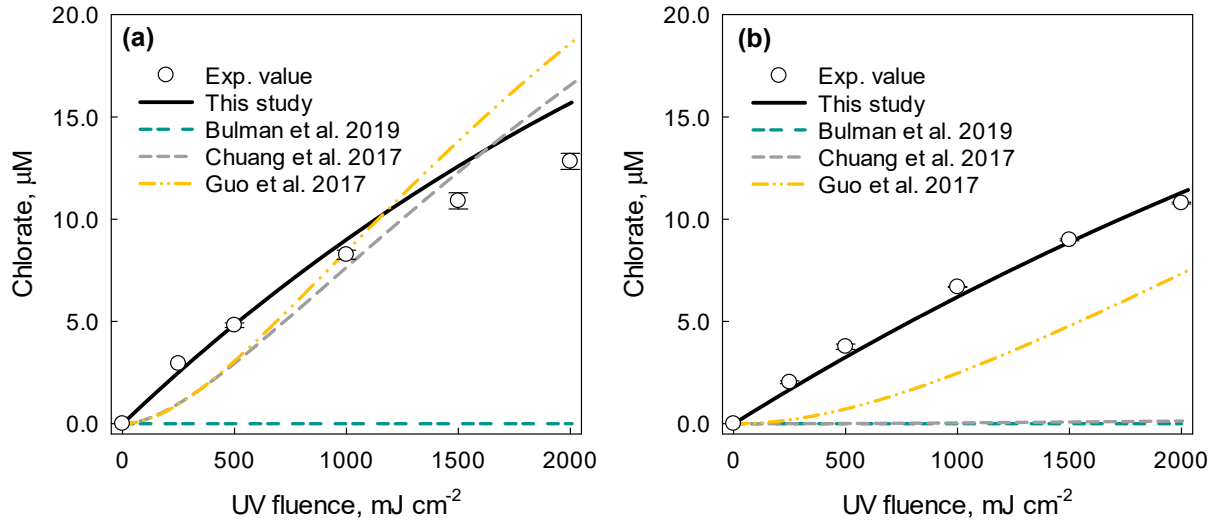

807

808 **Figure S17.** Comparison of experimental values with modeled values from the model developed

809 in this study and from the three previously reported models[37,45,48] for chlorate formation at (a) pH

810 6 and (b) pH 10 as a function of UV fluence in the UV/chlorine system.

811

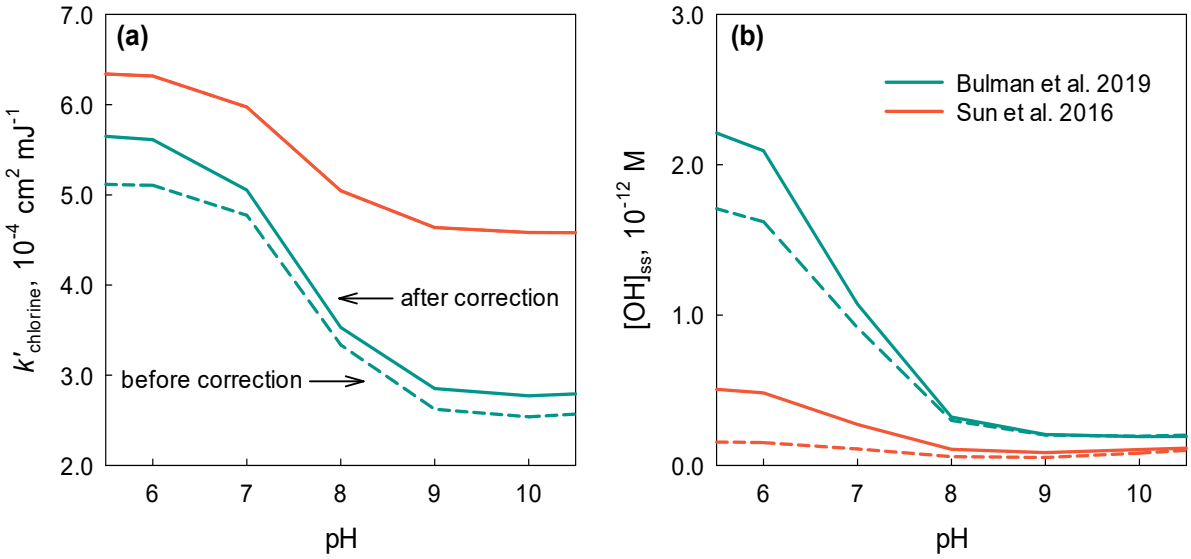

Figure S18. Effect of the illegal loop correction on the model prediction for the (a) fluence-based decomposition rate constant of chlorine ($k_{chlorine}$) and (b) steady-state concentration of •OH as a function of pH in the UV/chlorine system. Solid and dashed lines represent the model predictions after and before the illegal loop correction, respectively. The UV/chlorine models were applied to simulate the following condition ($[chlorine]_0$ = 140 μM, UV fluence rate = 3.7 mJ cm^{-2}). The results for before the illegal loop correction are shown in Figure 4 in the main text.

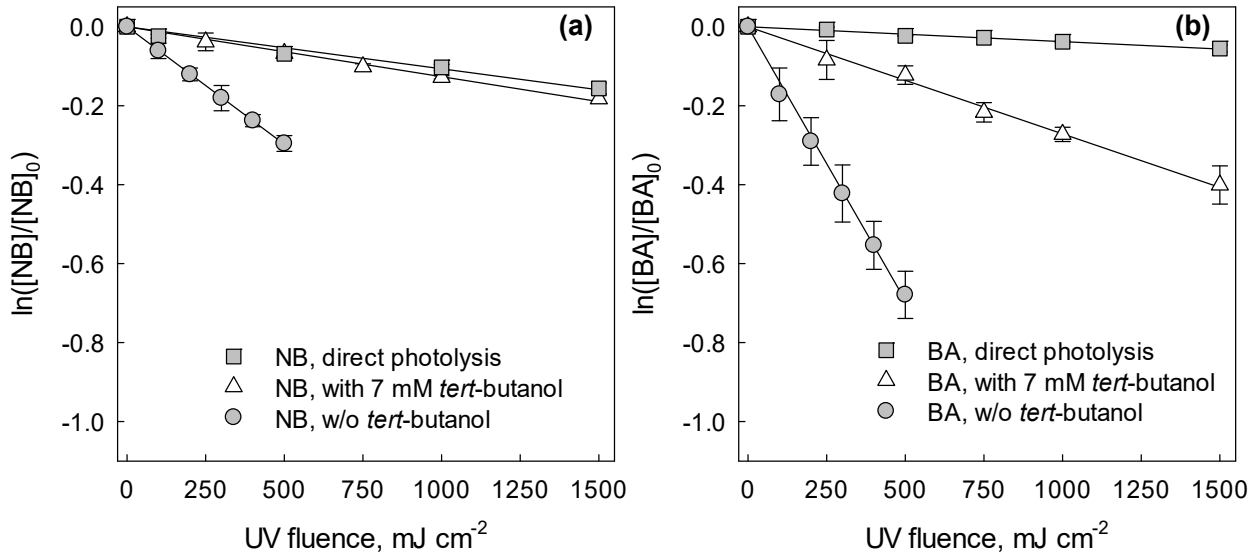

820

821 **Figure S19.** Logarithmic relative residual concentrations of (a) NB and (b) BA without and with
822 *tert*-butanol (7 mM) as a function of UV fluence during UV $_{254\ nm}$ photolysis of bromine (140 μM)
823 at pH 6. The initial concentrations of NB and BA were 1 μM. The symbols show the measured data
824 and error bars indicate one-standard deviation from triplicate measurements. Lines represent the
825 linear regression of the data.

826

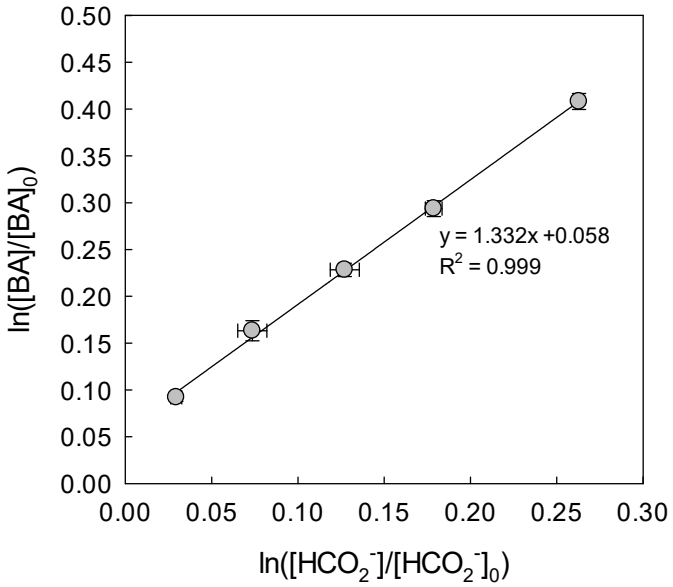

827

828 **Figure S20.** Competition kinetics plot of the logarithmic relative residual concentrations of BA
829 versus formate (HCO_2^-) during treatment with UV/bromine (140 μM) in the presence of *tert*-
830 butanol (7 mM) at pH 6. The initial concentrations of BA and formate were 10 μM and 100 μM,
831 respectively. The symbols show the measured data. The line represents the linear regression of the
832 data.

833

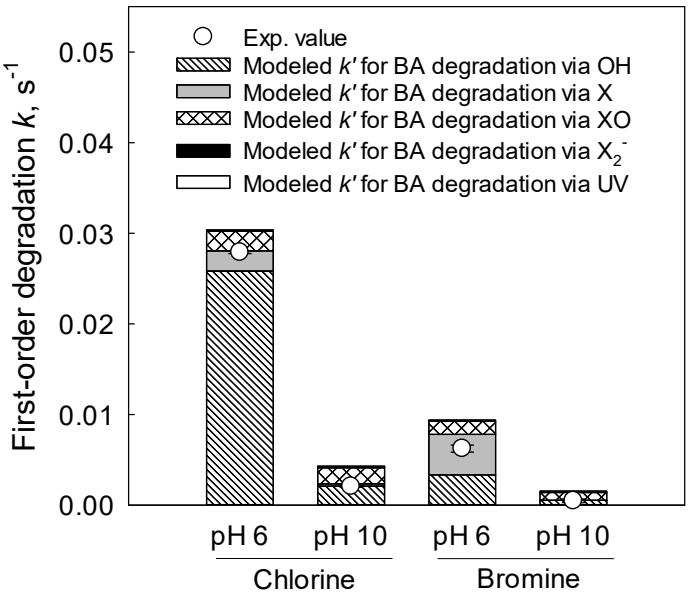

834

835 **Figure S21.** Experimental and modeled value for the first-order degradation rate constants of BA
836 (initial concentration = 1 μM) during UV photolysis (UV fluence rate = 3.7 mW cm^{-2}) of chlorine
837 and bromine (initial concentration = 140 μM each). Stacked bars represent the contributions of
838 each radical species and direct UV photolysis to the overall BA degradation rate. The contribution
839 of each radical species could be assessed by calculating the apparent degradation rate of BA by
840 each radical species ($k'_{BA,radical}$). This could be obtained from the second-order rate constant for the
841 reaction of BA with the radical species ($k_{radical,BA}$) and the concentration of the radical species
842 ([radical]) in the UV/chlorine system from the model prediction (Table S9) using $k'_{BA,radical}$ =
843 $k_{radical,BA}$×[radical].

844

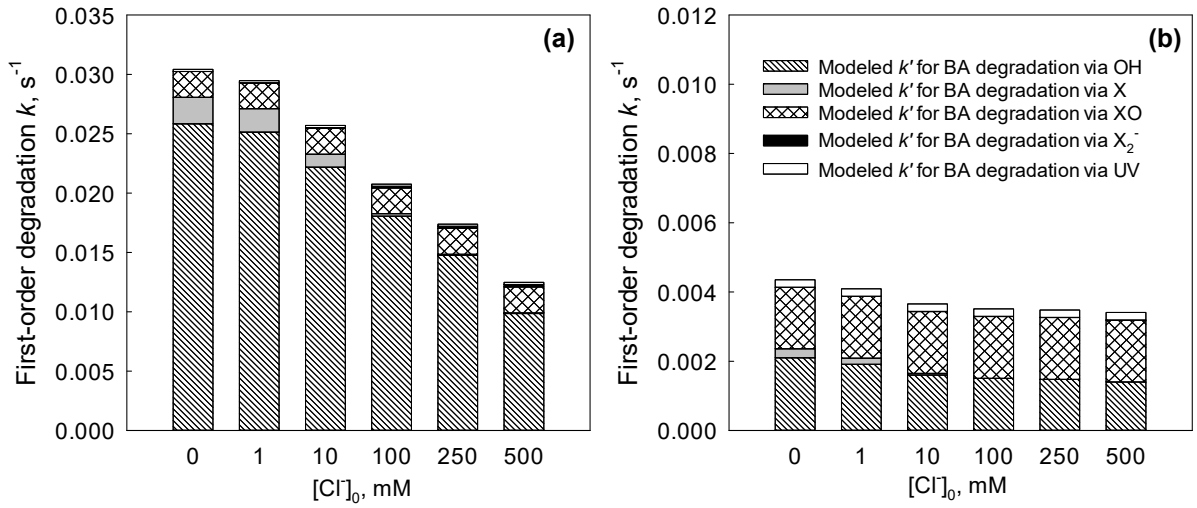

Figure S22. Experimental and modeled values for the first-order degradation rate constants of BA (initial concentration = 1 μM) during UV photolysis (UV fluence rate = 3.7 mW cm^{-2}) of chlorine (initial concentration = 140 μM each) at (a) pH 6 and (b) pH 10 as a function of the Cl^- level. Stacked bars represent the contributions of each radical species and direct UV photolysis to the overall BA degradation rate. The contribution of each radical species could be assessed by calculating the apparent degradation rate of BA by each radical species ($k'_{BA,radical}$). This could be obtained from the second-order rate constant for the reaction of BA with the radical species ($k_{radical,BA}$) and the concentration of the radical species ([radical]) in the UV/chlorine system from the model prediction using $k'_{BA,radical} = k_{radical,BA} \times [radical]$.

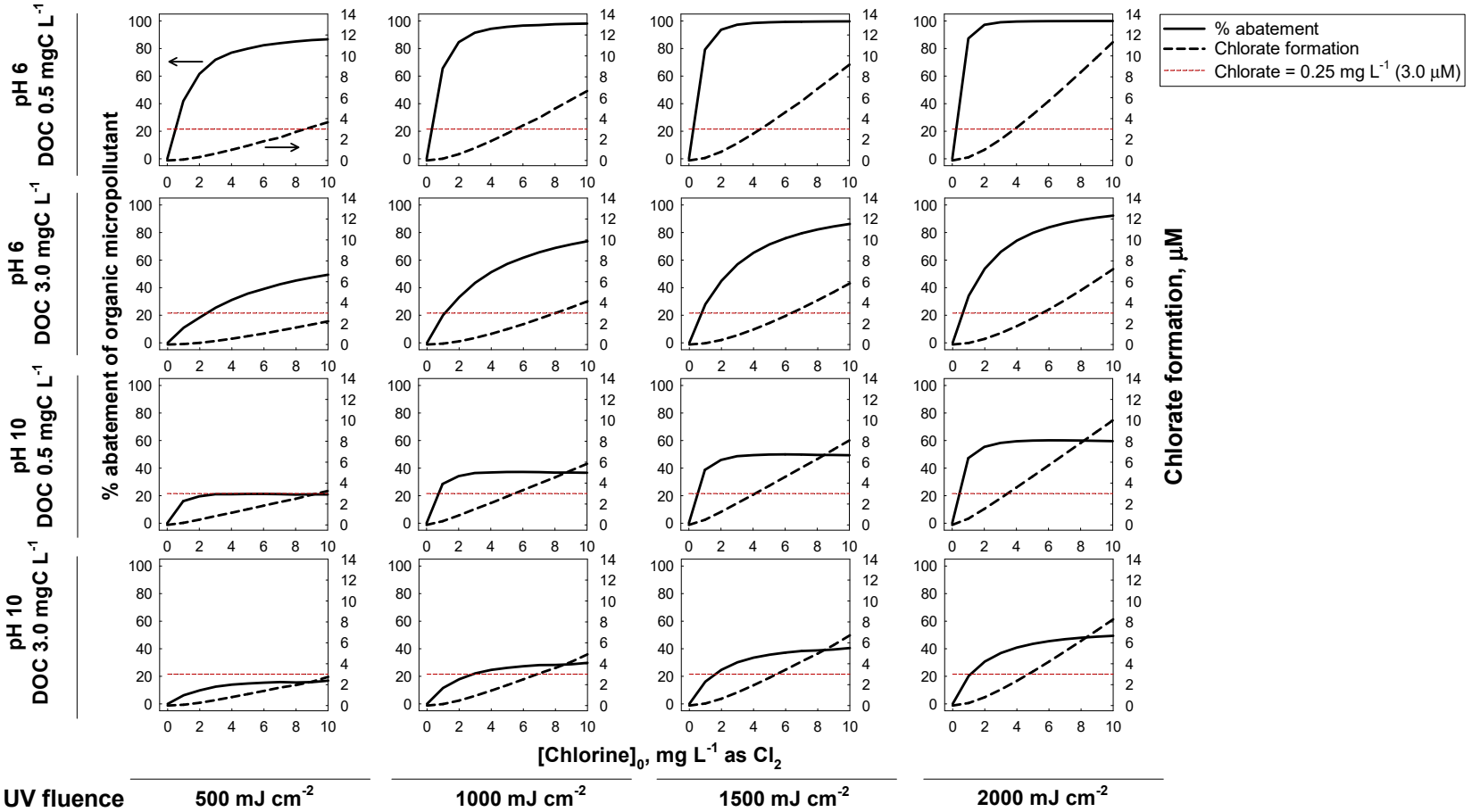

Figure S23. Model predictions for the percentage abatement of an organic micropollutant (OMP) (solid line) and ClO_3^- formation (dashed line) as a function of the initial chlorine concentration and UV fluence during UV photolysis of chlorine in the presence of DOC (0.5 and 3 mg L^{-1}) at pH 6 and pH 10. A compound reacting with $^{\bullet}OH$ at a $k_{^{\bullet}OH}$ of 5.0×10^9 $M^{-1}s^{-1}$ was hypothesized in the modeling as a representative OMP. The horizontal dotted line indicates the European drinking water guideline value of 0.25 mg L^{-1} (3.0 µM) for ClO_3^-.

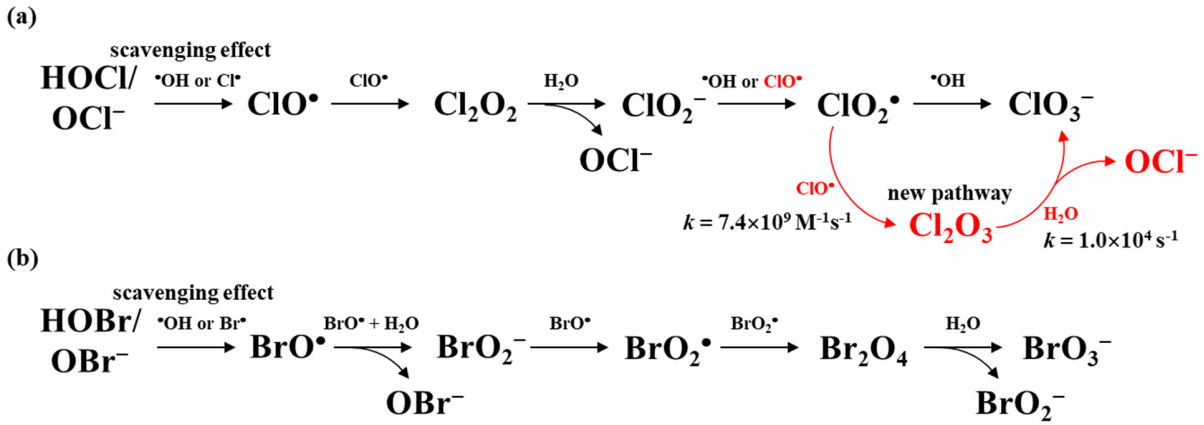

861

862 **Scheme S1.** Proposed formation pathway of (a) ClO_3^- in the UV/chlorine system and (b) BrO_3^- in

863 the UV/bromine system.

864

References

1. Furman, C. S.; Margerum, D. W., Mechanism of chlorine dioxide and chlorate ion formation from the reaction of hypobromous acid and chlorite ion. *Inorganic chemistry* **1998,** *37*, (17), 4321-4327.

2. Lei, H.; Mariñas, B. J.; Minear, R. A., Bromamine decomposition kinetics in aqueous solutions. *Environmental science & technology* **2004,** *38*, (7), 2111-2119.

3. Kumar, K.; Margerum, D. W., Kinetics and mechanism of general-acid-assisted oxidation of bromide by hypochlorite and hypochlorous acid. *Inorganic Chemistry* **1987,** *26*, (16), 2706-2711.

4. Troy, R. C.; Margerum, D. W., Non-metal redox kinetics: Hypobromite and hypobromous acid reactions with iodide and with sulfite and the hydrolysis of bromosulfate. *Inorganic Chemistry* **1991,** *30*, (18), 3538-3543.

5. Nash, T., The colorimetric estimation of formaldehyde by means of the Hantzsch reaction. *Biochemical Journal* **1953,** *55*, (3), 416-421.

6. Lee, Y.; Gerrity, D.; Lee, M.; Gamage, S.; Pisarenko, A.; Trenholm, R. A.; Canonica, S.; Snyder, S. A.; von Gunten, U., Organic Contaminant Abatement in Reclaimed Water by UV/H2O2 and a Combined Process Consisting of O3/H2O2 Followed by UV/H2O2: Prediction of Abatement Efficiency, Energy Consumption, and Byproduct Formation. *Environmental Science & Technology* **2016,** *50*, (7), 3809-3819.

7. Canonica, S.; Meunier, L.; Von Gunten, U., Phototransformation of selected pharmaceuticals during UV treatment of drinking water. *Water Research* **2008,** *42*, (1), 121-128.

8. Bicking, M. K.; Cooke, W. M.; Kawahara, F. K.; Longbottom, J. E., Effect of pH on the Reaction of 2, 4-Dinitrophenylhydrazine with Formaldehyde and Acetaldehyde. *Journal of Chromatography A* **1988,** *455*, 310-315.

9. Bolton, J. R.; Stefan, M. I., Fundamental photochemical approach to the concepts of fluence (UV dose) and electrical energy efficiency in photochemical degradation reactions. *Research on Chemical Intermediates* **2002,** *28*, (7), 857-870.

10. Guo, K.; Zheng, S.; Zhang, X.; Zhao, L.; Ji, S.; Chen, C.; Wu, Z.; Wang, D.; Fang, J., Roles of Bromine Radicals and Hydroxyl Radicals in the Degradation of Micropollutants by the UV/Bromine Process. *Environmental Science & Technology* **2020,** *54*, (10), 6415-6426.

11. Zhao, Q.; Shang, C.; Zhang, X., Effects of bromide on UV/chlorine advanced oxidation process. *Water Science and Technology: Water Supply* **2009,** *9*, (6), 627-634.

12. Rabani, J.; Klug-Roth, D.; Henglein, A., Pulse radiolytic investigations of OHCH2O2 radicals. *The Journal of Physical Chemistry* **1974,** *78*, (21), 2089-2093.
13. Staehelin, J.; Hoigne, J., Decomposition of ozone in water in the presence of organic solutes acting as promoters and inhibitors of radical chain reactions. *Environmental science & technology* **1985,** *19*, (12), 1206-1213.
14. Reisz, E.; Schmidt, W.; Schuchmann, H.-P.; von Sonntag, C., Photolysis of Ozone in Aqueous Solutions in the Presence of Tertiary Butanol. *Environmental Science & Technology* **2003,** *37*, (9), 1941-1948.
15. Flyunt, R.; Leitzke, A.; Mark, G.; Mvula, E.; Reisz, E.; Schick, R.; von Sonntag, C., Determination of •OH, O2•-, and Hydroperoxide Yields in Ozone Reactions in Aqueous Solution. *The Journal of Physical Chemistry B* **2003,** *107*, (30), 7242-7253.
16. Gilbert, B. C.; Stell, J. K.; Peet, W. J.; Radford, K. J., Generation and reactions of the chlorine atom in aqueous solution. *Journal of the Chemical Society, Faraday Transactions 1: Physical Chemistry in Condensed Phases* **1988,** *84*, (10), 3319-3330.
17. Merenyi, G.; Lind, J., Reaction mechanism of hydrogen abstraction by the bromine atom in water. *Journal of the American Chemical Society* **1994,** *116*, (17), 7872-7876.
18. Schuchmann, M. N.; Von Sonntag, C., Hydroxyl radical-induced oxidation of 2-methyl-2-propanol in oxygenated aqueous solution. A product and pulse radiolysis study. *Journal of Physical Chemistry* **1979,** *83*, (7), 780-784.
19. Piechowski, M. V.; Thelen, M. A.; Hoigné, J.; Bühler, R. E., tert-Butanol as an OH-Scavenger in the Pulse Radiolysis of Oxygenated Aqueous Systems. *Berichte der Bunsengesellschaft für physikalische Chemie* **1992,** *96*, (10), 1448-1454.
20. Held, A. M.; Halko, D. J.; Hurst, J. K., Mechanisms of chlorine oxidation of hydrogen peroxide. *Journal of the American Chemical Society* **1978,** *100*, (18), 5732-5740.
21. Von Gunten, U.; Oliveras, Y., Kinetics of the reaction between hydrogen peroxide and hypobromous acid: Implication on water treatment and natural systems. *Water Research* **1997,** *31*, (4), 900-906.
22. Bothe, E.; Schulte-Frohlinde, D., The bimolecular decay of the α-hydroxymethylperoxyl radicals in aqueous solution. *Zeitschrift für Naturforschung B* **1978,** *33*, (7), 786-788.
23. Long, C. A.; Bielski, B. H., Rate of reaction of superoxide radical with chloride-containing species. *The Journal of Physical Chemistry* **1980,** *84*, (5), 555-557.
24. Candeias, L. P.; Patel, K. B.; Stratford, M. R.; Wardman, P., Free hydroxyl radicals are

928 formed on reaction between the neutrophil-derived species superoxide anion and hypochlorous
929 acid. *FEBS letters* **1993,** *333*, (1-2), 151-153.
930 25. Schwarz, H. A.; Bielski, B. H. J., Reactions of hydroperoxo and superoxide with iodine
931 and bromine and the iodide (I2-) and iodine atom reduction potentials. *The Journal of Physical*
932 *Chemistry* **1986,** *90*, (7), 1445-1448.
933 26. Koppenol, W.; Butler, J., Energetics of interconversion reactions of oxyradicals. *Advances*
934 *in Free Radical Biology & Medicine* **1985,** *1*, (1), 91-131.
935 27. Ianni, J. C., Kintecus, Windows Version 6.51. In www.kintecus.com: 2018.
936 28. Ianni, J. C., Atropos, V1.20. In http://www.kintecus.com/atropos.htm: 2006.
937 29. NDRL/NIST Solution Kinetics Database; https://kinetics.nist.gov/solution/.
938 30. Buxton, G. V.; Subhani, M. S., Radiation chemistry and photochemistry of oxychlorine
939 ions. Part 2.—Photodecomposition of aqueous solutions of hypochlorite ions. *Journal of the*
940 *Chemical Society, Faraday Transactions 1: Physical Chemistry in Condensed Phases* **1972,** *68*,
941 958-969.
942 31. Biedenkapp, D.; Hartshorn, L. G.; Bair, E. J., The O (1D)+ H2O reaction. *Chemical*
943 *Physics Letters* **1970,** *5*, (6), 379-381.
944 32. Kläning, U. K.; Sehested, K.; Wolff, T., Ozone formation in laser flash photolysis of
945 oxoacids and oxoanions of chlorine and bromine. *Journal of the Chemical Society, Faraday*
946 *Transactions 1: Physical Chemistry in Condensed Phases* **1984,** *80*, (11), 2969-2979.
947 33. Buxton, G. V.; Subhani, M. S., Radiation chemistry and photochemistry of oxychlorine
948 ions. Part 3.—Photodecomposition of aqueous solutions of chlorite ions. *Journal of the Chemical*
949 *Society, Faraday Transactions 1: Physical Chemistry in Condensed Phases* **1972,** *68*, 970-977.
950 34. Haag, W. R.; Hoigné, J., Ozonation of water containing chlorine or chloramines. Reaction
951 products and kinetics. *Water Research* **1983,** *17*, (10), 1397-1402.
952 35. Forsyth, J. E.; Zhou, P.; Mao, Q.; Asato, S. S.; Meschke, J. S.; Dodd, M. C., Enhanced
953 inactivation of Bacillus subtilis spores during solar photolysis of free available chlorine.
954 *Environmental science & technology* **2013,** *47*, (22), 12976-12984.
955 36. Zhou, P.; Di Giovanni, G. D.; Meschke, J. S.; Dodd, M. C., Enhanced inactivation of
956 Cryptosporidium parvum oocysts during solar photolysis of free available chlorine. *Environmental*
957 *Science & Technology Letters* **2014,** *1*, (11), 453-458.
958 37. Bulman, D. M.; Mezyk, S. P.; Remucal, C. K., The Impact of pH and Irradiation
959 Wavelength on the Production of Reactive Oxidants during Chlorine Photolysis. *Environmental*

960 *Science & Technology* **2019,** *53*, (8), 4450-4459.
961 38. Matthew, B.; Anastasio, C., A chemical probe technique for the determination of reactive
962 halogen species in aqueous solution: Part 1–bromide solutions. *Atmospheric Chemistry and*
963 *Physics* **2006,** *6*, (9), 2423-2437.
964 39. Zehavi, D.; Rabani, J., Oxidation of aqueous bromide ions by hydroxyl radicals. Pulse
965 radiolytic investigation. *The Journal of Physical Chemistry* **1972,** *76*, (3), 312-319.
966 40. Kläning, U. K.; Wolff, T., Laser Flash Photolysis of HClO, ClO−, HBrO, and BrO− in
967 Aqueous Solution. Reactions of Cl-and Br-Atoms. *Berichte der Bunsengesellschaft für*
968 *physikalische Chemie* **1985,** *89*, (3), 243-245.
969 41. Shemer, H.; Sharpless, C. M.; Elovitz, M. S.; Linden, K. G., Relative rate constants of
970 contaminant candidate list pesticides with hydroxyl radicals. *Environmental science & technology*
971 **2006,** *40*, (14), 4460-4466.
972 42. Buxton, G. V.; Greenstock, C. L.; Helman, W. P.; Ross, A. B., Critical review of rate
973 constants for reactions of hydrated electrons, hydrogen atoms and hydroxyl radicals (· OH/· O− in
974 aqueous solution. *Journal of physical and chemical reference data* **1988,** *17*, (2), 513-886.
975 43. Mialocq, J. C.; Barat, F.; Gilles, L.; Hickel, B.; Lesigne, B., Flash photolysis of chlorine
976 dioxide in aqueous solution. *The Journal of Physical Chemistry* **1973,** *77*, (6), 742-749.
977 44. Alfassi, Z. B.; Huie, R. E.; Mosseri, S.; Neta, P., Kinetics of one-electron oxidation by the
978 ClO radical. *International Journal of Radiation Applications and Instrumentation. Part C.*
979 *Radiation Physics and Chemistry* **1988,** *32*, (1), 85-88.
980 45. Chuang, Y. H.; Chen, S.; Chinn, C. J.; Mitch, W. A., Comparing the UV/Monochloramine
981 and UV/Free Chlorine Advanced Oxidation Processes (AOPs) to the UV/Hydrogen Peroxide AOP
982 Under Scenarios Relevant to Potable Reuse. *Environ. Sci. Technol.* **2017,** *51*, (23), 13859-13868.
983 46. Eriksen, T. E.; Lind, J.; Merényi, G., Generation of chlorine dioxide from ClO–2 by pulse
984 radiolysis. *Journal of the Chemical Society, Faraday Transactions 1: Physical Chemistry in*
985 *Condensed Phases* **1981,** *77*, (9), 2115-2123.
986 47. Fang, J.; Fu, Y.; Shang, C., The roles of reactive species in micropollutant degradation in
987 the UV/free chlorine system. *Environmental science & technology* **2014,** *48*, (3), 1859-1868.
988 48. Guo, K.; Wu, Z.; Shang, C.; Yao, B.; Hou, S.; Yang, X.; Song, W.; Fang, J., Radical
989 chemistry and structural relationships of PPCP degradation by UV/chlorine treatment in simulated
990 drinking water. *Environmental science & technology* **2017,** *51*, (18), 10431-10439.
991 49. Li, W.; Jain, T.; Ishida, K.; Liu, H., A mechanistic understanding of the degradation of trace

992 organic contaminants by UV/hydrogen peroxide, UV/persulfate and UV/free chlorine for water
993 reuse. *Environmental Science: Water Research & Technology* **2017,** *3*, (1), 128-138.
994 50. Sun, P.; Lee, W. N.; Zhang, R.; Huang, C. H., Degradation of DEET and Caffeine under
995 UV/Chlorine and Simulated Sunlight/Chlorine Conditions. *Environ Sci Technol* **2016,** *50*, (24),
996 13265-13273.
997 51. Wu, Z.; Fang, J.; Xiang, Y.; Shang, C.; Li, X.; Meng, F.; Yang, X., Roles of reactive
998 chlorine species in trimethoprim degradation in the UV/chlorine process: Kinetics and
999 transformation pathways. *Water Research* **2016,** *104*, 272-282.
1000 52. Quiroga, S. L.; Perissinotti, L. J., Reduced mechanism for the 366 nm chlorine dioxide
1001 photodecomposition in N2-saturated aqueous solutions. *Journal of Photochemistry and*
1002 *Photobiology A: Chemistry* **2005,** *171*, (1), 59-67.
1003 53. Field, R. J.; Foersterling, H. D., On the oxybromine chemistry rate constants with cerium
1004 ions in the Field-Koeroes-Noyes mechanism of the Belousov-Zhabotinskii reaction: the
1005 equilibrium HBrO2+ BrO3-+ H+. dblharw. 2BrO. ovrhdot. 2+ H2O. *The Journal of Physical*
1006 *Chemistry* **1986,** *90*, (21), 5400-5407.
1007 54. Stanbury, D. M.; Harshman, J., Large-Scale Models of Radiation Chemistry and the
1008 Principle of Detailed Balancing. *The Journal of Physical Chemistry A* **2019,** *123*, (47), 10240-
1009 10245.
1010 55. Stanbury, D. M., Mechanisms of Advanced Oxidation Processes, the Principle of Detailed
1011 Balancing, and Specifics of the UV/Chloramine Process. *Environmental Science & Technology*
1012 **2020,** *54*, (7), 4658-4663.
1013 56. Stanbury, D. M.; Hoffman, D., Systematic Application of the Principle of Detailed
1014 Balancing to Complex Homogeneous Chemical Reaction Mechanisms. *The Journal of Physical*
1015 *Chemistry A* **2019,** *123*, (26), 5436-5445.
1016 57. Mártire, D. O.; Rosso, J. A.; Bertolotti, S.; Le Roux, G. C.; Braun, A. M.; Gonzalez, M. C.,
1017 Kinetic study of the reactions of chlorine atoms and Cl2•-radical anions in aqueous solutions. II.
1018 Toluene, benzoic acid, and chlorobenzene. *The Journal of Physical Chemistry A* **2001,** *105*, (22),
1019 5385-5392.
1020 58. Hasegawa, K.; Neta, P., Rate constants and mechanisms of reaction of chloride (Cl2-)
1021 radicals. *The Journal of Physical Chemistry* **1978,** *82*, (8), 854-857.
1022 59. Zhou, S.; Zhang, W.; Sun, J.; Zhu, S.; Li, K.; Meng, X.; Luo, J.; Shi, Z.; Zhou, D.;
1023 Crittenden, J. C., Oxidation Mechanisms of the UV/Free Chlorine Process: Kinetic Modeling and

1024 Quantitative Structure Activity Relationships. *Environmental science & technology* **2019,** *53*, (8),
1025 4335-4345.
1026 60. Watts, M. J.; Linden, K. G., Chlorine photolysis and subsequent OH radical production
1027 during UV treatment of chlorinated water. *Water Research* **2007,** *41*, (13), 2871-2878.
1028 61. Feng, Y.; Smith, D. W.; Bolton, J. R., Photolysis of aqueous free chlorine species (HOCl
1029 and OCl-) with 254 nm ultraviolet light. *Journal of Environmental Engineering and Science* **2007,**
1030 *6*, (3), 277-284.
1031 62. Jin, J.; El-Din, M. G.; Bolton, J. R., Assessment of the UV/chlorine process as an advanced
1032 oxidation process. *Water Res* **2011,** *45*, (4), 1890-1896.
1033 63. Thomsen, C. L.; Madsen, D.; Poulsen, J. A.; Thøgersen, J.; Jensen, S. J. K.; Keiding, S. R.,
1034 Femtosecond photolysis of aqueous HOCl. *The Journal of Chemical Physics* **2001,** *115*, (20), 9361-
1035 9369.
1036 64. Von Sonntag, C.; Von Gunten, U., *Chemistry of ozone in water and wastewater treatment*.
1037 IWA publishing: 2012.
1038 65. Treinin, A., The photochemistry of oxyanions. *Israel Journal of Chemistry* **1970,** *8*, (2),
1039 103-113.
1040 66. Buxton, G. V.; Bydder, M.; Salmon, G. A., Reactivity of chlorine atoms in aqueous solution:
1041 Part 1. The equilibrium Cl. + Cl- ⇌ Cl2. *Journal of the Chemical Society, Faraday Transactions*
1042 **1998,** *94*, (5), 653-657.
1043 67. Buxton, G. V.; Bydder, M.; Salmon, G. A.; Williams, J. E., The reactivity of chlorine atoms
1044 in aqueous solution. Part III. The reactions of Cl• with solutes. *Physical Chemistry Chemical*
1045 *Physics* **2000,** *2*, (2), 237-245.
1046 68. Grigor'ev, A.; Makarov, I.; Pikaev, A., Formation of Cl 2-in the bulk of solution during
1047 radiolysis of concentrated aqueous solutions of chlorides. *Khimiya Vysokikh Ehnergij* **1987,** *21*, (2),
1048 123-126.
1049 69. Yu, X.-Y.; Barker, J. R., Hydrogen peroxide photolysis in acidic aqueous solutions
1050 containing chloride ions. I. Chemical mechanism. *The Journal of Physical Chemistry A* **2003,** *107*,
1051 (9), 1313-1324.
1052 70. Ferraudi, G., Magnetic field effects on the rates of Cl2-and Br2-reactions: the dependence
1053 of the rates of radical disporportionation and oxidation of Mn (II) complexes on field intensity.
1054 *Journal of physical chemistry* **1993,** *97*, (11), 2793-2797.
1055 71. McElroy, W. J., A laser photolysis study of the reaction of sulfate (1-) with chloride and

the subsequent decay of chlorine (1-) in aqueous solution. *Journal of Physical Chemistry* **1990,** *94*, (6), 2435-2441.

72. Huie, R. E.; Clifton, C. L., Temperature dependence of the rate constants for reactions of the sulfate radical, SO4-, with anions. *Journal of Physical Chemistry* **1990,** *94*, (23), 8561-8567.

73. Hynes, A. J.; Wine, P., Time-resolved resonance Raman study of the spectroscopy and kinetics of the Cl− 2 radical anion in aqueous solution. *The Journal of chemical physics* **1988,** *89*, (6), 3565-3572.

74. Lierse, C.; Sullivan, J. C.; Schmidt, K. H., Rates of oxidation of selected actinides by Cl2. *Inorganic Chemistry* **1987,** *26*, (9), 1408-1410.

75. Gogolev, A.; Makarov, I.; Pikaev, A., Pulsed Radiolysis of Concentrated Hydrochloric-acid. *High Energy Chemistry* **1984,** *18*, (6), 390-395.

76. Navaratnam, S.; Parsons, B.; Swallow, A. J., Some reactions of the dichloride anion radical. *Radiation Physics and Chemistry (1977)* **1980,** *15*, (2-3), 159-161.

77. Zansokhova, A.; Kabakchi, S.; Pikaev, A., Mechanism of Cl 2-formation during pulsed radiolysis of neutral aqueous solutions of alkali metal chlorides. *Khimiya Vysokikh Ehnergij* **1977,** *11*, (1), 67-71.

78. Broszkiewicz, R. K., On the effect of Br-on formation of Cl-2 in the pulse radiolysis of the aqueous chloride solutions. *Bulletin de l'Academie Polonaise des Sciences. Serie des Sciences Chimiques* **1976,** *24*, (2), 123-131.

79. Woods, R.; Lesigne, B.; Gilles, L.; Ferradini, C.; Pucheault, J., Pulse radiolysis of aqueous lithium chloride solutions. *The Journal of Physical Chemistry* **1975,** *79*, (24), 2700-2704.

80. Zhestkova, T.; Pikaev, A., Destruction rate of Cl 2− anion-radicals during pulse radiolysis of concentrated aqueous lithium chloride solutions. *Bulletin of the Academy of Sciences of the USSR, Division of chemical science* **1974,** *23*, (4), 877-878.

81. Broszkiewicz, R., Pulse radiolysis studies on chloro-complexes of palladium. *International Journal for Radiation Physics and Chemistry* **1974,** *6*, (4), 249-258.

82. Thornton, A. T.; Laurence, G. S., Kinetics of oxidation of transition-metal ions by halogen radical anions. Part I. The oxidation of iron (II) by dibromide and dichloride ions generated by flash photolysis. *Journal of the Chemical Society, Dalton Transactions* **1973**, (8), 804-813.

83. Patterson, L. K.; Bansal, K.; Bogan, G.; Infante, G.; Fendler, E.; Fendler, J., Micellar effects on Cl2.-reactivity. Reactions with surfactants and pyrimidines. *Journal of the American Chemical Society* **1972,** *94*, (26), 9028-9032.

84. Ward, J.; Kuo, I., Steady state and pulse radiolysis of aqueous chloride solutions of nucleic acid components. In ACS Publications: 1968.
85. Langmuir, M. E.; Hayon, E., Flash photolysis study of mercury (II) halide complexes in aqueous solutions. Rates of reaction X2-radical antons. *The Journal of Physical Chemistry* **1967,** *71*, (12), 3808-3814.
86. Grebel, J. E.; Pignatello, J. J.; Mitch, W. A., Effect of Halide Ions and Carbonates on Organic Contaminant Degradation by Hydroxyl Radical-Based Advanced Oxidation Processes in Saline Waters. *Environmental Science & Technology* **2010,** *44*, (17), 6822-6828.
87. Connick, R. E., The interaction of hydrogen peroxide and hypochlorous acid in acidic solutions containing chloride ion. *Journal of the American Chemical Society* **1947,** *69*, (6), 1509-1514.
88. Mialocq, J.-C.; Barat, F.; Gilles, L.; Hickel, B.; Lesigne, B., Flash photolysis of chlorine dioxide in aqueous solution. *The Journal of Physical Chemistry* **1973,** *77*, (6), 742-749.
89. Mártire, D. O.; Rosso, J. A.; Bertolotti, S.; Carrillo Le Roux, G.; Braun, A. M.; Gonzalez, M. C., Kinetic study of the reactions of chlorine atoms and Cl2•- radical anions in aqueous solutions. II. Toluene, benzoic acid, and chlorobenzene. *Journal of Physical Chemistry A* **2001,** *105*, (22), 5385-5392.
90. Bobrowski, K.; Zagórski, Z., Kinetics of transient oxygen compounds formation measured from Čerenkov emission in pulse radiolysis. *Radiation Effects* **1977,** *33*, (1), 39-42.
91. von Sonntag, C.; Schuchmann, H. P.; Alfassi, Z. B., *Peroxyl radicals in aqueous solutions*. John Wiley & Sons: 1997.
92. Bothe, E.; Schuchmann, M. N.; Schulte-Frohlinde, D.; Sonntag, C. v., HO2 elimination from α-hydroxyalkylperoxyl radicals in aqueous solution. *Photochemistry and photobiology* **1978,** *28*, (4-5), 639-643.
93. Harris, D. C., *Quantitative Chemical Analysis, Sixth Edition*. W. H. Freeman: 2003.
94. Buxton, G. V., Pulse radiolysis of aqueous solutions. Rate of reaction of OH with OH–. *Transactions of the Faraday Society* **1970,** *66*, 1656-1660.
95. Bielski, B. H., Reevaluation of the spectral and kinetic properties of HO2 and O2-free radicals. *Photochemistry and Photobiology* **1978,** *28*, (4-5), 645-649.
96. Lide, D. R., *CRC handbook of chemistry and physics*. 82 ed. ed.; CRC Press: Boca Raton, FL: 2001.
97. Tao, L.; Han, J.; Tao, F.-M., Correlations and predictions of carboxylic acid p K a values

using intermolecular structure and properties of hydrogen-bonded complexes. *The Journal of Physical Chemistry A* **2008,** *112*, (4), 775-782.

98. Buxton, G. V.; Dainton, F. S., The radiolysis of aqueous solutions of oxybromine compounds; the spectra and reactions of BrO and BrO2. *Proceedings of the Royal Society of London. Series A. Mathematical and Physical Sciences* **1968,** *304*, (1479), 427-439.

99. Amichai, O.; Treinin, A., Oxybromine radicals. *The Journal of Physical Chemistry* **1970,** *74*, (20), 3670-3674.

100. Leitner, N. K. V.; De Laat, J.; Dore, M., Photodecomposition du bioxyde de chlore et des ions chlorite par irradiation uv en milieu aqueux-partie II. Etude cinetique. *Water Research* **1992,** *26*, (12), 1665-1672.

101. Buxton, G. V.; Subhani, M. S., Radiation chemistry and photochemistry of oxychlorine ions. Part 1.—Radiolysis of aqueous solutions of hypochlorite and chlorite ions. *Journal of the Chemical Society, Faraday Transactions 1: Physical Chemistry in Condensed Phases* **1972,** *68*, 947-957.

102. Sehested, K.; Corfitzen, H.; Holcman, J.; Hart, E. J., Decomposition of ozone in aqueous acetic acid solutions (pH 0-4). *The Journal of Physical Chemistry* **1992,** *96*, (2), 1005-1009.

103. Sehested, K.; Holcman, J.; Bjergbakke, E.; Hart, E. J., A pulse radiolytic study of the reaction hydroxyl+ ozone in aqueous medium. *The Journal of Physical Chemistry* **1984,** *88*, (18), 4144-4147.

104. Buhler, R.; Staehelin, J.; Hoigne, J., Ozone Decomposition in Water Studied by Pulse Radiolysis 1. HO2/O2-and HO3/O3-as Intermediates-Correction. *The Journal of Physical Chemistry* **1984,** *88*, (22), 5450-5450.

105. Nizkorodov, S. A.; Harper, W. W.; Blackmon, B. W.; Nesbitt, D. J., Temperature dependent kinetics of the OH/HO2/O3 chain reaction by time-resolved IR laser absorption spectroscopy. *The Journal of Physical Chemistry A* **2000,** *104*, (17), 3964-3973.

106. Elliot, A. J.; McCracken, D. R., Effect of temperature on O∅ reactions and equilibria: A pulse radiolysis study. *International Journal of Radiation Applications and Instrumentation. Part C. Radiation Physics and Chemistry* **1989,** *33*, (1), 69-74.

107. Sehested, K.; Holcman, J.; Bjergbakke, E.; Hart, E. J., Formation of ozone in the reaction of hydroxyl with O3-and the decay of the ozonide ion radical at pH 10-13. *The Journal of Physical Chemistry* **1984,** *88*, (2), 269-273.

108. Hoigné, J.; Bader, H., Kinetics of reactions of chlorine dioxide (OClO) in water—I. Rate

1152 constants for inorganic and organic compounds. *Water Research* **1994,** *28*, (1), 45-55.
1153 109. Klaning, U.; Sehested, K.; Holcman, J., Standard Gibbs energy of formation of the
1154 hydroxyl radical in aqueous solution. Rate constants for the reaction chlorite (ClO2-)+ ozone.
1155 dblarw. ozone (1-)+ chlorine dioxide. *The Journal of Physical Chemistry* **1985,** *89*, (5), 760-763.
1156 110. Crittenden, J. C.; Hu, S.; Hand, D. W.; Green, S. A., A kinetic model for H2O2/UV process
1157 in a completely mixed batch reactor. *Water research* **1999,** *33*, (10), 2315-2328.
1158 111. Sidgwick, N. V., *The chemical elements and their compounds*. Oxford Press: Oxford: 1952;
1159 Vol. 2.
1160 112. Amichai, O.; Czapski, G.; Treinin, A., Flash photolysis of the oxybromine anions. *Israel*
1161 *Journal of Chemistry* **1969,** *7*, (3), 351-359.
1162 113. Wagner, I.; Strehlow, H., On the flash photolysis of bromide ions in aqueous solutions.
1163 *Berichte der Bunsengesellschaft für physikalische Chemie* **1987,** *91*, (12), 1317-1321.
1164 114. Matthew, B. M.; George, I.; Anastasio, C., Hydroperoxyl radical (HO2•) oxidizes
1165 dibromide radical anion (• Br2−) to bromine (Br2) in aqueous solution: Implications for the
1166 formation of Br2 in the marine boundary layer. *Geophysical research letters* **2003,** *30*, (24).
1167 115. Mamou, A.; Rabani, J.; Behar, D., Oxidation of aqueous bromide (1-) by hydroxyl radicals,
1168 studies by pulse radiolysis. *The Journal of Physical Chemistry* **1977,** *81*, (15), 1447-1448.
1169 116. Field, R.; Raghavan, N.; Brummer, J., A pulse radiolysis investigation of the reactions of
1170 bromine dioxide radical (BrO2. cntdot.) with hexacyanoferrate (II), manganese (II), phenoxide ion,
1171 and phenol. *The Journal of Physical Chemistry* **1982,** *86*, (13), 2443-2449.
1172 117. Sander, R.; Vogt, R.; Harris, G. W.; Crutzen, P. J., Modelling the chemistry of ozone,
1173 halogen compounds, and hydrocarbons in the arctic troposphere during spring. *Tellus B: Chemical*
1174 *and Physical Meteorology* **1993,** *45*, (5), 522-532.
1175 118. Ershov, B. G., Kinetics, mechanism and intermediates of some radiation-induced reactions
1176 in aqueous solutions. *Russian chemical reviews* **2004,** *73*, (1), 101-113.
1177 119. Donati, A. Spectroscopic and kinetic investigations of halogen containing radicals in the
1178 tropospheric aqueous phase. Verlag nicht ermittelbar, 2002.
1179 120. Simic, M.; Hoffman, M. Z., Acid-base properties of the radicals produced in the pulse
1180 radiolysis of aqueous solutions of benzoic acid. *The Journal of Physical Chemistry* **1972,** *76*, (10),
1181 1398-1404.
1182 121. Grabner, G.; Getoff, N.; Schwoerer, F., Pulsradiolyse von H3PO4, H2PO4-, HPO42-und
1183 P2O74-in Wässriger Lösung—I. Geschwindigkeitskonstanten der reaktionen mit den

primärprodukten der wasserradiolyse. *International Journal for Radiation Physics and Chemistry* **1973,** *5*, (5), 393-403.

122. Jiang, P.-Y.; Katsumura, Y.; Domae, M.; Ishikawa, K.; Nagaishi, R.; Ishigure, K.; Yoshida, Y., Pulse radiolysis study of concentrated phosphoric acid solutions. *Journal of the Chemical Society, Faraday Transactions* **1992,** *88*, (22), 3319-3322.

123. Zuo, Z.; Katsumura, Y.; Ueda, K.; Ishigure, K., Reactions between some inorganic radicals and oxychlorides studied by pulse radiolysis and laser photolysis. *Journal of the Chemical Society, Faraday Transactions* **1997,** *93*, (10), 1885-1891.

124. Nowell, L. H.; Hoigné, J., Photolysis of aqueous chlorine at sunlight and ultraviolet wavelengths—II. Hydroxyl radical production. *Water Research* **1992,** *26*, (5), 599-605.